NONLINEAR GRAVITY WAVE-WIND INTERACTIONS
AND JET STREAM GRAVITY WAVE GENERATION

by

DONALD LEE PAUL

B.S., Massachusetts Institute of Technology

M.S., Massachusetts Institute of Technology

SUBMITTED IN PARTIAL FULFILLMENT OF THE REQUIREMENTS

FOR THE DEGREE OF

DOCTOR OF PHILOSOPHY

at the

MASSACHUSETTS INSTITUTE OF TECHNOLOGY

January 1977

Signature of Author_____
                    Department of Earth & Planetary Sciences

Certified by_____
                                        Thesis Supervisor

Accepted by_____
              Chairman, Departmental Committee on Graduate Students

NONLINEAR GRAVITY WAVE-WIND INTERACTIONS AND

JET STREAM GRAVITY WAVE GENERATION

by

Donald Lee Paul

Submitted to the Department of Earth and Planetary Sciences
in January 1977, in partial fulfillment of the requirements
for the degree of Doctor of Philosophy.

ABSTRACT

Theoretical gravity wave source models have been
developed to explain observed ground pressure fluctuation
measurements associated with overhead jet streams. The first
theory was developed using a multiple-scale analysis for
finite amplitude gravity waves in a sheared flow. This anal-
ysis is equivalent to a nonlinear WKB approximation and cal-
culations show the assumption of spatial smoothness of the
medium will be violated for the low Richardson numbers
associated with jet stream source regions. A quasi-linear
theory was next developed which is not limited in applica-
bility to large Richardson number shears. The quasi-linear
theory allows the essence of the nonlinear wave-wind inter-
action to be explored, yet retains the features of linear
wave propagation away from critical levels. For transient
gravity wave sources in the jet stream, numerical experiments

show two major effects. First, the initial disturbance is amplified in the source region at the expense of the wind and gravity waves are radiated from the source region up the jet and down toward the ground. An observed peak to peak surface pressure fluctuation of 0.5 millibar would correspond to maximum peak to peak sources region wave wind velocities of approximately 6 m/s. The second effect is a transfer of wind energy from the upper critical level to the lower critical level. This results from the upper critical level absorbing negative momentum waves that propagate up from the source region, while the lower critical absorbs positive momentum waves that propagate down to and are reflected back from the ground. The total energy transferred can be considerably larger than the original disturbance energy when the source region Richardson number is low.

A possible mechanism for generating the initial disturbances involves the generation of propagating subharmonics by their nonlinear wave-wave interaction with an unstable mode associated with shears having Richardson numbers less than 0.25. This possibility was studied using linear stability theory for stratified shear flows and an approximate theory for nonlinear wave-wave interactions. The time history predicted for this interaction is compatible with that of the subharmonic-mean wind interaction previously modeled. The more complete modeling involving the interactions of the unstable mode, the subharmonic, and the mean wind remains as an extension of the current study. The unstable modes have

periods less than the Brünt period and the periods of their
subharmonics will be from 1.2 to 1.6 Brünt periods which
falls within the range of commonly observed jet stream
gravity wave spectra.

TABLE OF CONTENTS

TABLE OF CONTENTS (continued)

LIST OF FIGURES

NONLINEAR GRAVITY WAVE-WIND INTERACTIONS AND
JET STREAM GRAVITY WAVE GENERATION

INTRODUCTION

Ground level pressure fluctuation measurements with an
array of micro-barographs have shown that most of the fluctu-
ation energy in the period range of minutes to an hour behave
as propagating atmospheric gravity waves. These waves are
especially strong when a well developed tropospheric jet
stream is located overhead. Linear wave theory is able to
account for many features of these waves. The frequency
spectrum of the waves shows a sharp high frequency cutoff at
the Brünt frequency. This was shown to be due to the evanes-
cent wave behavior for waves with frequencies above the Brünt
frequency and which have subsonic horizontal phase velocities.
The phase velocity of the waves can be used to determine the
height of the source region, since one can assume the source
region is convected with the mean wind, and in the troposphere
the wind velocity is usually monotonically increasing with
height. On examining the upper air wind and temperature
records it was found that the source regions represented
those levels of the jet that were least stable as based on
the Richardson number (Claerbout, 1967; Madden and Claerbout,
1968). Linear theory is unable to predict the source charac-
teristics, however, as the theory breaks down in the vicinity

1

of the critical level, that level where the wind velocity
equals the wave phase velocity. Linear theory predicts
growing wave amplitudes and decreasing vertical wavenumbers
as one approaches the critical level (Booker and Bretherton,
1967; Claerbout, 1967), so that unstable wind shears would
result from the waves themselves. Linear theory also predicts
that the wave is able to interact with the wind at the criti-
cal level (Bretherton, 1968; Garret, 1968; Hazel, 1967), and
this interaction could greatly alter the resulting wave
behavior. Since linear theory cannot predict how the inter-
action proceeds, one must incorporate nonlinear terms in
order to study the real situation existing in the jet stream
source regions.

A nonlinear investigation of gravity wave behavior
near the source region and the relation to ground pressure
observations and energy transport within the jet stream
seemed a worthy topic of investigation since waves involving
surface pressure variations of only fractions of a millibar
could become important in the jet stream due to the strong
and nonlinear behavior near critical levels. In addition,
the association of the source regions with low Richardson
numbers was an indication that a study of possible gravity
wave source generation by shear flow instability would also
be valuable.

A start on such a nonlinear study of gravity wave-wind
interactions was made by Breeding (1971). In that study the
nonlinear critical level phenomenon was investigated by means

of finite difference equations. The study showed how wave energy and momentum is taken up by the mean wind and how some higher harmonic wave generation also results. Unfortunately, the finite difference calculations require large amounts of computer time, and without a more analytic basis it is difficult to generate a complete understanding of the phenomenon. In addition, there remains the question of source generation and transient behavior in full jet stream models. Breeding's calculations did show, however, that with realistic wave amplitudes, the time scale of the changes in the waves and the wind could be slow relative to a wave period. This result could justify certain simplifications in the analysis and opens up the possibility of using more analytic methods to efficiently study these interactions.

In Section I a multiple scale analysis is applied to gravity wave propagation in a sheared flow. This analysis is based on the concept that while the wave amplitudes are finite so that second-order products cannot be neglected, the changes in the system are slow relative to the wave and spatially smooth compared to the wave phase structure. After considerable algebraic manipulation one is led to a much simpler set of equations for the waves and mean flow that is equivalent to a nonlinear WKB approximation for gravity wave propagation. Unfortunately, in the jet stream environment the condition of spatial smoothness is not upheld, and this analysis gives unrealistic results. The important parameter to define spatial variations is the wave impedance change

per radian. From linear theory we know that this parameter
is inversely proportional to the square root of the
Richardson number, and is therefore not small in regions of
interest where the waves are generated.

Breeding's analysis also showed that the wave harmonic
generation is much smaller than the mean flow - fundamental
interaction, and thus an expansion in horizontal Fourier com-
ponents is justified. Such an approach is taken up in Section
II. This method also leads to simplified numerical calcula-
tions, but in this case good agreement is obtained with
Breeding's two-dimentional finite difference calculations. A
similar expansion was also developed by Boer (1970).

This quasi-linear analysis can be given a rather
simple interpretation. On the whole the waves behave as in
linear theory, but in a time-varying medium. The spatial
and temporal variations of the medium are straightforwardly
related to nonlinear wave terms. From linear theory we are
aware of the large reflection effects occurring because of
rapid impedance changes with height in regions of low
Richardson number, and it is the presence of these partial
reflections which invalidated the multiple-scale analysis.
These reflections, which are included in the quasi-linear
theory, greatly influence the resulting wave-wind interac-
tions.

In Section III the quasi-linear theory is used in a
numerical study of the behavior of finite amplitude gravity
wave transients in a jet stream model as a function of source

characteristics and source region Richardson number. Calculations will show that gravity waves provide a very efficient coupling between the source region critical level and the critical level at the top of the jet. The steady state result is a transfer of wind energy from the topside to the underside critical level, the amount of energy transport rapidly increasing for decreasing Richardson number. Calculations will also show that source region wave-wind velocities of a 6 m/s can produce the observed pressure fluctuation amplitudes of 0.5 millibar at the ground.

In the final section we examine the question of gravity wave source generation itself. From linear stability theory for stratified shear flows we know that a certain range of wavenumbers will be unstable and grow at the expense of the wind if the Richardson number is less than 0.25 (Collyer, 1970; Drazin, 1958; Drazin and Howard, 1966; Hazel, 1972; Howard, 1963; Jones, 1968; Miles, 1961 and 1963; Richardson, 1920). However, these unstable wave modes have frequencies above the Brünt frequency cutoff and are trapped in the jet stream. Untrapped waves can be generated through wave-wave interaction among unstable modes. The development of such waves is studied in Section IV using linear stability theory and an approximate nonlinear wave-wave interaction formulation. The analysis shows that such effects are a possible explanation for the generation of observed gravity waves.

I. MULTIPLE-SCALE ANALYSIS OF NONLINEAR GRAVITY WAVES IN A BOUSSINESQ FLUID WITH A SHEARED MEAN FLOW

A. Mathematical Development for Finite Amplitude Waves

We wish to examine in detail one method of approximation to deal with finite amplitude gravity waves interacting with a sheared mean flow. In an attempt to eliminate algebraic complexities without altering the basic nature of the problem, we shall assume the equations of motion are those describing a Boussinesq fluid. The use of the Boussinesq approximation implies that the speed of sound and scale height of the mean density are very large compared to the phase velocities and vertical wavelengths of the fluid motions (Spiegel and Veronis, 1960). The mean vertical density structure is then described by the Brünt-Vasailia frequency Ω_B, and is otherwise considered a constant.

We then wish to examine the interaction of a train of internal gravity waves with a mean horizontal flow. The mean flow is assumed to be sheared and initially independent of time; however, nonlinear interactions with the wave train will introduce both time and spatial variations on the initial structure.

The governing equations and variables are given as follows:

$$(1.1) \quad \frac{\partial}{\partial t}(u+\bar{U}) + \frac{\partial}{\partial x}\left[(u+\bar{U})^2 + P\right] + \frac{\partial}{\partial z}\left[(u+\bar{U})w\right] = 0$$

$$(1.2) \quad \frac{\partial w}{\partial t} + \frac{\partial}{\partial x}\left[w(u+\bar{U})\right] + \frac{\partial}{\partial z}\left[w^2 + P\right] + \phi = 0$$

6

(1.3) $\quad \dfrac{\partial \phi}{\partial t} + \dfrac{\partial}{\partial x}\left[(u+\bar{U})\phi\right] + \dfrac{\partial}{\partial z}\left[w\phi\right] - \Omega_B^2 w = 0$

(1.4) $\quad \dfrac{\partial}{\partial x}\left[u+\bar{U}\right] + \dfrac{\partial w}{\partial z} = 0$

where

$\quad$ u $\quad$ = Horizontal wave velocity field

$\quad \bar{U} \quad$ = mean horizontal velocity field

$\quad$ w $\quad$ = vertical wave velocity field

$\quad$ P $\quad$ = (wave pressure field) $/\bar{\rho}$

$\quad \bar{\rho} \quad$ = mean density field

$\quad \phi \quad$ = wave bouyancy function $\equiv$

$$\Omega_{B^2} = g\left[\tfrac{1}{c^2}\left(\bar{P}\,\bar{P}_{\bar{z}} + \bar{P}\,\bar{P}_{\bar{z}}\right) - \tfrac{1}{\bar{\rho}}\bar{\rho}_{\bar{z}}\right].$$

For future reference, it can easily be shown that an energy conservation equation can be derived from (1.1) - (1.4) as:

(1.5) $\quad \dfrac{\partial E}{\partial t} + \dfrac{\partial}{\partial x}\left[(u+\bar{U})(E+P)\right] + \dfrac{\partial}{\partial z}\left[w(E+P)\right] = 0$

where $\quad E = \tfrac{1}{2}\left[(u+\bar{U})^2 + w^2 + \phi^2/\Omega_B^2\right].$

The nonlinear terms in the Reynold's stress in Equations (1.1) - (1.4) make a general solution to the above system virtually impossible, However, under certain approximations one can look for special solutions which may give insight into the particular problem. One method available is that of multiple-scale analysis. This method is essentially a generalized nonlinear WKB approximation for application to hyperbolic partial differential equations, and has been shown (Whitham, 1970) to be equivalent to the

phase-averaged techniques developed by Whitham (1965). The method of multiple scales has been applied to general nonlinear one-dimensional dispersive wave systems by Nayfeh and Hassen (1971), and by Grimshaw (1972) to gravity waves in fluids without sheared mean flows. The following development represents a new application of the method to the study of the propagation finite amplitude internal gravity waves and their critical level interaction with a sheared mean flow.

The basic assumption of the multiple-scale analysis is that there exist two space-time regimes, one representing the rapid phase fluctuations in the wave train, and one representing variation of such variables as amplitude, frequency, wavenumber, and properties of the medium. In order to describe mathematically the multiple-scale procedure, we introduce a small parameter $\epsilon \ll 1$, such that

$$(1.6) \quad \underline{X} = \epsilon \underline{x} \ , \ T = \epsilon t$$

where $(\underline{x}, t)$ refer to the short-term phase behavior of the wavetrain and $(\underline{X}, T)$ to the long-term behavior of the wave amplitude, phase derivatives (frequency and wavenumber) and medium properties. In linear theory one usually deals with the derivatives of the phase $\theta = wt - \underline{k} \cdot \underline{x}$. In the multiple-scale analysis a parallel development follows as the variables $(\underline{x}, t)$ are introduced through a rapidly-varying phase variable θ. The time and spatial derivatives can then be written as:

(1.7) a) $\dfrac{\partial}{\partial t} = \sigma \dfrac{\partial}{\partial \theta} + \varepsilon \dfrac{\partial}{\partial T}$

b) $\dfrac{\partial}{\partial x} = -k \dfrac{\partial}{\partial \theta} + \varepsilon \dfrac{\partial}{\partial X}$

c) $\dfrac{\partial}{\partial z} = -\ell \dfrac{\partial}{\partial \theta} + \varepsilon \dfrac{\partial}{\partial Z}$.

In general, the frequency σ and wavenumbers k and ℓ are also functions of the variables (X, Z, T). Finally, we introduce an asymptotic series in powers of ε for each dependent wave variable as functions of $(\theta, \underline{X}, T)$. The specific notation will be as follows:

(1.8) a) $u = u_0(\theta, \underline{X}, T) + \varepsilon u_1(\theta, \underline{X}, T) + \cdots$

b) $W = W_0(\theta, \underline{X}, T) + \varepsilon W_1(\theta, \underline{X}, T) + \cdots$

c) $P = P_0(\theta, \underline{X}, T) + \varepsilon P_1(\theta, \underline{X}, T) + \cdots$

d) $\phi = \phi_0(\theta, \underline{X}, T) + \varepsilon \phi_1(\theta, \underline{X}, T) + \cdots$.

It should be noted that the wave field variables are not considered small, that is of $O(\varepsilon)$, so that quadratic products of zero order in the governing equations may not be neglected as is the case in linear theory. Furthermore, since the wave-train amplitude is not to be considered $O(\varepsilon)$ relative to ambient values, one would also expect wave-wind and wave-wave interactions to produce changes in the medium properties. The total field variables will then be written as:

(1.9) a) $u = \bar{U}(Z) + \Delta u(\underline{X}, T) + u_0(\theta, \underline{X}, T) + O(\varepsilon)$

b) $W = \Delta W(\underline{X}, T) + W_0(\theta, \underline{X}, T) + O(\varepsilon)$

c) $P = \Delta P(\underline{X},T) + P_0(\theta,\underline{X},T) + O(\varepsilon)$

d) $\phi = \Delta\phi(\underline{X},T) + \phi_0(\theta,\underline{X},T) + O(\varepsilon)$.

Note that we initially assume only a horizontal shear $\bar{U}(z)$ and hydrostatic equilibrium so that $\bar{P}(z)$ and $\bar{\phi}(z)$ do not appear in the Boussinesq equations (1.1)- (1.4) and in (1.9) c, d.

Zero and First Order Equations

Upon substitution of the scaled derivatives and the asymptotic series for the field variables into the governing equations, one obtains a sequence of systems of partial differential equations after ordering by powers of ε. Of immediate interest are the systems of equations corresponding to $O(\varepsilon^0)$ and $O(\varepsilon^1)$. The $O(\varepsilon^0)$ system contains only derivatives with respect to θ and gives the phase dependence of the leading terms of the wave field variables. The $O(\varepsilon^0)$ system is as follows:

$$(1.10) \quad \frac{\partial}{\partial\theta}\Big[\sigma(u_0+\bar{U}+\Delta u)-k(u_0+\bar{U}+\Delta u)^2 - k(P_0+\Delta P)$$
$$- \ell(u_0+\bar{U}+\Delta u)(W_0+\Delta W)\Big] = 0$$

$$(1.11) \quad \frac{\partial}{\partial\theta}\Big[\sigma(W_0+\Delta W)-k(u_0+\bar{U}+\Delta u)(W_0+\Delta W)-\ell(P_0+\Delta P)$$
$$-\ell(W_0+\Delta W)^2\Big] + \phi_0 + \Delta\phi = 0$$

$$(1.12) \quad \frac{\partial}{\partial\theta}\Big[\sigma(\phi_0+\Delta\phi) - k(u_0+\bar{U}+\Delta u)(\phi_0+\Delta\phi)$$
$$-\ell(W_0+\Delta W)(\phi_0+\Delta\phi)\Big] - \Omega_B^2(W_0+\Delta W) = 0$$

$$(1.13) \quad \frac{\partial}{\partial\theta}\Big[k(u_0+\bar{U}+\Delta u) + \ell(W_0+\Delta W)\Big] = 0.$$

In the above equations σ, K, ℓ have been collected

inside the brackets as they are a function only of $(\underline{X}, T)$ and
not θ. Also, since $\bar{U}$, Δu, Δw, ΔP and $\Delta\phi$ are not functions of
θ, some terms could be deleted but are retained for conveni-
ence in the manipulations that follow.

Equations (1.10) and (1.13) can be integrated with
respect to θ directly. From (1.13),

$$(1.14) \quad K(u_0 + \bar{U} + \Delta u) + \ell(w_0 + \Delta w) \equiv f_0(\underline{X}, T)$$

and from (1.10)

$$(1.15) \quad (u_0 + \bar{U} + \Delta u)(\sigma - f_0(\underline{X},T)) - K(P_0 + \Delta P) \equiv K M_0(\underline{X},T).$$

Eliminating $(P_0 + \Delta P)$ and $(u_0 + \bar{U} + \Delta u)$ in favor of $(w_0 + \Delta w)$ in
(1.11) gives

$$(1.16) \quad (\sigma - f_0)\left(1 + \frac{\ell^2}{K^2}\right)\frac{\partial}{\partial\theta}(w_0 + \Delta w) + (\phi_0 + \Delta\phi) = 0$$

and finally eliminating $(\phi_0 + \Delta\phi)$ yields

$$(1.17) \quad \left(\frac{\sigma - f_0}{\Omega_B}\right)^2\left(1 + \frac{\ell^2}{K^2}\right)\frac{\partial^2}{\partial\theta^2}(w_0 + \Delta w) + (w_0 + \Delta w) = 0.$$

If we normalize the period of θ to 2π, the solution is

$$(1.18) \quad w_0 + \Delta w = W(\underline{X},T)e^{i\theta} + W^*(\underline{X},T)e^{-i\theta}$$

which requires from (1.17) that

$$(1.19) \quad (\sigma - f_0)^2(K^2 + \ell^2) = K^2\Omega_B^2.$$

The relation (1.19) defines a "local" dispersion relation and
if $f_0(\underline{X},T) = K\bar{U}(z)$, one would have the linear dispersion
relation for internal gravity waves in a Boussinesq fluid
with horizontal shear flow. Since $w_0 = w_0(\theta,\underline{X},T)$ and
$\Delta w = \Delta w(\underline{X},T)$, we can take $\Delta w = 0$ and then

$$(1.20) \quad W_o(\theta,\underline{X},T) = W(\underline{X},T)e^{i\theta} + W^*(\underline{X},T)e^{-i\theta}.$$

Referring back to Equation (1.14), we can write

$$(1.21) \quad \left[Ku_o + \ell(We^{i\theta} + W^*e^{-i\theta}) \right] + K(\bar{U} + \Delta u) = f_o(\underline{X},T)$$

and since $u_o = u_o(\theta,\underline{X},T)$ this can only hold for all $\theta,\underline{X},T$ if

$$(1.22) \quad u_o(\theta,\underline{X},T) = -\frac{\ell}{K}(We^{i\theta} + W^*e^{-i\theta})$$

and

$$(1.23) \quad f_o(\underline{X},T) = K[\bar{U}(z) + \Delta u(\underline{X},T)].$$

We observe then that the "local" dispersion relation (1.15) is exactly analogous to the dispersion relation of linear theory wherein the initial mean horizontal flow $\bar{U}(z)$ is replaced by the instantaneous mean horizontal flow $\bar{U}(Z) + \Delta u(\underline{X},T)$. The mean flow is modified by the term $\Delta u(\underline{X},T)$ resulting from nonlinear wave-wave interaction, and this will in turn modify the wave train via wave-wind interaction.

The remaining amplitude relationships can be determined straight away.

$$(1.24) \quad K^2 P_o = -\ell(\sigma - f_o)(We^{i\theta} + W^*e^{-i\theta})$$

$$(1.25) \quad (\sigma - f_o)(\bar{U} + \Delta u) - K\Delta P = KM_o(\underline{X},T)$$

$$(1.26) \quad \phi_o + \Delta\phi = -i(\sigma - f_o)\left(1 + \frac{\ell^2}{K^2}\right)(We^{i\theta} - W^*e^{-i\theta})$$

which in turn allows us to take $\Delta\phi = 0$. The amplitude and polarization relations are exactly analogous to those for linear theory in terms of the lowest order wavefield variables. The effect of the finite amplitude of the wave train is

observed in the contribution to altering the mean horizontal flow and mean pressure field, which in turn will modify the wave train itself. The $0(\varepsilon^0)$ system has yielded the phase relationships within the wavetrain and the $0(\varepsilon^1)$ system will give the dependence of the zero-order solution on $(\underline{X},T)$.

The $0(\varepsilon^1)$ system is:

(1.27)
$$\frac{\partial}{\partial\theta}\left[(\sigma-f_0)u_1-kP_1\right] = -\left[\frac{\partial}{\partial T}(u_0+\bar{U}+\Delta u)\right.$$
$$\left. +\frac{\partial}{\partial X}\left[(u_0+\bar{U}+\Delta u)^2+P_0+\Delta P\right]+\frac{\partial}{\partial Z}\left[(u_0+\bar{U}+\Delta u)W_0\right]\right]$$
$$\equiv A_1(\theta,\underline{X},T)$$

(1.28)
$$\frac{\partial}{\partial\theta}\left[(\sigma-f_0)W_1-\ell P_1\right] = -\left[\frac{\partial W_0}{\partial T}+\frac{\partial}{\partial X}\left[W_0(u_0+\bar{U}+\Delta u)\right]\right.$$
$$\left. +\frac{\partial}{\partial Z}\left[W_0^2+P_0+\Delta P\right]\right] \equiv B_1(\theta,\underline{X},T)$$

(1.29)
$$\frac{\partial}{\partial\theta}\left[(\sigma-f_0)\phi_1\right]-\mathcal{Q}_\beta^2 W_1 = -\left[\frac{\partial\phi_0}{\partial T}+\frac{\partial}{\partial X}\left[\phi_0(u_0+\bar{U}+\Delta u)\right]\right.$$
$$\left. +\frac{\partial}{\partial Z}(W_0\phi_0)\right] \equiv C_1(\theta,\underline{X},T)$$

(1.30)
$$\frac{\partial}{\partial\theta}\left[ku_1+\ell W_1\right]=-\left[\frac{\partial}{\partial X}(u_0+\bar{U}+\Delta u)+\frac{\partial W_0}{\partial Z}\right] \equiv D_1(\theta,\underline{X},T).$$

We observe that the homogeneous part of the system of partial differential equations for u_1, w_1, P_1 and ϕ_1 is identical to that of the corresponding $0(\varepsilon^0)$ variables. In general then, we can expect terms which are secular (non-periodic) in θ to be generated in the inhomogeneous solution to the system (1.27) - (1.30). To maintain an asymptotic series which will be uniform in θ, at least to $0(\varepsilon^1)$, certain necessary conditions must exist concerning the inhomogeneous portion of the $0(\varepsilon)$ equations. The removal of secular terms at $\theta(\varepsilon)$ will generate the equations required to describe the

behavior of the $0(\varepsilon^0)$ variables with respect to $(\underline{X},T)$.

Since there are four independent equations, in general we would expect four conditions and this proves to be the case. Immediately from equations (1.27) and (1.30), we see that removal of secularities requires

(1.31) $\int_0^{2\pi} d\Theta \, A_1(\Theta, \underline{X}, T) = 0$

and

(1.32) $\int_0^{2\pi} d\Theta \, D_1(\Theta, \underline{X}, T) = 0.$

Explicitly this requires

(1.33) $\dfrac{\partial \Delta u}{\partial T} + \dfrac{\partial}{\partial X}\left[(\Delta u)^2 + 2\dfrac{\ell^2}{K^2} W W^* + \Delta P\right] + \dfrac{\partial}{\partial Z}\left[-2\dfrac{\ell}{K} W W^*\right] = 0$

and

(1.34 $\dfrac{\partial \Delta u}{\partial X} = 0.$

To find the remaining two secular conditions, we derive the governing second-order differential equation for W_1:

(1.35) $\left[\left(\dfrac{\sigma - f_0}{\Omega_B}\right)^2\left(1 + \dfrac{\ell^2}{K^2}\right)\right]\dfrac{\partial^2 W_1}{\partial \Theta^2} + W_1$

$= \dfrac{1}{\Omega_B^2}\left[(\sigma - f_0)\left[\dfrac{\partial B_1}{\partial \Theta} - \dfrac{\ell}{K}\dfrac{\partial A_1}{\partial \Theta} + (\sigma - f_0)\dfrac{\ell}{K^2}\dfrac{\partial P_1}{\partial \Theta}\right] - C_1$

$\equiv E_1(\Theta, \underline{X}, T).$

Since $\left[\left(\dfrac{\sigma - f_0}{\Omega_B}\right)^2\left(1 + \dfrac{\ell^2}{K^2}\right)\right] = 1$ from the $0(\varepsilon^0)$ calculations, we are reduced to the form:

(1.36) $\dfrac{\partial^2 W_1}{\partial \Theta^2} + W_1 = E_1(\Theta, \underline{X}, T)$.

The two remaining secular conditions follow directly.
Multiplying both sides of W_o and integrating over θ from
0 to 2π gives

(1.37) $\displaystyle\int_0^{2\pi} d\Theta \left[W_o \dfrac{\partial^2 W_1}{\partial \Theta^2} + W_o W_1 \right] = \int_0^{2\pi} d\Theta \left[W_o \dfrac{\partial^2 W_1}{\partial \Theta^2} - W_1 \dfrac{\partial^2 W_o}{\partial \Theta^2} \right]$

$= \left[W_o \dfrac{\partial W_1}{\partial \Theta} - W_1 \dfrac{\partial W_o}{\partial \Theta} \right]_0^{2\pi} = \displaystyle\int_0^{2\pi} d\Theta\, W_o E_1(\Theta, \underline{X}, T)$

and since W_o and $\dfrac{\partial W_o}{\partial \theta}$ are periodic over 2π and W_1 and $\dfrac{\partial W_1}{\partial \theta}$
are also required to be periodic over 2π (with secularities
removed) then

(1.38) $\displaystyle\int_0^{2\pi} d\Theta\, W_o E_1(\Theta, \underline{X}, T) = 0.$

In an exactly analogous way, multiplying by $\dfrac{\partial W_o}{\partial \theta}$ and
integrating (1.36) over 2π gives:

(1.39) $\displaystyle\int_0^{2\pi} d\Theta\, \dfrac{\partial W_o}{\partial \Theta} E_1(\Theta, \underline{X}, T) = 0.$

As a simple example, consider the case where
$E_1(\theta, \underline{X}, T) = \alpha(\underline{X}, T) W_o + \beta(\underline{X}, T) \dfrac{\partial W_o}{\partial \theta}$. The secular term removed
conditions (1.38) and (1.39) give $\alpha = \beta = 0$. The exact
solution to (1.36) using E_1 as above is
$W_1 = W_o(1 + \beta\theta/2) + \dfrac{\partial W_o}{\partial \theta}(1 - \alpha\theta/2)$ which clearly will have
secular terms in θ unless $\alpha = \beta = 0$ is required.

The derivation of the amplitude equations for the
zero-order field variables based on removal of secular terms
in θ provides the mathematical foundation for a more intui-
tive approach. Whitham (1965) has shown that if the original

equations can be put into conservation form, the amplitude
equations can be derived by simply phase-averaging. A con-
servation equation will have the form

(1.40) $\dfrac{\partial M}{\partial T} + \dfrac{\partial F_x}{\partial X} + \dfrac{\partial F_z}{\partial Z} = 0$ and for the system (1.1) - (1.4),

there are three conservation forms. The governing amplitude
equations are:

(1.41) $\dfrac{\partial \Delta u}{\partial T} + \dfrac{\partial}{\partial X}\left[(\bar{U}+\Delta u)^2 + \langle u_0^2 \rangle_\theta + \Delta P\right]$

$+ \dfrac{\partial}{\partial Z}\left[\langle u_0 W_0 \rangle_\theta\right] = 0$ (horizontal momentum conserva-

tion)

(1.42) $\dfrac{\partial}{\partial T}\langle E_0 \rangle_\theta + \dfrac{\partial}{\partial X}\left[(\bar{U}+\Delta u)\Delta P + \langle u_0 E_0 \rangle_\theta + \langle u_0 P_0 \rangle_\theta \right.$

$\left. + (\bar{U}+\Delta u)\langle E_0 \rangle_\theta\right]$ (energy conservation)

$+ \dfrac{\partial}{\partial Z}\left[\langle W_0 E_0 \rangle_\theta + \langle W_0 P_0 \rangle_\theta\right] = 0$

where $\langle E_0 \rangle_\theta = \dfrac{1}{2}\left[(\bar{U}+\Delta u)^2 + \langle u_0^2 \rangle_\theta + \langle W_0^2 \rangle_\theta + \dfrac{\langle \phi_0^2 \rangle_\theta}{\Omega_B^2}\right]$

(1.43) $\dfrac{\partial \Delta u}{\partial X} = 0$ (mass conservation) .

In addition there are two phase conservation
equations,

(1.44) $\dfrac{\partial k}{\partial T} + \dfrac{\partial \sigma}{\partial X} = 0$

(1.45) $\dfrac{\partial \ell}{\partial T} + \dfrac{\partial \sigma}{\partial Z} = 0$

and one dispersion relation

$$(1.46) \quad \left[\sigma - k(\bar{U} + \Delta u)\right]^2 (k^2 + \ell^2) = k^2 \Omega_B^2$$

which complete the system.

A particularly important case arises when the amplitudes and medium properties are considered only to be functions of (Z,T). The wavetrain will then retain an x-dependence only in the phase through the horizontal wave number K. The resulting theory corresponds to a time-dependent WKB approximation for finite amplitude gravity waves.

Even though the x-dependence in the wavetrain amplitudes is ignored, the equations remain nonlinear and numerical computations are required in even the simplist of cases. However, the two-dimensional problem has been reduced to a one-dimensional one resulting in a considerable reduction in computation effort.

B. <u>Applications of the Method of Characteristics to</u>
    <u>Low-Frequency Gravity Waves -- Some Analytical Results</u>

Let us examine more closely the time-dependent, finite amplitude WKB approximation for the case of very low frequency gravity waves, that is, when the doppler-shifted frequency is such that $\varpi^2 \ll \Omega_B^2$. For algebraic convenience, let us introduce a mean wind velocity scale v_o and define the nondimensional variables:

$$(1.47) \quad a) \quad \phi \equiv \left(\frac{WW^*}{V_o^2}\right)\left(\frac{\Omega_B}{\varpi}\right) \quad , \quad \varpi \equiv \sigma - k(\bar{U} + \Delta u)$$

$$b) \quad \eta \equiv \frac{\bar{U} + \Delta u}{V_o}$$

$$c) \quad \varsigma \equiv \frac{\varpi}{\Omega_B} \; .$$

The governing equations for the low-frequency case ($\zeta^2 \ll 1$) are:

(1.48) $\dfrac{\partial \eta}{\partial T} - 2V_0 \dfrac{\partial \phi}{\partial Z} = 0$ (horizontal momentum conservation)

(1.49) $\dfrac{\partial \phi}{\partial T} + \dfrac{\partial}{\partial Z}(V_g \phi) - 2V_0 \zeta \phi \dfrac{\partial \eta}{\partial Z} = 0$ (energy conservation)

(1.50) $\dfrac{\partial \zeta}{\partial T} + V_g \dfrac{\partial \zeta}{\partial Z} - V_0 \zeta^2 \dfrac{\partial \eta}{\partial Z} = 0$ (phase conservation)

where $V_g = -\dfrac{\Omega_B}{K}\zeta^2$. In linear wave propagation theory, V_g would be the vertical group velocity for wavetrains moving in the negative z-direction.

The system (1.48) - (1.50) can be put in matrix form, defining the nondimensional vector

(1.51) $\underline{V} \equiv (\phi, \zeta, \eta)$

(1.52) $\dfrac{\partial \underline{V}}{\partial T} + \underline{\underline{A}} \cdot \dfrac{\partial \underline{V}}{\partial Z} = 0$

where

(1.53) $\underline{\underline{A}} = \begin{bmatrix} V_g & -2V_g(\phi/\zeta) & -2V_0\zeta\phi \\ 0 & V_g & -V_0\zeta^2 \\ -2V_0 & 0 & 0 \end{bmatrix}$.

Then there will exist a set of three characteristic curves c_i, i = 1, 2, 3, defining functions $\psi_i(Z,T) = 0$, which are given from the differential equations:

(1.54) $\dfrac{dZ}{dT} = \lambda_i$; $\lambda_i \dfrac{\partial \psi_i}{\partial Z} + \dfrac{\partial \psi_i}{\partial T} = 0$

where λ_i are the roots of the deterministic equation:

(1.55) $\det [\underline{A} - \lambda \underline{\underline{I}}] = 0.$ ($\underline{\underline{I}}$ = identity matrix)

The eigenvalues, with $\underline{\underline{A}}$ given in (1.53) are:

(1.56) a) $\lambda_1 = 0$

  b) $\lambda_2 = V_g + 2V_0\sqrt{\phi\xi} = V_g + 2|W|$

  c) $\lambda_3 = V_g - 2V_0\sqrt{\phi\xi} = V_g - 2|W|$

and the corresponding left eigenvectors are:

(1.57) a) $\ell_1 = \left[1, -\dfrac{2\phi}{\xi}, \dfrac{V_g}{2V_0}\right]$

  b) $\ell_2 = \left[1, \dfrac{V_g\sqrt{\phi\xi}}{V_0\xi^2}, -\sqrt{\phi\xi}\right]$

  c) $\ell_3 = \left[1, \dfrac{-V_g\sqrt{\phi\xi}}{V_0\xi^2}, \sqrt{\phi\xi}\right].$

We see that all the eigenvalues are real so the system is totally hyperbolic in character. The system can then be put in canonical form such that in each equation all quantities are differentiated along the same characteristic direction.

(1.58) $\dfrac{\partial\phi}{\partial T} - \dfrac{2\phi}{\xi}\dfrac{\partial\xi}{\partial T} - \dfrac{V_g}{2V_0}\dfrac{\partial\eta}{\partial T} = 0$

(1.59) $\left[\dfrac{\partial}{\partial T} + (V_g + 2V_0\sqrt{\phi\xi})\dfrac{\partial}{\partial Z}\right]\phi$

$\qquad - \dfrac{V_g\sqrt{\phi\xi}}{V_0\xi^2}\left[\dfrac{\partial}{\partial T} + (V_g + 2V_0\sqrt{\phi\xi})\dfrac{\partial}{\partial Z}\right]\xi$

$\qquad - \sqrt{\phi\xi}\left[\dfrac{\partial}{\partial T} + (V_g + 2V_0\sqrt{\phi\xi})\dfrac{\partial}{\partial Z}\right]\eta = 0$

(1.60) $\left[\dfrac{\partial}{\partial T} + (V_g - 2V_0\sqrt{\phi\xi})\dfrac{\partial}{\partial Z}\right]\phi + \dfrac{V_g\sqrt{\phi\xi}}{2V_0\xi^2}\left[\dfrac{\partial}{\partial T} + \right.$

$\qquad \left. (V_g - 2V_0\sqrt{\phi\xi})\dfrac{\partial}{\partial Z}\right]\eta + \sqrt{\phi\xi}\left[\dfrac{\partial}{\partial T} + (V_g - 2V_0\sqrt{\phi\xi})\dfrac{\partial}{\partial Z}\right]\xi = 0.$

The details are still quite complicated at this point; however, two important observations about the system can be made.

First, in the small amplitude limit where $|w| \to 0$, the eigenvalues (1.56) coalesce to a single value V_g, and the system reduces immediately to the linear theory result

$$(1.61) \qquad \frac{\partial \phi}{\partial T} + V_g \frac{\partial \phi}{\partial Z} = 0.$$

This demonstrates that the total wave energy is conserved as it must be, since there can be no wave-wind energy exchange without nonlinear interactions.

The second immediate result from the canonical formulation is that there exists one exact integral. Equation (1.58) can be rewritten as

$$(1.62) \qquad \frac{\partial}{\partial T} \left[\eta - \frac{z V_0 \phi}{V_g} \right] = 0$$

which can be integrated directly since ϕ, ζ, and η are all known functions of z at T = 0 in an initial value problem. Making use of this exact integral, the system can be reduced further to one containing only two dependent variables. The remaining equations are still highly nonlinear, however, the use of the multiple scale approximation has resulted in a considerable simplification of the original Boussinesq system given in (1.1) - (1.4).

C. The Limitations of Multiple-Scale Analysis and the Question of Partial Reflections

The primary assumption of the multiple-scale analysis is that there exist at least two time-space scales in the

problem under examination. In the foregoing analysis, we
have assumed that the phase fluctuations of the wavetrain were
much more rapid than the corresponding time and space varia-
tions in the wave amplitudes and properties of the medium.
This assumption means that only a minor amount of wave reflec-
tion can take place and thus the wave impedance change per
vertical wavelength must be small. If the reflected waves are
of order ε compared to the transmitted wave they will be con-
tained in the amplitude equations resulting from the elimin-
ation of secular terms of order ε^2.

From linear theory we can evaluate the criteria for
strong reflections. If temperature and density variations
are slow only the wind variations modify the wave impedance,
and strong reflections result if the Richardson number is
less than 1. In the nonlinear theory one cannot develop such
an explicit constraint, but it is reasonable to expect diffi-
culties with the multiple scale analysis in regions of strong
wind shears. In Figure 1 we show some results of calcula-
tions using the multiple-scale analysis for a wave-wind inter-
action in a region where the Richardson number is 0.53, and
compare them with Breeding's more exact numerical calcula-
tions. The multiple-scale analysis retains the proper
qualitative features, but the amplitudes are considerably in
error. Breeding's calculations showed that a substantial
reflected wave was present as would be expected with a low
Richardson number, and thus much of the wave energy was turned
back before it interacted with the mean wind. The multiple-

CHANGE IN THE MEAN WIND NEAR THE CRITICAL LEVEL
— CALCULATION METHODS COMPARISON

RICHARDSON NUMBER = 0.53
t = 2190 S.

□ — — □   MULTIPLE SCALE ANALYSIS
————   FIRST AND ZERO HARMONIC
O — O   R. BREEDING NUMERICAL
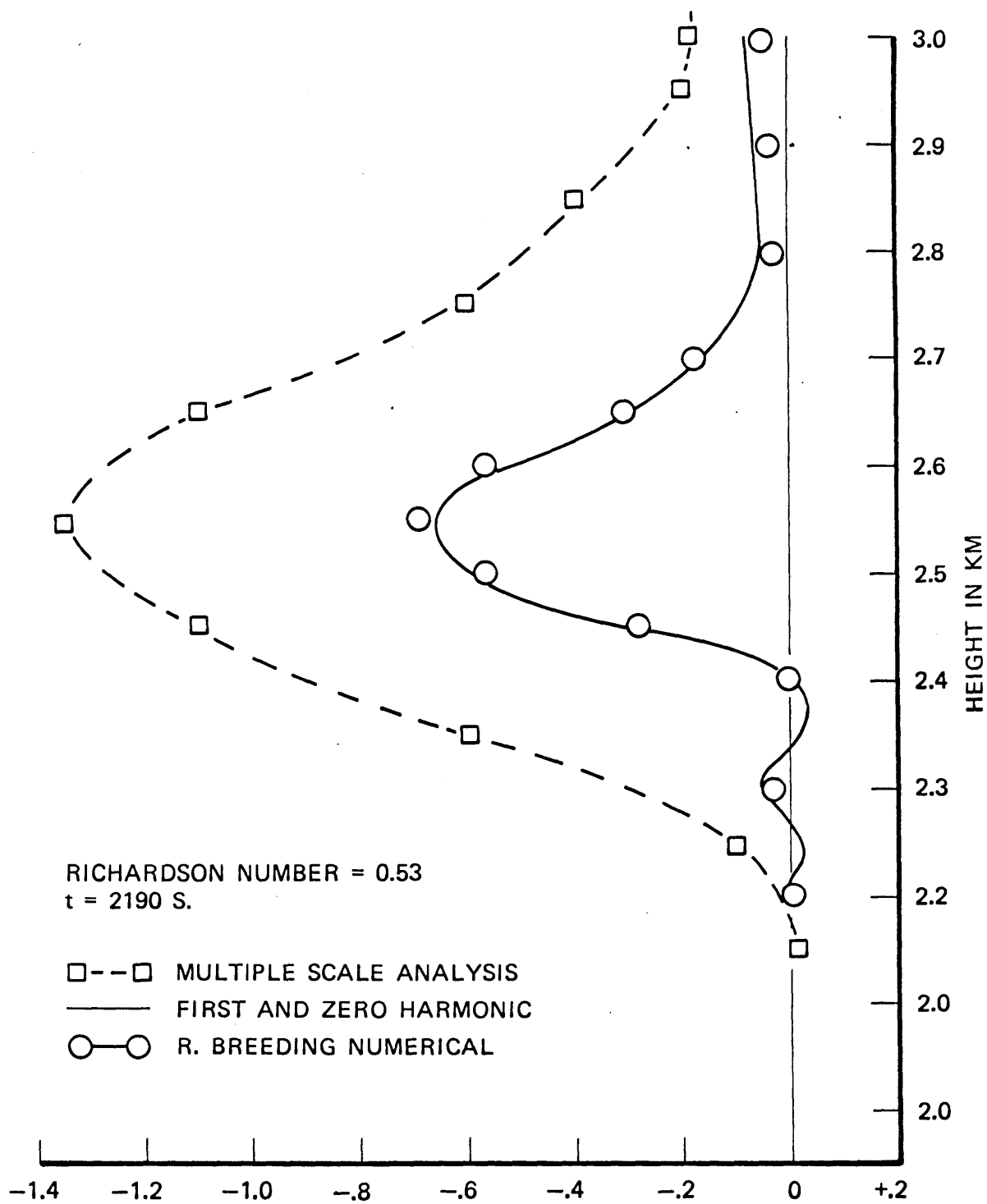
FIGURE 1

CHANGE IN MEAN WIND IN M/S

scale analysis which did not properly account for reflected waves thus gave too large a mean wind modification, and the discrepancy would continue to grow with time.

When the Richardson number is large, the conditions necessary for justifying the multiple-scale analysis will be upheld and then the methods described above can yield good approximations with a considerable reduction in computational effort. Unfortunately, in our jet stream studies, the areas of greatest interest are those with the lowest Richardson number, and these analysis methods will fail to give us adequate representations of the actual behavior of these regions. Thus, we are led to find a different approach to these problems, which is taken up in the next section.

II. HORIZONTAL FOURIER EXPANSION ANALYSIS

A. Development of the Governing Equations

In the previous section the multiple-scale approxi-
mation was used to analyze qualitative features of the non-
linear gravity wave - jet stream interaction. While this
method allows certain problems to be attacked by analytical
means the approximation appears inadequate for obtaining
detailed results in several physical situations. In particu-
lar, the important problem of interpretation of gravity wave
pressure fluctuations observed at the ground in terms of
possible jet stream source parameters appears to lie beyond
the scope of the multiple-scale approach.

The key to any attempt at inverting gravity wave
pressure fluctuation measurements involves the development of
an efficient, accurate method of solving the nonlinear
hydrodynamic problem under a wide range of initial conditions.
A direct approach would be to use a full nonlinear numerical
model such as that of R. Breeding. Such a study involves the
use of two-space and one time coordinate finite difference
grid, and while quite general in application, can require a
large computation effort.

An examination of R. Breeding's work indicates that
there is a useful approximation which can be employed to
greatly reduce computation effott while yielding quite satis-
factory results under realistic conditions.

The above numerical integration scheme requires the
application of cyclical horizontal boundary conditions, hence

the dependent field variables are required to be periodic over some distance, L, in the horizontal direction. Therefore, the velocity, pressure, and density field can be expanded in a Fourier series in x, where the amplitudes are functions of (z, t) only:

$$(2.1) \quad u(x,z,t) = u_0(z,t) + \sum_{n=1}^{\infty}\left[u_n(z,t)e^{-iknx} + u_n^*(z,t)e^{iknx}\right]$$

$$(2.2) \quad w(x,z,t) = w_0(z,t) + \sum_{n=1}^{\infty}\left[w_n(z,t)e^{-iknx} + w_n^*(z,t)e^{iknx}\right]$$

$$(2.3) \quad p(x,z,t) = p_0(z,t) + \sum_{n=1}^{\infty}\left[p_n(z,t)e^{-iknx} + p_n^*(z,t)e^{iknx}\right]$$

$$(2.4) \quad \phi(x,z,t) = \phi_0(z,t) + \sum_{n=1}^{\infty}\left[\phi_n(z,t)e^{-iknx} + \phi_u^*(z,t)e^{iknx}\right]$$

where $K = \frac{2\pi}{L}$.

Substituting the above expressions for the field variables in the Boussinesq fluid equations (1.1) - (1.4) and equating Fourier coefficients we have:

for n = 0, 1

$$(2.5) \quad \frac{\partial u_0}{\partial t} + \frac{\partial}{\partial z}\left[u_0 w_0 + \sum_{p=1}^{\infty}(u_p w_p^* + u_p^* w_p)\right] = 0$$

$$(2.6 \quad \frac{\partial w_0}{\partial t} + \frac{\partial}{\partial z}\left[p_0 + w_0^2 + z\sum_{p=1}^{\infty}(w_p w_p^*)\right] + \phi_0 = 0$$

$$(2.7) \quad \frac{\partial \phi_0}{\partial t} + \frac{\partial}{\partial z}\left[\phi_0 w_0 + \sum_{p=1}^{\infty}(w_p \phi_p^* + w_p^* \phi_p)\right] - \mathcal{L}_B^2 w_0 = 0$$

$$(2.8) \quad \frac{\partial w_0}{\partial z} = 0$$

$$(2.9) \quad \frac{\partial u_1}{\partial t} - ik\left[P_1 + 2u_0 u_1 + 2\sum_{P=1}^{\infty}(u_P^* u_{P+1})\right]$$
$$+ \frac{\partial}{\partial z}\left[u_0 w_1 + u_1 w_0 + \sum_{P=1}^{\infty}(u_P^* w_{P+1} + u_{P+1} w_P^*)\right] = 0$$

$$(2.10) \quad \frac{\partial w_1}{\partial t} - ik\left[u_0 w_1 + u_1 w_0 + \sum_{P=1}^{\infty}(u_P^* w_{P+1} + u_{P+1} w_P^*\right]$$
$$+ \frac{\partial}{\partial z}\left[P_1 + 2w_0 w_1 + 2\sum_{P=1}^{\infty}(w_P^* w_{P+1})\right] + \phi_1 = 0$$

$$(2.11) \quad \frac{\partial \phi_1}{\partial t} - ik\left[u_0 \phi_1 + u_1 \phi_0 + \sum_{P=1}^{\infty}(u_P^* \phi_{P+1} + u_{P+1} \phi_P^*)\right]$$
$$+ \frac{\partial}{\partial z}\left[w_0 \phi_1 + w_1 \phi_0 + \sum_{P=1}^{\infty}(w_P^* \phi_{P+1} + w_{P+1} \phi_P^*)\right] - \Omega_B^2 w_1 = 0$$

$$(2.12) \quad -iku_1 + \frac{\partial w_1}{\partial z} = 0,$$

and for $n \geq 2$.

$$(2.13) \quad \frac{\partial u_n}{\partial t} - ikn\left[2u_0 u_n + \sum_{P=1}^{n-1}(u_P u_{n-P}) + 2\sum_{P=1}^{\infty}(u_P^* u_{P+n}) + P_n\right]$$
$$+ \frac{\partial}{\partial z}\left[u_0 w_n + u_n w_0 + \sum_{P=1}^{n-1}(u_{n-P} w_P)\right.$$
$$\left. + \sum_{P=1}^{\infty}(u_{P+n} w_P^* + u_P^* w_{P+n})\right] = 0$$

$$(2.14) \quad \frac{\partial w_n}{\partial t} - ikn\left[u_0 w_n + u_n w_0 + \sum_{P=1}^{n-1}(u_{n-P} w_P) + \sum_{P=1}^{\infty}(u_{P+n} w_P^*\right.$$
$$\left. + u_P^* w_{P+n})\right] + \frac{\partial}{\partial z}\left[P_n + 2w_0 w_n + \sum_{P=1}^{n-1}(w_P w_{n-P})\right.$$
$$\left. + 2\sum_{P=1}^{\infty}(w_P^* w_{P+n})\right] + \phi_n = 0$$

$$(2.15) \quad \frac{\partial \phi_n}{\partial t} - ikn\left[u_0 \phi_n + u_n \phi_0 + \sum_{P=1}^{n-1}(u_{n-P} \phi_P) + \sum_{P=1}^{\infty}(u_{P+n} \phi_P^*\right.$$
$$\left. + u_P^* \phi_{P+n})\right] + \frac{\partial}{\partial z}\left[w_0 \phi_n + w_n \phi_0 + \sum_{P=1}^{n-1}(w_{n-P} \phi_P)\right.$$
$$\left. + \sum_{P=1}^{\infty}(w_{P+n} \phi_P^* + w_P^* \phi_{P+n})\right] - \Omega_B^2 w_n = 0$$

$$(2.16) \quad -iknu_n + \frac{\partial w_n}{\partial z} = 0.$$

In addition, there are complex conjugate equations for
$n \geq 1$. A similar development, including compressibility
effects (other than through the Brünt period), was used by
Boer (1970) to examine shear flow interaction with a continu-
ous sinusoidal gravity wave source produced by forced motion
on the lower boundary. At this point no approximation has
been made, given that cyclical boundary conditions are
involved. There has also been no savings in computation
effort at this step, for if computations are made using N
coefficients, the method is equivalent to a finite difference
net using 2N horizontal points. However, R. Breeding's calcu-
lations have shown that if the source structure has a dominant
horizontal wavelength $\lambda_x = 2\pi/k$, then under most conditions
the higher harmonic coefficients corresponding to n = 2, 3,...
etc., will generally have much smaller amplitudes than the
fundamental corresponding to n = 1. For example, Figure 2
shows the production of second harmonics due to nonlinearities
using a source containing only the fundamental as calculated
by R. Breeding (1971). Even for a Richardson number of 0.53,
the second harmonic amplitude seldom reaches 15% of the funda-
mental and the third harmonic will be correspondingly less.
Therefore, a good approximation can be obtained by retaining
on the first few Fourier coefficients with a considerable
reduction in computation effort.

The simplist approximation available is to consider
the interaction between the mean horizontal flow and the first
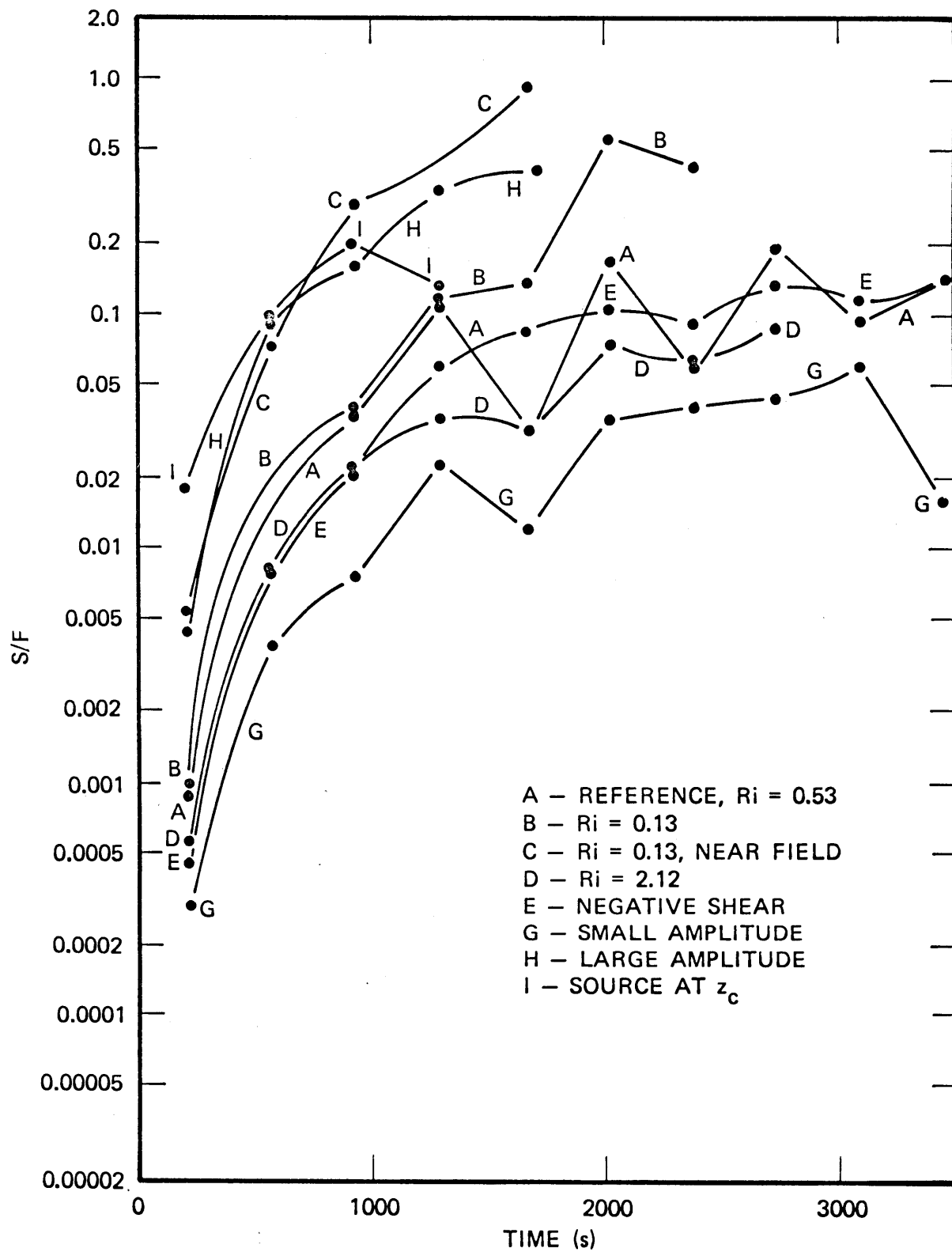
FIGURE 2

S/F, THE ABSOLUTE VALUE OF THE RATIO OF THE SECOND
HARMONIC IN u, AS A FUNCTION ABOUT 100m ABOVE z_c
(FROM BREEDING (1971))

harmonic wave field. In this case, the governing equations become:

$$(2.17) \quad \frac{\partial u_0}{\partial t} + \frac{\partial}{\partial z}\left[u_1 w_1^* + u_1^* w_1\right] = 0$$

$$(2.18) \quad \frac{\partial u_1}{\partial t} - ik\left[P_1 + 2u_0 u_1\right] + \frac{\partial}{\partial z}\left[u_0 w_1\right] = 0$$

$$(2.19) \quad \frac{\partial w_1}{\partial t} - ik\left[u_0 w_1\right] + \frac{\partial P_1}{\partial z} + \phi_1 = 0$$

$$(2.20) \quad \frac{\partial \phi_1}{\partial t} - ik\left[u_0 \phi_1\right] - \Omega_B^2 w_1 = 0$$

$$(2.21) \quad -iku_1 + \frac{\partial w_1}{\partial z} = 0 \;.$$

If u_0 is constrained to be independent of time and equal to the initial mean flow, the basic equations of linear gravity wave theory result. Thus the system of equations (2.17) - (2.21) can be interpreted in a very simple manner. The gravity waves follow the linear theory for an atmosphere which is slowly varying in time. The atmospheric variations in time result from one nonlinear equation (2.17). The time variations of the mean wind have the effect of preventing the catastrophic build-up of the wave amplitude near the critical level that linear theory predicts if the atmosphere is considered time invariant. This result was also seen in the multiple-scale analysis. In this present analysis, however, we clearly see the failing of the multiple-scale approximation.

The vertical variations of the mean wind can alter the linear wave impedance, and thus reflected waves can be set up, and these are not included in the multiple-scale approach which is a WKB type of analysis. For linear waves in a constant mean wind shear, the relative change of wave impedance per radian of vertical wavenumber if $1/R_i^{1/2}$ and is independent of actual wavelength. Thus the shortening of the vertical wave-length as one approaches the critical level does not help justify a WKB approximation, and for Richardson numbers close to or less than 1, large errors result if the reflected wave energy is ignored.

Again referring to Figure 1, we show comparisons of the results of various computational methods on predicting the mean wind variations caused by wave-wind interaction near the critical level. Solutions to equations (2.17) - (2.21) give excellent agreement with the finite difference solution of the full nonlinear equations. Again we note that the multiple scale analysis has overestimated the effect, since the wave reduction due to partial reflections was not taken into account.

B. Stream Function - Vorticity Formulation

The numerical integration of the fluid equations for incompressible Boussinesq fluids requires the reformulation of the problem in terms of a scalar stream function ψ, and a vector vorticity $\underline{\lambda}$, rather than the standard Eulerian velocity and pressure fields. Since the velocity field in an incompressible or Boussinesq fluid is divergence-free, one

introduces ψ and $\underline{\lambda}$ in terms of the horizontal fluid velocity u and vertical fluid velocity w as:

(2.22) $\quad u = -\dfrac{\partial \psi}{\partial z} \quad ; \quad w = \dfrac{\partial \psi}{\partial x}$

and

(2.23) $\quad \underline{\lambda} = \nabla_x \underline{u} = \hat{y}\left(\dfrac{\partial u}{\partial z} - \dfrac{\partial w}{\partial x}\right).$

In the case of only two velocity components, $\underline{\lambda}$ has only one component and the resulting stream function/vorticity equation is scalar:

(2.24) $\quad \dfrac{\partial^2 \psi}{\partial x^2} + \dfrac{\partial^2 \psi}{\partial z^2} = -\lambda$

where $\underline{\lambda} \equiv \hat{Y}\lambda$.

Finally, the equation of vorticity transport is developed by taking the curl of the momentum transport equation. This operation eliminates the pressure explicitly from the governing equations. This is beneficial for numerical examination of divergence - free flows, where the time derivative of the pressure is not readily available.

Employing a first harmonic vorticity λ_1 and stream function ψ_1, the basic system truncated at the first harmonic becomes:

(2.25) $\quad \dfrac{\partial u_0}{\partial t} + ik\left[\psi_1^* \lambda_1 - \psi_1 \lambda_1^*\right] = 0$

(2.26) $\quad \dfrac{\partial \phi_0}{\partial t} + ik\dfrac{\partial}{\partial z}\left[\psi_1^* \phi_1 - \psi_1 \phi_1^*\right] = 0$

(2.27) $\quad \left(\dfrac{\partial}{\partial t} - iku_0\right)\lambda_1 - ik\psi_1\dfrac{\partial^2 u_0}{\partial z^2} + ik\phi_1 = 0$

(2.28) $\quad \left(\dfrac{\partial}{\partial t} - iku_0\right)\phi_1 - ik\psi_1\left(\dfrac{\partial \phi_0}{\partial z} - \Omega_B^2\right) = 0$

(2.29) $\left(\dfrac{\partial^2}{\partial z^2} - \kappa^2\right)\psi_1 = -\lambda_1$

where $u_1 = -\dfrac{\partial \psi_1}{\partial z}$; $\omega_1 = -i\kappa\psi_1$.

The specification of the boundary condition at the ground, $z = 0$, is straightforward since ψ_1 must be a constant on a rigid surface. Further, since ψ_1 is directly proportional to the vertical velocity w_1 because of the Fourier expansion in x, then $\psi_1 = 0$ on $z = 0$. The condition at the upper boundary $z = H$, requires more care. Ideally, an outward radiation condition would be imposed; however, the use of a steady-state radiation condition will cause errors in a transient calculation; and the addition of a viscous region as considered by Yanowitch (1967) and Houghten and Jones (1968), will be computationally inefficient since an additional grid region several wavelengths in dimension must be included. Fortunately, the existence of large Richardson number shears in the upper jet stream structure resolves these upper boundary condition difficulties. Numerical results have confirmed the calculations of J. Booker and F. Bretherton (1967) that for large Richardson number shears, internal gravity waves are attenuated by approximately a factor $\exp\left[-2\pi\left(R-\tfrac{1}{4}\right)^{1/2}\right]$ as they pass through a critical level. For the case of $R_i = 4.8$, as per Figure 3, up-going gravity wave amplitudes would be attenuated by a factor of about 10^{-12}. Since very little wave energy will penetrate the upper shear, the imposition of a rigid boundary condition above the upper shear will not give rise to spurious reflections. Subsequent numerical results have substantiated this assumption. At the upper boundary the appropriate boundary value of the wave stream function is $\psi_1 = 0$ at $z = H$.

III. NUMERICAL EXPERIMENTS: WAVE-WIND INTERACTIONS FOR
TRANSIENT GRAVITY WAVE SOURCES

A. Computational Procedure

In this section we wish to examine through a series
of numerical experiments the nonlinear interaction of a
single harmonic transient gravity wave source with simple
models of the jet stream. The purpose is not to formally
invert the observed ground pressure fluctuation measurements,
but to examine the qualitative features of the interaction in
terms of the vertical distribution and strength of the source
and initial Richardson number in the source region. Of
particular interest is the wave-wind interaction in the pres-
ence of strong shear (Ri<0.5), since observed gravity waves
often appear to originate from regions of low Richardson
number.

1. The Finite Difference Equations

The equations describing the wave-wind interaction
(2.25) - (2.29) contain nonlinear coupling terms so that a
numerical approach is dictated. The finite difference approx-
imation employed here is the so-called "leap-frog" method,
which is an explicit scheme using spatial and temporal
centered differencing. Let the time spacing be δt and the
vertical spacing be δz. Then for notation purposes, define

$$(3.1) \quad \lambda(j\delta z, n\delta t) \equiv \lambda_j^n$$
$$\phi(j\delta z, n\delta t) \equiv \phi_j^n$$
$$\psi(j\delta z, n\delta t) \equiv \psi_j^n$$

$$u_0(j\delta z, n\delta t) \equiv u_{0j}^{n}$$

$$\phi_0(j\delta z, n\delta t) \equiv \phi_{0j}^{n} \;.$$

The governing finite difference approximations to equations (2.17) through (2.21) are:

(3.2) $\quad \dfrac{1}{2\delta t}\left[u_{0j}^{n+1} - u_{0j}^{n-1}\right] + ik\left[\psi_j^{n*}\lambda_j^{n} - \psi_j^{n}\lambda_j^{n*}\right] = 0$

(3.3) $\quad \dfrac{1}{2\delta t}\left[\phi_{0j}^{n+1} - \phi_{0j}^{n-1}\right] + \dfrac{ik}{2\delta z}\left[\psi_{j+1}^{n*}\phi_{j+1}^{n} - \psi_{j+1}^{n}\phi_{j+1}^{n*}\right]$

$\qquad -\dfrac{ik}{2\delta z}\left[\psi_{j-1}^{n*}\phi_{j-1}^{n} - \psi_{j-1}^{n}\phi_{j+1}^{n*}\right] = 0$

(3.4) $\quad \dfrac{1}{2\delta t}\left[\lambda_j^{n+1} - \lambda_j^{n-1} - 2ik\delta t\, u_{0j}^{n}\lambda_j^{n}\right] + ik\phi_j^{n}$

$\qquad -\dfrac{ik}{(\delta z)^2}\psi_j^{n}\left[u_{0j+1}^{n} + u_{0j-1}^{n} - 2u_{0j}^{n}\right] = 0$

(3.5) $\quad \dfrac{1}{2\delta t}\left[\phi_j^{n+1} - \phi_j^{n-1} - 2ik\delta t\, u_{0j}^{n}\phi_j^{n}\right] + ik\Omega_B^2\psi_j^{n}$

$\qquad -\dfrac{ik}{2\delta z}\psi_j^{n}\left[\phi_{0j+1}^{n} - \phi_{0j-1}^{n}\right] = 0$

(3.6) $\quad \psi_{j+1}^{n+1} - 2\left(1 + \dfrac{(k\delta z)^2}{2}\right)\psi_j^{n+1} + \psi_{j-1}^{n+1} = -(\delta z)^2\lambda_j^{n+1}.$

The last equation is solved at the end of each iteration as a boundary value problem with $\psi_1^{n+1} = \psi_{JMAX}^{n+1} = 0$, where j = 1 and j = J MAX are the end points of the finite difference grid. Two other approaches to solving the stream function-vorticity equation involve an integral method using Green's functions and a transform method using Fast Fourier Transform (FFT) techniques. Solution of the tridiagonal system (3.6) and the FFT method are about equal in computing time, whereas the Green's function method is much slower. The

FFT method is, in principle, more accurate than the second-order difference approach given in equation (3.6). However, a fourth-order differencing scheme,

$$(3.7) \quad \left(1 - \frac{(K\delta z)^2}{2}\right)\left[\psi_{j+1}^{n+1} + \psi_{j-1}^{n+1}\right] - 2\left(1 - \frac{5(K\delta z)^2}{12}\right)\psi_j^{n+1}$$
$$= -\frac{(\delta z)^2}{12}\left[\lambda_{j+1}^{n+1} + 10\lambda_j^{n+1} + \lambda_{j-1}^{n+1}\right]$$

gives much better accuracy with only a slight increase in computing cost over the use of the FFT. All three methods were tested in practice and gave quite similar results. In the case of very low Richardson number shears, the fourth-order scheme was used because of the short wavelengths involved.

2. Convergence, Stability and Grid Dispersion

Of fundamental importance in applying finite difference approximations to the solution of partial differential equations are the questions of convergence, numerical stability and accuracy. When dealing with wave propagation phenomena, lack of accuracy of the solution usually manifests itself as grid dispersion. Unfortunately, analysis of these effects is limited to a linear, point-wise approach. The global analysis of a given finite difference scheme is fully as difficult as solving the originally partial differential equation.

To examine the point-wise characteristics of the difference equations it is useful to derive the governing finite difference dispersion relation. Since this is a local analysis, let ϕ_{0j}^n = constant and $U_{0j}^n = \bar{U}$ = constant.

This is not a limitation in terms of the derived stability criteria, but greatly simplifies the algebra. Consider plane wave solutions for the field variables as:

$$(3.8) \quad \lambda_j^n = \hat{\lambda} e^{i\Theta(j,n)}$$
$$\phi_j^n = \hat{\phi} e^{i\Theta(j,n)}$$
$$\psi_j^n = \hat{\psi} e^{i\Theta(j,n)}$$

where $\Theta(j,n) = (\omega\delta t)n + (\ell\delta z)j$ is the phase, and $(\omega\delta t)$ and $(\ell\delta z)$ are the normalized frequency and vertical wave-numbers respectively. Substituting into equations (3.4), (3.5) and (3.6) and defining,

$$(3.9) \quad \alpha \equiv \ell\delta z \;,\; \beta^2 \equiv \frac{(\kappa\delta z)^2}{2} \;,\; A \equiv \sin(\omega\delta t) - \kappa\delta t\bar{U}$$

gives, in matrix form

$$(3.10) \quad \begin{bmatrix} A & \kappa\delta t & 0 \\ 0 & A & -\kappa\delta t\Omega_B^2 \\ \beta^2/\kappa & 0 & (1+\beta^2-\cos\alpha) \end{bmatrix} \begin{bmatrix} \hat{\lambda} \\ \hat{\phi} \\ \hat{\psi} \end{bmatrix} = \begin{bmatrix} 0 \\ 0 \\ 0 \end{bmatrix}.$$

Setting the determinant in (3.10) to zero yields the dispersion relation,

$$(3.11) \quad \sin(\omega\delta t) = \kappa\delta t\bar{U} \pm \frac{\beta\delta t\Omega_B}{\sqrt{\beta^2+(1-\cos\alpha)}} \;.$$

In the limit that $\delta t, \delta z \to 0$ (3.11) becomes

$$(3.12) \quad \omega = \kappa\bar{U} \pm \frac{\kappa\Omega_B}{\sqrt{\kappa^2+\ell^2}}$$

which is exactly the dispersion relation for the continuum

equations. Convergence is therefore established, at least on a point-wise basis.

The wave solutions described by the finite difference dispersion relation will, in general, differ from those of the continuum case. In certain instances, completely extraneous wave modes arise which correspond to complex frequencies. Since these modes will occur as complex conjugate pairs, the exponentially growing mode leads to numerical instability. From equation (3.11), unconditional stability requires that $\sin(\omega \delta t) \leq 1$ for all wavenumbers α. The maximum value of $\sin(\omega \delta t)$ will occur at $\cos \alpha = 1$ for the plus root:

$$(3.13) \quad \text{Max.} \left[\sin(\omega \delta t) \right] = \delta t (\kappa \bar{U} + \Omega_B).$$

The requirement on the time step δt for unconditional local stability is then

$$(3.14) \quad \delta t \leq 1 / (\kappa \bar{U} + \Omega_B).$$

Grid dispersion in a finite difference scheme arises because the stable modes of (3.11) corresponding to a wavenumber-frequency pair are not equal to the same wavenumber-frequency pair in (3.12) for finite δt, δz. Subsequently, the phase velocity of a given mode will also differ from that of the continuum, and in general this correspondence will vary as a function of wavenumber and propagation angle. Therefore, superimposed on the wave dispersion of the continuum system will be a propagation-angle dependent numerical or grid dispersion. The loss of accuracy resulting from grid dispersion is inherent in all finite difference approximations

and can only be minimized, with the lower bound on grid spacing usually determined by computation cost. All numerical computations were done with a step size of $\delta z = 25m$ in regions where short wavelengths are expected, such as near critical levels and source regions. Reasonable accuracy is then expected for wavelengths greater than about 100m. with only moderate to poor resolution for shorter wavelengths.

B. Basic Jet Stream and Gravity Wave Source Models

For use in the numerical experiments a basic jet stream mean flow model was employed. The initial jet stream velocity profile was assumed to be uniform in the horizontal plane with a vertical wind profile. The direction of the mean wind was chosen to coincide with the x-axis. The general model is shown in Figure 3, which is divided into three regions. Region II is taken to be 2.0 km wide centered about the source. The source subregion itself will range in width from about 125 m to 550 m. Region I extends from the ground to a height of 4.0 km. The remainder of the jet and computational grid is contained in Region III with an initial jet core speed of 50 m/s. Except for the source subregion, the Richardson number in the lower and upper shears is fixed for all models at $R_{i_{II}} = 0.925$ and $R_{i_{III}} = 4.80$ respectively. The source subregion is centered at 5.0 km and the width and initial Richardson number are specified for each model. All shears are initially taken to be linear.

The basic structure of the jet stream model was developed from examination of typical Weather Bureau balloon

MODEL JET STREAM PROFILE
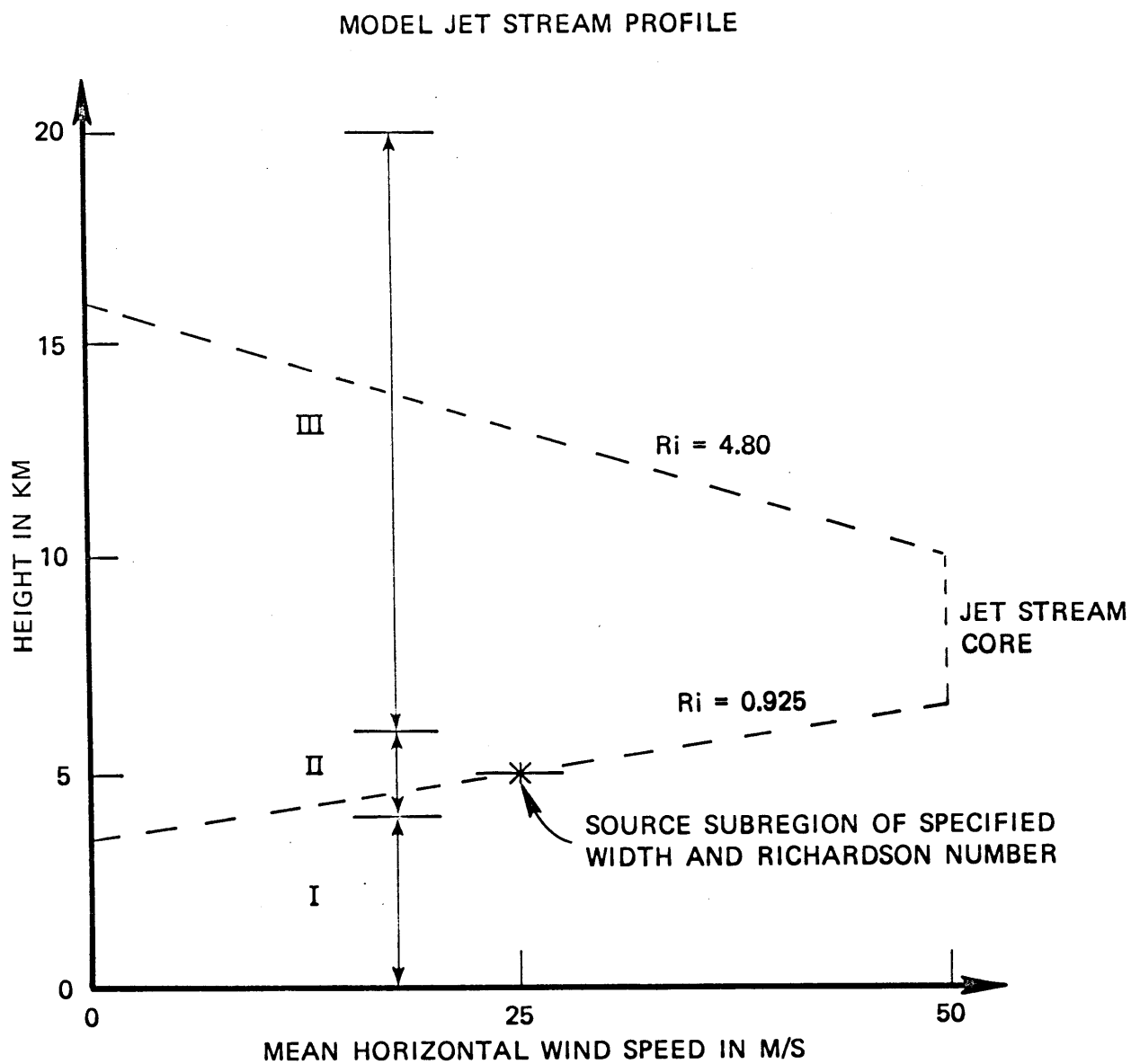
FIGURE 3

SCHEMATIC OF MODEL JET STREAM PROFILE
INCLUDING REGIONAL AND SOURCE SUBREGIONAL
CONFIGURATION

measurements over Nantucket Island. In general, the balloon measurements indicate the jet stream velocity profile to be quite symmetrical; however, because of the change in the temperature lapse rate above the jet core, a higher Richardson number results in the upper sheared region. Therefore, in order to use a constant Brünt frequency model in the calculations, the shear in the upper region has been decreased so as to yield an appropriate value for the Richardson number.

The simplest source models which will retain the essentials of the nonlinear interaction between finite amplitude gravity waves and the mean jet stream flow are those containing only the first harmonic component of the general horizontal Fourier expansion described in Section II. The general form of the numerical experiments is to specify a gravity wave source structure implanted in the model jet stream flow as an initial condition. The behavior of the model is then governed by the finite difference equations (3.2) - (3.6), which describe the interaction of the zeroth and first harmonic terms.

The development of theoretical atmospheric gravity wave source models represents a very difficult problem in its own right. A recently developed approach to gravity wave source generation by wave-wave interaction will be discussed in Section IV. However, at this point a more heuristic approach will be taken. Although the specific choice of a model is admittedly arbitrary, there are constraints on physical grounds and in terms of linear theory behavior.

Gravity wave-wind interactions essentially only exist around
a narrow region about the critical level. Therefore it is
reasonable to locate the source at a critical level and
require it to rapidly decay away with distance. Linear
theory shows that the horizontal wave-wind velocity has
opposite signs on different of the critical level. Further,
the vertical wave-wind velocity must go to zero at the crit-
ical level while the horizontal wave-wind velocity becomes
discontinuous with infinite amplitude. Any source model
should approach these limits as the amplitude of vertical
velocity and the source width go to zero for a source of
fixed total energy.

Under these constraints, a simple source model is
chosen with a Gaussian distributed stream function:

$$(3.15) \quad \psi_1(x, z, t=0) = 2A e^{-\alpha^2 (z-z_c)^2} \cos kx .$$

The associated velocity field is:

$$(3.16) \quad w_1(x, z, t=0) = -2Ak e^{-\alpha^2 (z-z_c)^2} \sin kx$$

$$(3.17) \quad u_1(x, z, t=0) = 4\alpha^2 A(z-z_c) e^{-\alpha^2 (z-z_c)^2} \cos kx.$$

If we consider the limit as $A \to 0$ and $\alpha \to \infty$, the con-
straint of constant total source energy requires $A^2 \alpha$ = con-
straint, then $w \to \alpha^{-1/2}$ and $u \to \alpha^{3/2}(z-z_c)$, so that linear
theory behavior at the critical level is obtained.

Wave and Wind Energy Calculations

In a Boussinesq fluid, the conservation of energy is given as

$$(3.18) \quad \frac{\partial E}{\partial t} + \frac{\partial}{\partial x}(uE) + \frac{\partial}{\partial z}(wE) = 0$$

where u and w are the total horizontal and vertical veloci-ties, and E is the total energy density. Expressing E in terms of the field variables, u, w, ϕ and P, we have:

$$(3.19) \quad E = \frac{1}{2}\left[u^2 + w^2 + \phi^2/\Omega_B^2\right] + P$$

(recalling that P = pressure/mean density).

If we consider the total Eulerian field to be com-posed of a mean flow and finite amplitude single harmonic wave, the total energy density averaged over a horizontal wavelength is

$$(3.20) \quad \langle E \rangle_x = \frac{1}{2}U_0^2(z,t) + u_1u_1^* + w_1w_1^* + \phi_1\phi_1^*/\Omega_B^2 \ .$$

The equation of energy conservation for this system is obtained from averaging (3.18):

$$(3.21) \quad \frac{\partial}{\partial t}\langle E \rangle_x + \frac{\partial}{\partial z}\langle wE \rangle_x = 0$$

or equivalently,

$$(3.22) \quad \frac{\partial}{\partial t}\langle E \rangle_x + \frac{\partial}{\partial z}\left[u_0(w_1u_1^* + w_1^*u_1) + (P_1w_1^* + P_1^*w_1)\right] = 0.$$

One can easily demonstrate that the energy conservation form developed directly from the zero and first harmonic expansion equations yield an identical result. Integrating

(3.21) over z from 0 to H gives

$$(3.23) \quad \frac{\partial}{\partial t} \int_0^H dz \langle E \rangle_x + \langle wE \rangle_x \Big|_0^H = 0.$$

If we assume rigid surfaces to exist at z = 0 and z = H, then the vertical velocity must vanish there. Therefore,

$$(3.24) \quad \frac{\partial}{\partial t} \int_0^H dz \langle E \rangle_x = 0$$

and the total integrated energy per wavelength must be a constant over time in such a closed system. The behavior of the computed total system energy as a function of time provides one of the constraints on the global behavior of the finite difference scheme.

It will be useful in the analysis of the numerical experiments to examine the behavior of wave and wind components of the total energy as a function of time in each of the three regions of the model.

Since the total kinetic energy of the mean wind is very large with respect to the other components of the total energy, it is useful to redefine the total system energy excluding the total wind kinetic energy at t = 0. Changes in the wind energy will then be reflected by alterations in the mean flow caused by wave-wind interactions. Under this definition, the total energy of the system will be equal to the total source energy at t = 0. Using this definition, the wave and wind energy densities are from (3.20).

$$(3.25) \quad \langle E \rangle_x \Big|_{WIND} = \bar{U}(z) \Delta u(z,t) + \frac{1}{2} (\Delta u(z,t))^2$$

$$(3.26) \quad \langle E \rangle_x \big|_{WAVE} = u_1 u_1^* + w_1 w_1^* + \phi_1 \phi_1^* / \Omega_B^2$$

where $\bar{U}(z) = U_0(z, t=0)$ and $\Delta u(z,t)$ is the time-varying change in the mean wind.

To determine the total energy input to each model we need the total source energy. Since the energy decays away from the critical level as $e^{-\alpha^4 (z-z_s)^4}$ and the source width is at most a few hundred meters, the integration interval 0 to H = 20 km can be extremely well approximated by $(-\infty, \infty)$. In this case the source energy at t = 0 is

$$(3.27) \quad E_0 = \langle E \rangle_x \big|_{WAVE} (t=0) = \sqrt{\frac{\pi}{2}} \frac{A^2}{\alpha} (\alpha^2 + \kappa^2).$$

The total system energy and the source width parameter α can be used as input parameters to completely describe the source model.

C. Transient Behavior of Finite Amplitude Gravity Wave Sources in Low Richardson Number Shears

The gravity wave source and jet stream models to be examined numerically will have the following fixed and variable parameters.

Fixed parameters for all models:

(1) Jet stream mean flow structure excepting the source subregion:

(a) upper shear R_i = 4.800

(b) lower shear R_i = 0.925

(c) jet core speed 50 m/s

(2) Source centered at 5.0 km.

(3) Wind speed at source initially 25 m/s.

(4) Brünt period   300 s.

(5) Horizontal wavelength   10 km.

Variable parameters:

(1) Total source energy E_o at t = 0.

(2) Source width at t = 0.

(3) Richardson number of source subregion at t = 0.

Specific models given in figures:

MODEL A at t = 0

R_i = 0.200

width = 318 m

peak wave velocities

   horizontal = 0.085 m/s

   vertical   = 0.010 m/s

MODEL B at t = 0

R_i = 0.250

width = 318 m

peak wave velocities

   horizontal = 0.85 m/s

   vertical   = 0.10 m/s

MODEL C at t = 0

R_i = 0.500

width = 318 m

peak wave velocities

   horizontal = 0.85 m/s

   vertical = 0.10 m/s

MODEL D at t = 0

R_i = 0.500

width = 136.5 m

peak wave velocities

    horizontal = 1.30 m/s

    vertical   = .066 m/s

MODEL E at t = 0

R_i = 0.500

width = 273 m

peak wave velocities

    horizontal = 0.92 m/s

    vertical   = 0.092 m/s

MODEL F at t = 0

R_i = 0.500

width = 546 m

peak wave velocities

    horizontal = 0.64 m/s

    vertical   = 0.13 m/s

The phenomena observed during the wave-jet interaction will be discussed in terms of the time-energy curves given in Figures 4 through 7. The detailed vertical distribution of wave and wind velocities in regions I and II for Model A are given as a function of time in Appendix C. The energies shown refer to the integrated energy densities within each of the three regions shown in Figure 3. The time-energy curves give spatially integrated values for both the wave motion and changes in the mean wind structure, whereas the time-net energy curves refer to the total system energy integrated over each region.
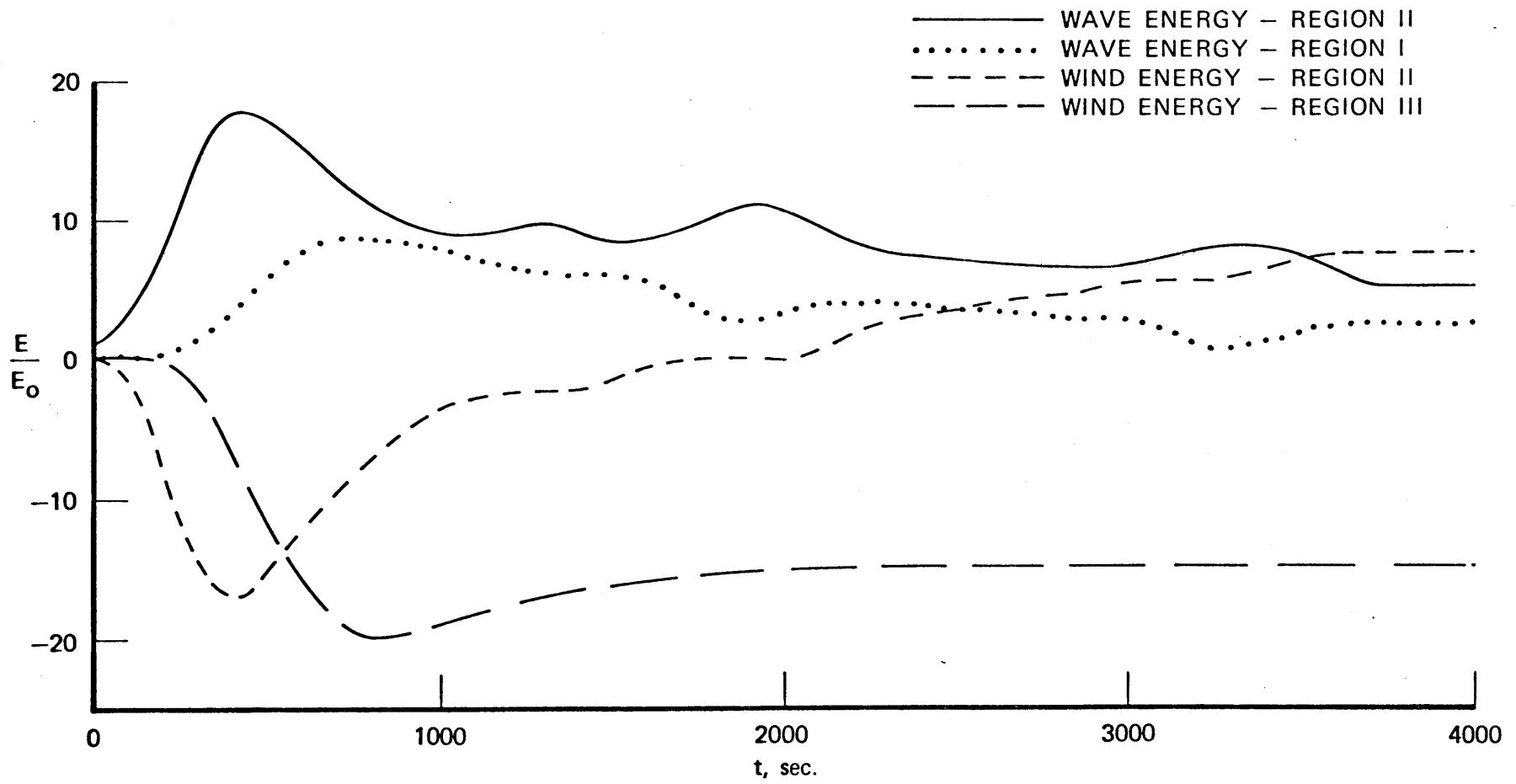
FIGURE 4

TIME ENERGY CURVES FOR MODEL A
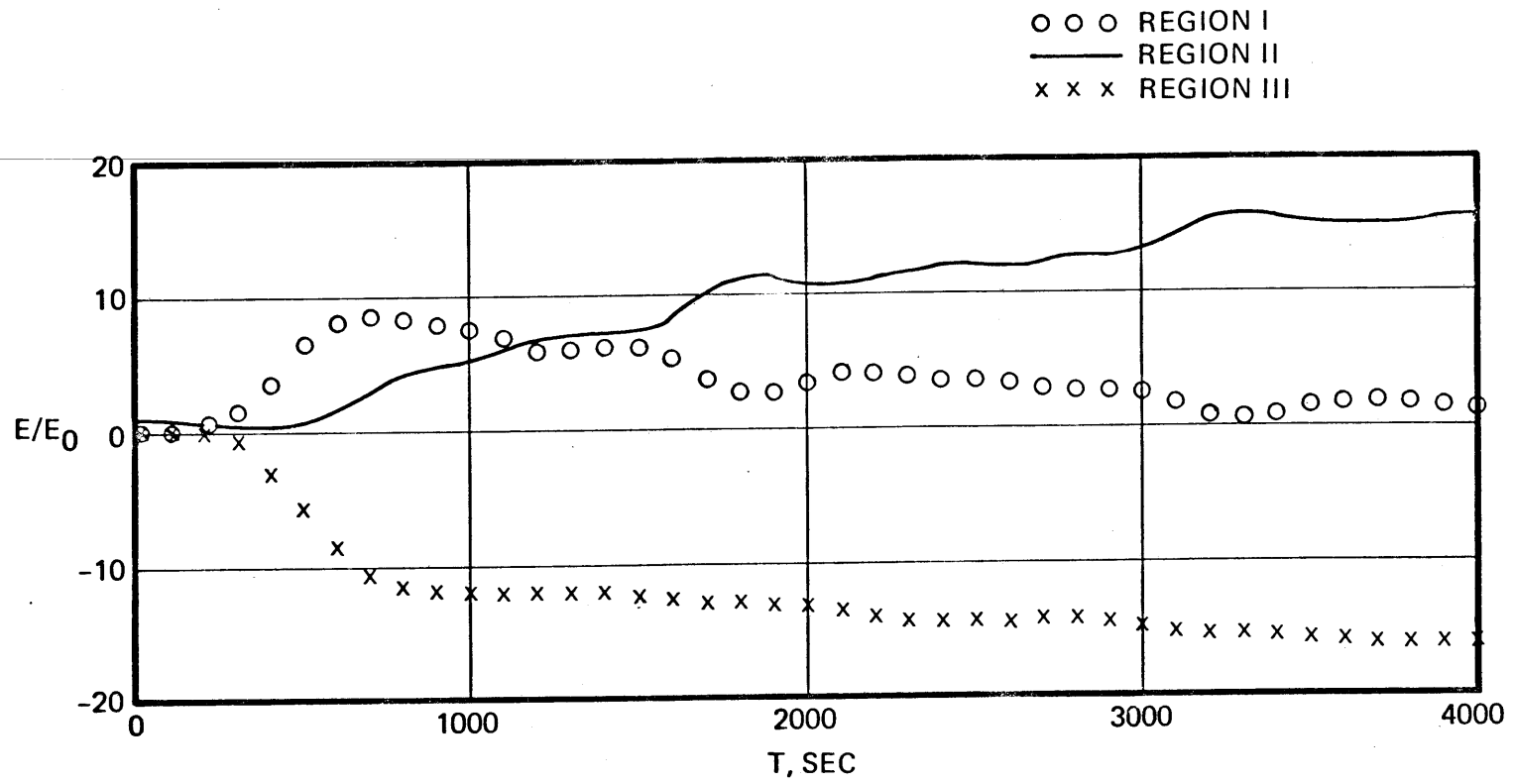
FIGURE 5
TIME — NET ENERGY CURVES FOR MODEL A

MODEL B R_i = .250

MODEL C R_i = .500

$\frac{E}{E_o}$

0   1000   2000

t, sec.
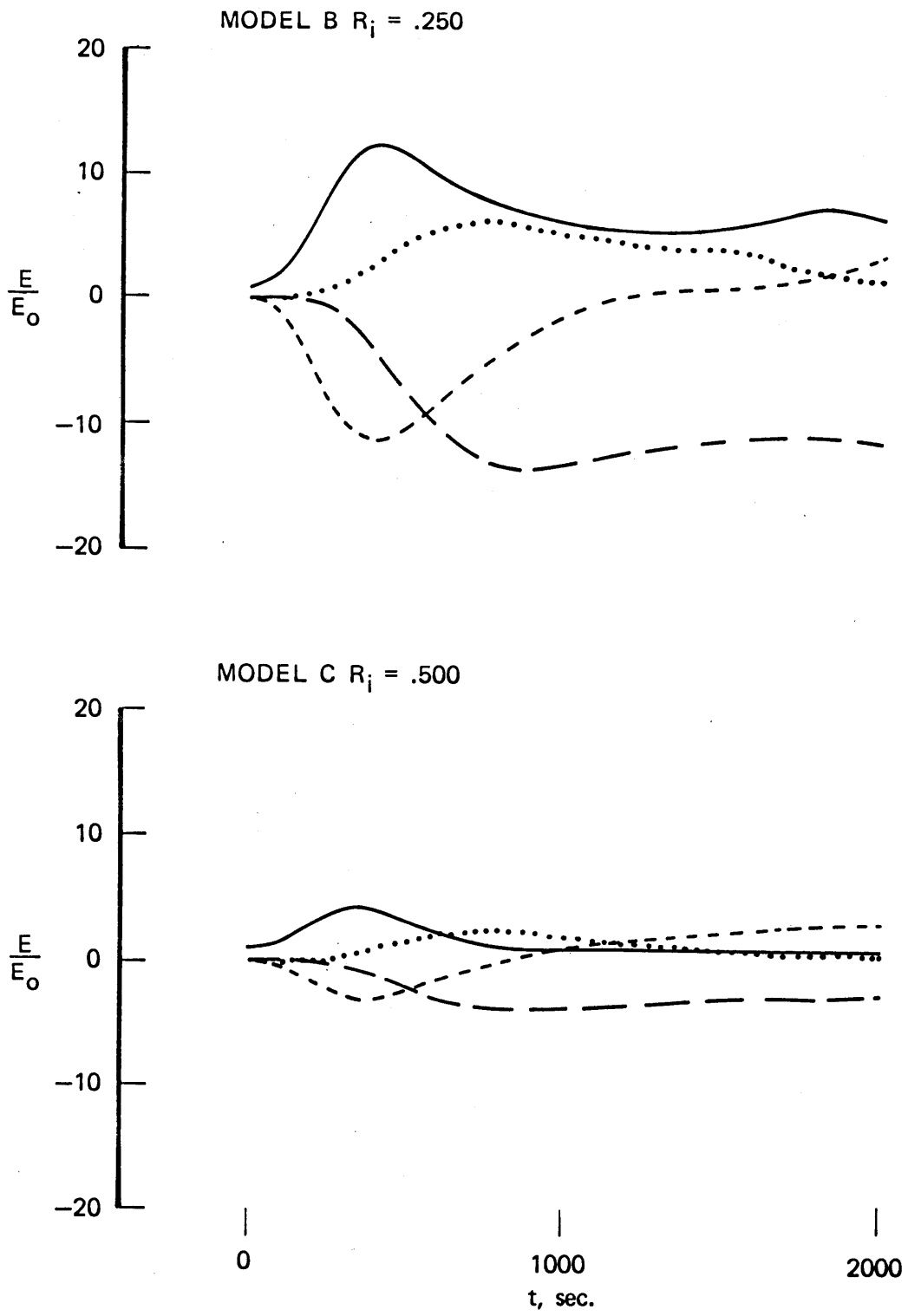
FIGURE 6

TIME ENERGY CURVES — RICHARDSON NUMBER EFFECTS

MODEL D WIDTH = 136.5 m

MODEL E WIDTH = 273.0 m

MODEL F WIDTH = 546.1 m
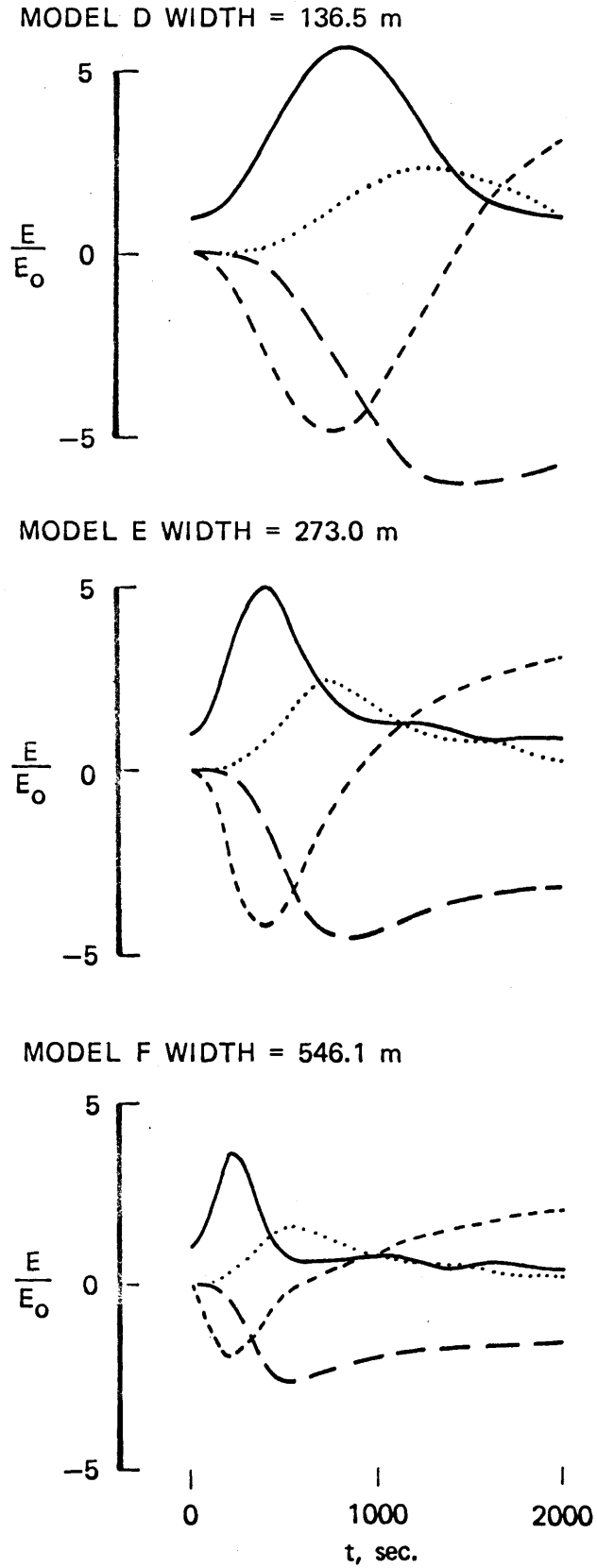
FIGURE 7

TIME ENERGY CURVES — SOURCE WIDTH EFFECTS

All energies shown are normalized to the total integrated input source energy, E_o, at t = 0. Wind energies then refer to changes from the mean flow state at t = 0. The boundary conditions of ·the jet model require that the total system energy integrated over the entire model remain constant and provides an estimate of cumulative truncation effects of the finite difference solution. A maximum deviation of eight percent from the condition of constant total system energy was observed after 400 time steps for the case of R_i = .200. The total system energy typically oscillated about a slowly decreasing mean value. The period of the oscillations was about 100 time steps with an amplitude of less than $0.01E_o$. The mean value decreased as a function of the number of time steps as very short wavelength disturbances are dissipated by the finite difference scheme. The total system energy after 200 time steps (= 2000 s in model time) ranged from $E = .995E_o$ for R_i = 0.925 to $E = .97E_o$ for R_i = 0.200.

Results:

The initial interaction in the source region extracts considerable wave energy at the expense of the wind. The amount of wave amplification increases dramatically with decreasing Richardson number as seen in the time-energy curves, but is observed in all cases even when the Richardson number was greater than 0.25. As the wave energy in the source region nears a maximum, substantial gravity wave energy is being radiated away from the region as observed from the increase in wave energy in region I. Approximately

equal amounts are radiated up the jet and toward the surface.
Waves traveling up the jet transport negative momentum and
will decrease the wind in the region about the topside criti-
cal level. Waves traveling toward the surface are carrying
positive momentum.

Until the return to the source region of ground
reflected wave energy, the net energy in the source region
declined slightly but remains near its initial value of E/E_o
= 1.0. The two-way travel time from the source critical level
for the surface reflection can be shown to be approximately
700 s on the basis of linear calculations, and at about this
time the net energy in the source region is rising rapidly.
Since the ground reflected waves are moving faster than the
wind as they approach the critical level, they are carrying
positive momentum and will increase the mean wind and net
energy in the source region on being absorbed.

Waves traveling up the jet are moving slower than
the wind as they approach the topside critical level so
$\partial E/\partial t < 0$ in this region. If no secondary sources are gener-
ated and no additional gravity waves are emitted from the
source region, the net energy in Region III will approach a
negative constant as wave motions are converted to mean flow
deformations. For $R_i > .25$ this was the observed process,
however at lower Richardson numbers secondary sources do
result with subsequent gravity wave radiation into Regions I
and III. For Model A this process is observed in Figure 5
with slight increases in Region I and corresponding decreases
in Region III being seen at t = 1400 s. Additional secondary

radiation occurs at t = 2100 and t = 3400, although the system remains stable with each subsequent radiation process being less energetic than its predecessor. The radiation, reflection and reabsorption processes will continue until virtually all wave motion has been converted to mean flow deformations through the efficient gravity wave - mean flow coupling mechanism at the source and topside critical levels.

Of particular interest is the amount of energy transport provided by the gravity wave coupling of the topside and source region critical levels. The amount of net energy transport from the critical level at the top of the jet to the source region critical level is shown in Figure 9 and is a strong function of the initial source subregion Richardson number. For the case of R_i = 0.200, 16 energy units per unit of input have been transported from the top of the jet to the source region. Even for a Richardson number of 0.500, the energy transport is three times that of the source input.

For a fixed initial total source energy, the effect of decreasing the width is to increase the efficiency of the energy transport process and lengthen the time scale of the interaction. The time scale of the interaction can be seen from Figure 6 to be directly proportional to 1/width. For instance, the wave energy maximum in the source region occurs at 900, 450 and 225 s for corresponding widths of 136.5, 273.0 and 546.1 m.

The effect of absolute wave amplitudes on the system behavior is approximately linear. Shown in Figure 8 is the source region wave amplification as a function of initial

source input energy for a fixed width of 318 m.. The net
energy transport also shows a slight, but definite increase
with increasing source energy input. However, the ampli-
tude behavior is essentially linear over decade variations in
input energy. For very large source wave amplitudes (greater
than 10 m/s), rapid and large variations in the mean wind
can occur with subsequent Richardson number reduction to
below 0.10 and generation of short vertical wavelength dis-
turbances. Neither of these effects can be dealt with accu-
rately by the current numerical procedure and probably
invalidate the initial assumption of a single component - mean
flow interaction model. The maximum wave amplitudes success-
fully modelled were observed to be less than 8 m/s in the
source region.

Of fundamental importance is the magnitude of wave
velocities in the source region necessary to produce the peak
to peak pressure fluctuations observed at the ground. Typi-
cal measurements of jet stream associated gravity waves in
eastern Massachusetts show peak to peak pressure amplitude
variations of 0.1 to 0.5 millibars, although disturbances
occasionally 1.0 mb or greater in amplitude are observed.
Shown in Figure 10 are the calculated peak to peak ground
pressure amplitudes as a function of the maximum rms wave
velocity in the source region for models with varying initial
source subregion Richardson numbers. The observed 0.2-0.5 mb
pressure amplitudes are being produced by source region wave
velocities of 1-2 m/s which are well within the limitations
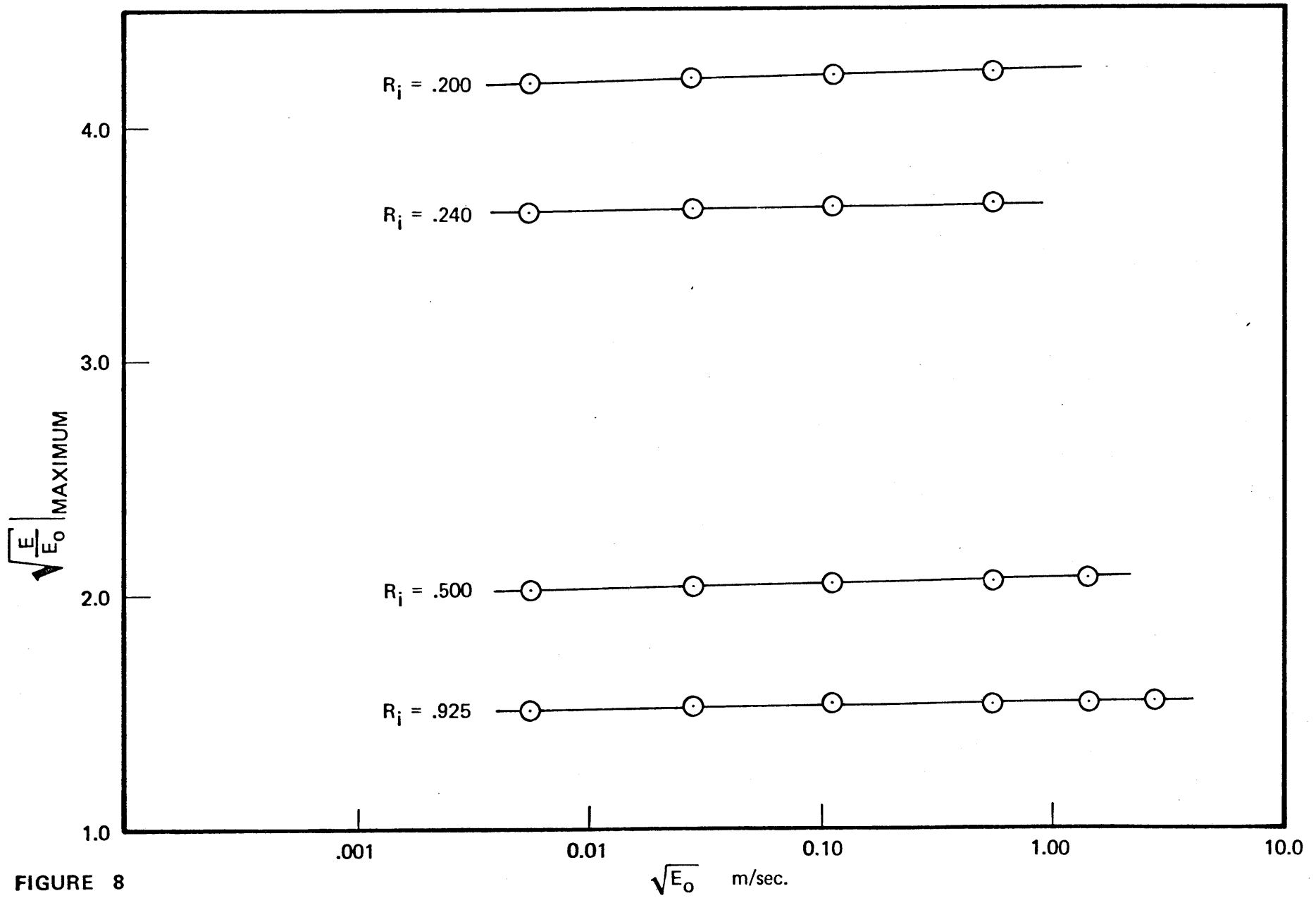
FIGURE 8

SOURCE REGION WAVE ENERGY:
AMPLIFICATION FACTOR vs.
MEAN INITIAL ENERGY DENSITY
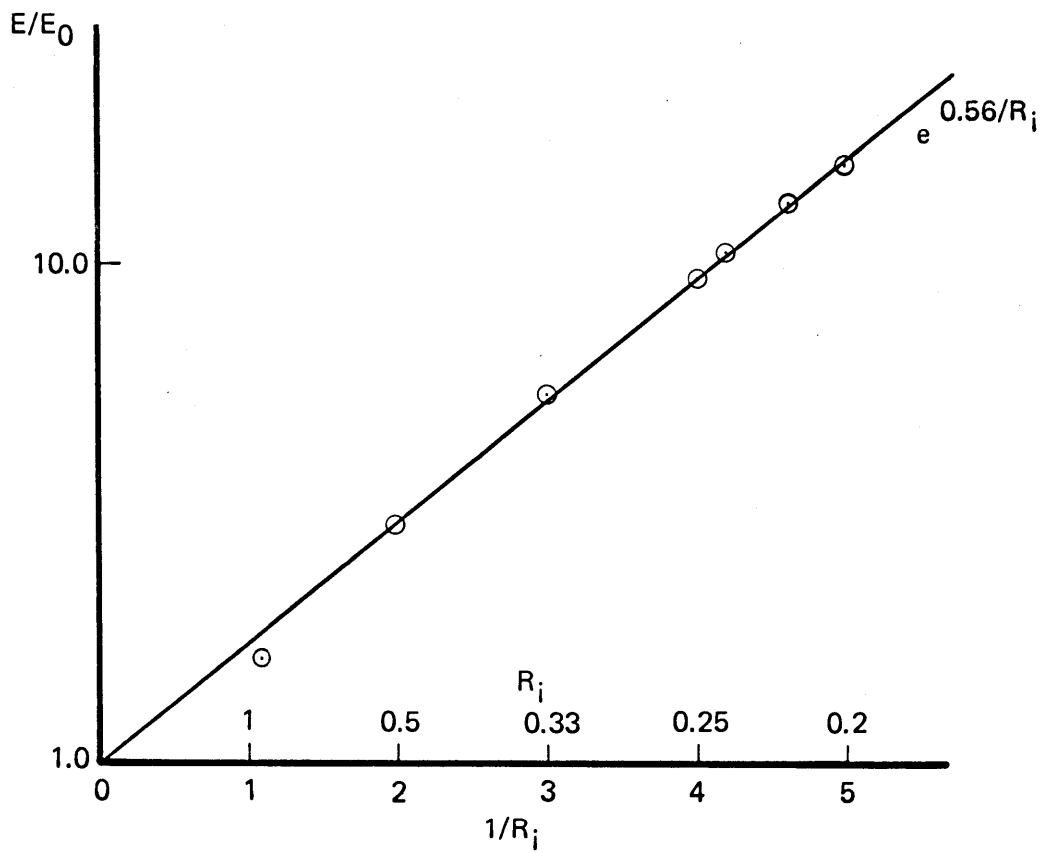
FIGURE 9
NET ENERGY TRANSPORT BY GRAVITY WAVES AS A FUNCTION
OF SOURCE SUBREGION RICHARDSON NUMBER
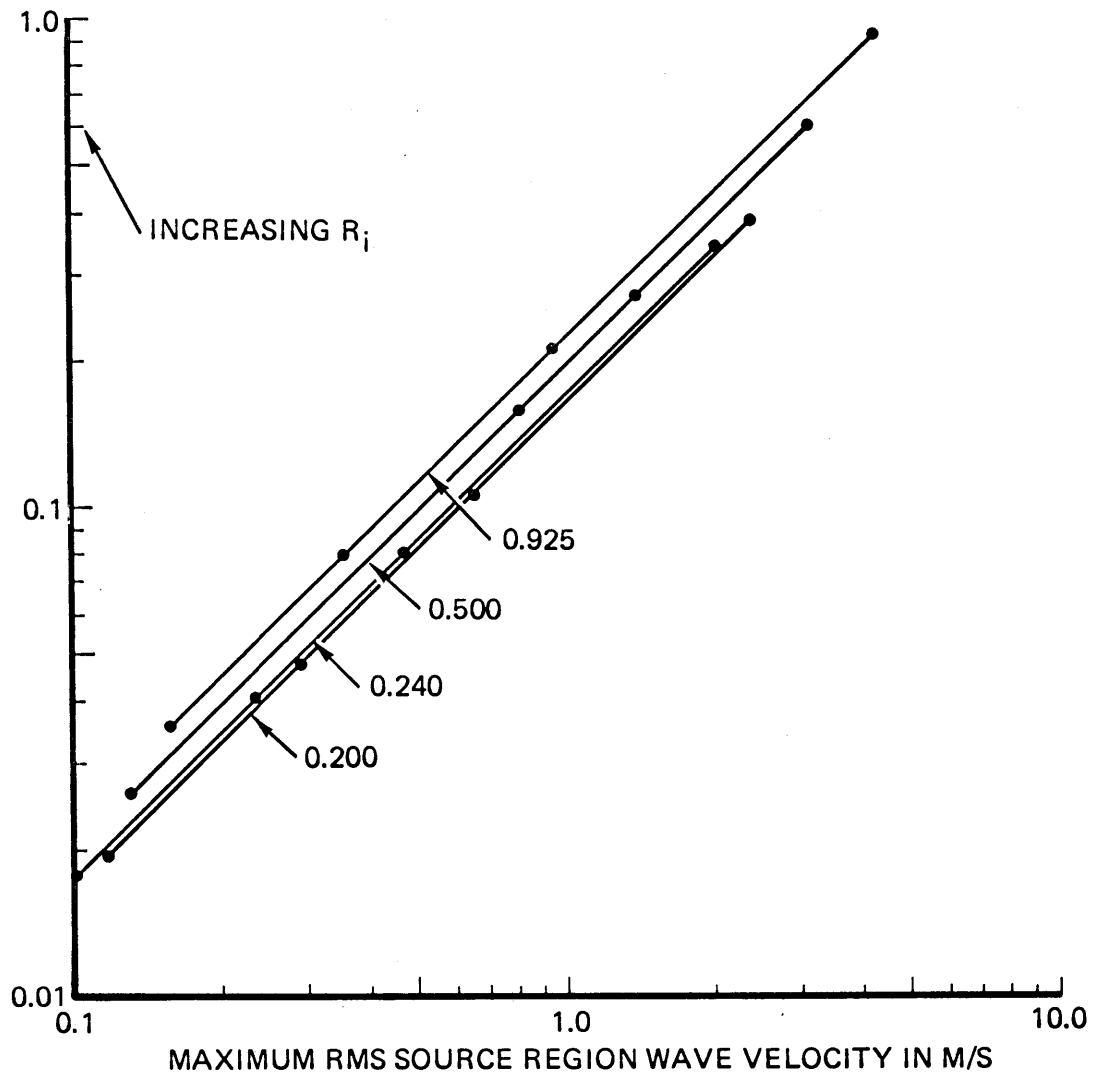
FIGURE 10
PEAK-PEAK GROUND PRESSURE FLUCTUATIONS IN MB

of the model. The increase in transmission efficiency for
higher Richardson number is due to the relative decrease in
the partial reflections in the source region resulting from
reduced impedance change per wavelength.

IV. THE DEVELOPMENT OF JET STREAM GRAVITY WAVE SOURCES BY
WAVE-WAVE INTERACTIONS

A. Introductory Remarks

The results developed thus far describe the propaga-
tion effects and energy transport in the jet stream due to
single harmonic finite amplitude gravity wave sources. The
question of the origin of natural jet stream sources has been
left unanswered. In this section we will discuss a possible
mechanism for the generation of such gravity wave sources.

Observational information shows a strong correlation
between horizontal phase velocities of gravity wave pressure
fluctuations at the ground and jet stream velocities in
regions of low Richardson number (Claerbout, 1967). A natural
mechanism would seem to be the amplification of small dis-
turbances due to dynamic instability in regions of the jet
stream where the Richardson number falls below 0.25. A large
body of literature exists on the instability of shear flows to
small perturbations within the appropriate range of horizontal
wavenumbers and Richardson numbers (see References). However,
the wavenumber dependence of instability is such that expon-
entially growing waves in the jet stream source regions will
have periods less than the Brünt period and are essentially
trapped within the jet stream. Typical power spectra of
ground pressure fluctuations show a sharp cutoff for periods
less than the Brünt period (Fig.11). The dominant observed
periods correspond to waves which are predicted by linear
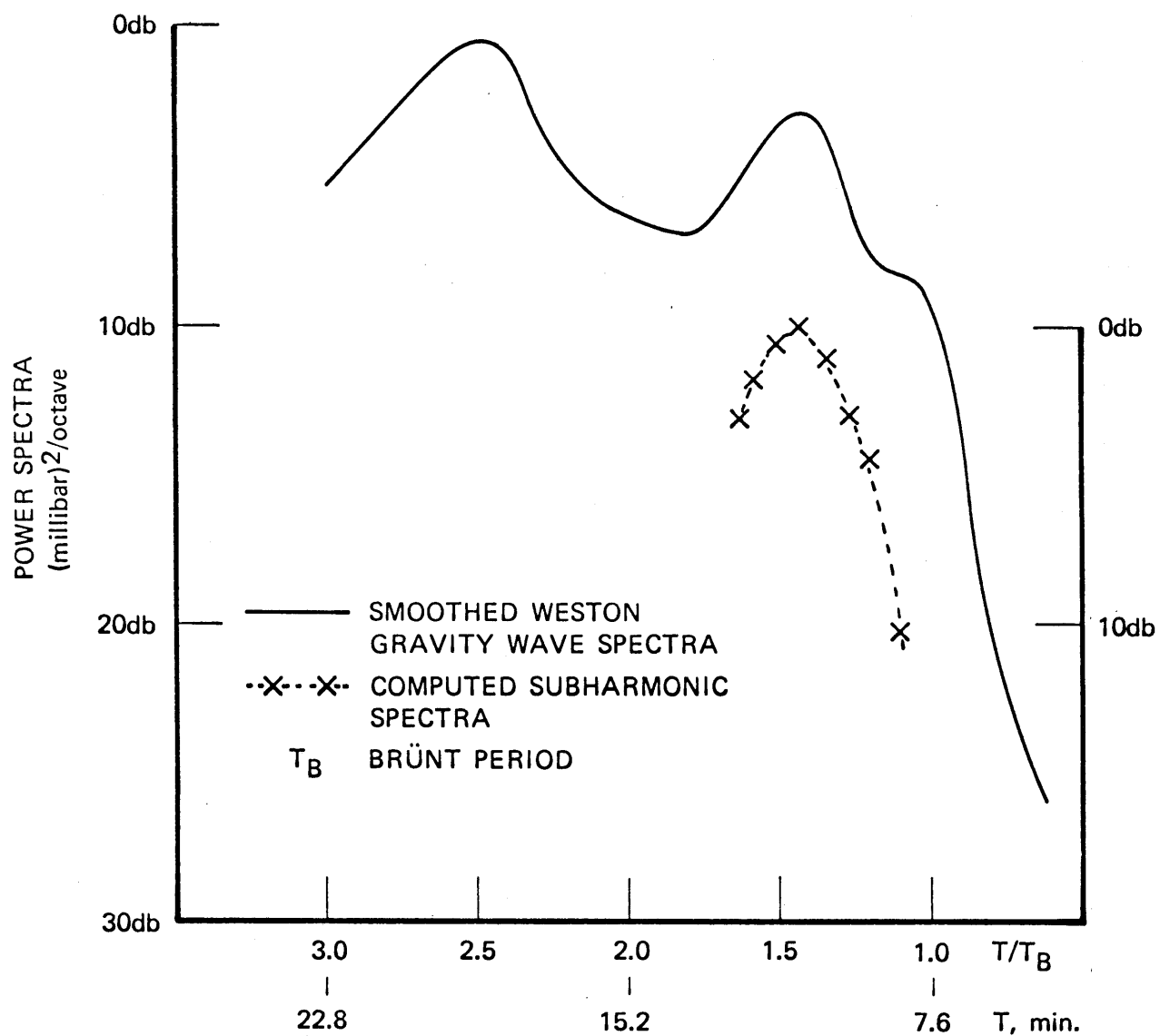
FIGURE 11

SMOOTHED TYPICAL GRAVITY WAVE SPECTRA (NORMALIZED)
OBSERVED AT WESTON, MASS. AND THEORETICAL VALUES FROM
SUBHARMONIC GENERATION.

stability theory to be stable in source regions even if the Richardson number is less than 0.25. These observational difficulties can be resolved through a wave-wave interaction mechanism.

B. Brief Review of Linear Stability Theory

The infinitesimal stability of inviscid, parallel, stratified shear flows is an area of extensive study in fluid mechanics and applied mathematics. Using a single Fourier component of the vertical perturbation velocity w(z), with horizontal wavenumber k, the linear stability of the flow is governed by the Taylor-Goldstein equation in the Boussinesq approximation,

$$(4.1) \quad \frac{d^2 w}{dz^2} + w\left[\frac{\Omega_B^2}{(v(z)-c)^2} - \frac{d^2 v/dz^2}{v(z)-c} - k^2\right] = 0$$

where v(z) is the mean flow and C the horizontal phase speed. Together with appropriate boundary conditions, it defines an eigenvalue problem for C given K, or vice-versa, for a specified mean flow v(z) and Brünt frequency Ω_B.

Often of particular importance is the calculation of "neutral curves," which for a given value of $R_e(C)$ divide the $I_m(C)$-Richardson number plane into regions of stability ($I_m(C) > 0$, say) and instability ($I_m(C) < 0$, say). There are mathematical subtleties. However, for asymmetric flows, it can be shown that the neutral curves separate simply-connected regions (Miles, 1961, 1963). Separate flows have been examined in the literature (Collyer (1970), Drazin and Howard (1966), Hazel (1972), Maslowe and Kelly (1971); however, for

the sake of explicitness the remainder of the chapter will concentrate on the hyperbolic tangent mean velocity profie.

Stability of the Hyperbolic Tangent Mean Wind Profile with Constant Brünt Frequency

Let the mean wind $v(z)$ be written in scaled terms as

$$(4.2) \qquad v(z) = v_o \left[1 + \tanh(z/d) \right]$$

where d is a vertical scale length. We can then introduce further scaling,

$$(4.3) \qquad \xi \equiv \frac{\omega/K}{v_o}; \quad \alpha \equiv Kd$$

and the Richardson number dependence upon z is

$$(4.4) \qquad R_i(z) = J_o \cosh^4 (z/d),$$

where $J_o \equiv \dfrac{\Omega_B^2 d^2}{v_o^2}$ is the minimum value of $R_1(z)$ occurring at

$z = 0$. The appropriate boundary conditions are $w(z) \to 0$ as $|z| \to \infty$. All eigenvalues have the same real part, $R_e(C) = 1$, and the neutral curve $\left[I_m(C) = 0 \right]$, was first obtained by Drazin (1958) and is given analytically as

$$(4.5) \qquad J_o = \alpha^2 (1 - \alpha^2).$$

The eigenvalues, except on the neutral curve where $C = 1$, are not available analytically and must be computed numerically (see Appendix A). The stability diagram for this flow is given in Figure 12, showing the neutral curve, intermediate eigenvalues at $J_o = .15$ and $.20$, all with the curve

$J_o = \alpha^2$. The latter represents a condition of Brünt frequency reflection somewhere in the shear for wave with phase velocities of $C = 1$ (see Appendix B). Of course, if $I_m(C) \neq 0$, there will not be total reflection; however, the attenuation lengths for $J_o > \alpha^2$ are much greater than for $J_o < \alpha^2$. If $c_i^2 \ll 1$, the attenuation lengths are given approximately by

(4.6)

$$J_o > \alpha^2: \quad \ell \simeq d\frac{\sqrt{J_o - \alpha^2}}{J_o c_i}$$

$$J_o < \alpha^2: \quad \ell \simeq \frac{-(J_o - \alpha^2)}{(J_o - \alpha^2)^2 + J_o^2 c_i^2}.$$

Since $c_i^2 \ll 1$ we observe that unstable waves are effectively trapped in the source region, which strongly supports the observational evidence. Furthermore, frequently observed ground pressure fluctuations must represent waves which are theoretically stable in the source region.

C. Source Generation by Subharmonic Wave-Wave Interaction

One possible mechanism for generating observed waves is through a wave-wave interaction involving an unstable mode of horizontal wavenumber 2K and a stable (observable) wavenumber K. Laboratory experiments by Browland (1965), Miksad (1970) and Scotti and Corcos (1972) on free shear layers indicate that a growing fundamental mode interacting with the background noise could generate substantial energy at the subharmonic frequency. An examination of the stability

diagram (Figure 12) indicates that the subharmonics corresponding to the unstable modes would have periods of about 1.2 to 1.6 times the Brünt period, which fall in the range of substantial observable gravity wave energy.

To examine the plausability of the subharmonic generation mechanism one could employ the zeroth, first and second harmonic equations developed in Chapter II using very samll initial values for the primary and subharmonic waves. The unstable mode would first be expected to grow exponentially at a rate determined from linear theory. The growth of the subharmonic is proportional to the amplitude of the primary so eventually its growth will be very large, thereby altering significantly the primary wave growth, perhaps even stopping it altogether. Unfortunately, the finite difference solution will be very costly because of the small time steps required to accurately follow the large expected growth rates. This problem is indigenous to finite difference simulations of physically unstable systems. However, an approximate approach can be taken to qualitatively examine this generation mechanism.

Let us assume that each wave behaves as it would in linear theory, excepting that the nonlinear wave-wave interaction terms will produce a time variation in the amplitude. The horizontal (complex) wave velocities are given then as:

$$(4.7) \quad u_1 = A e^{-i(kx - \omega_r t)} f_1(z)$$

$$u_2 = B e^{-2i(kx - \omega_r t)} e^{\sigma t} f_2(z)$$
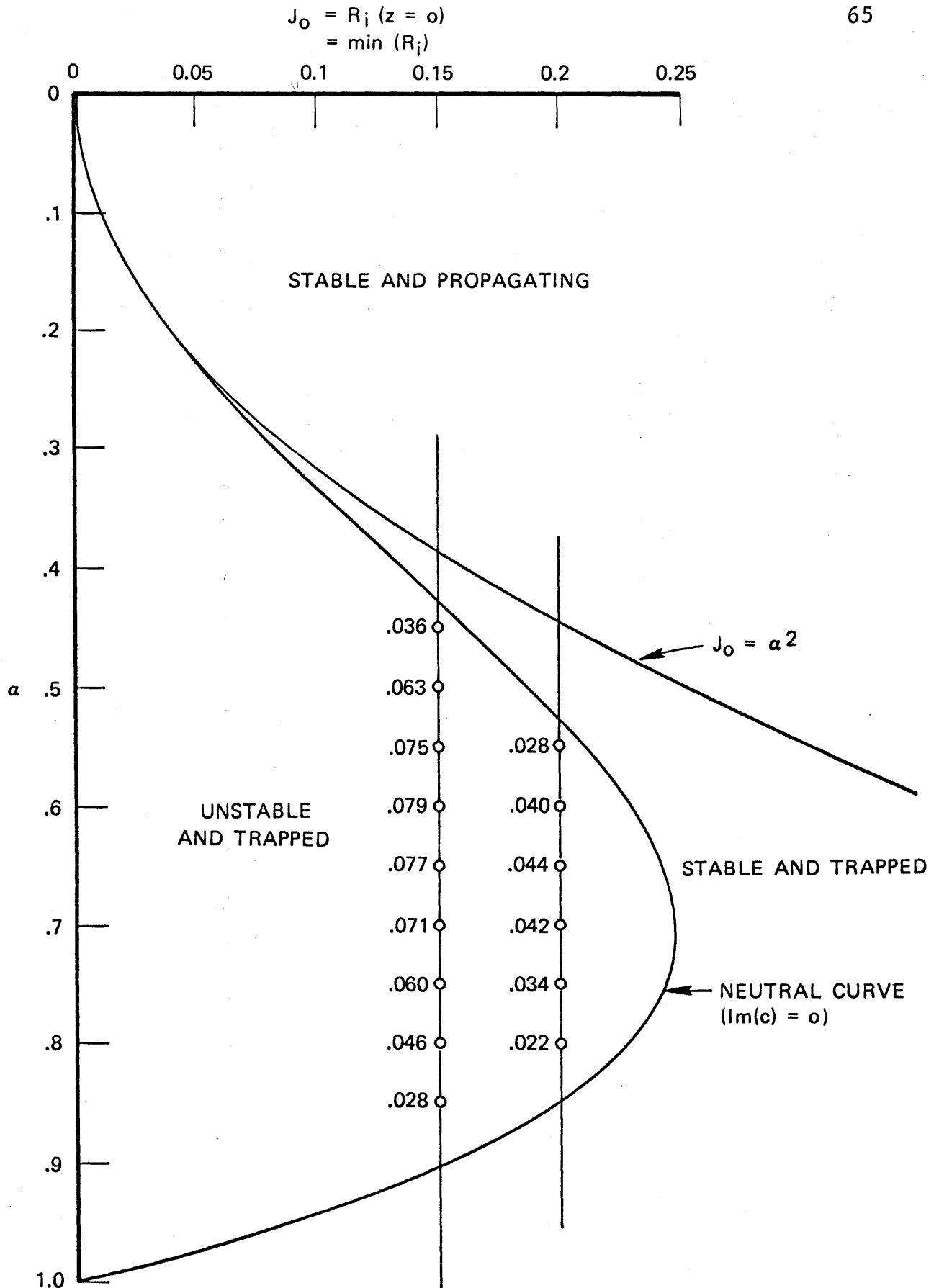
FIGURE 12

STABILITY DIAGRAM FOR HYPERBOLIC TANGENT PROFILE
AND COMPUTED EIGENVALUES
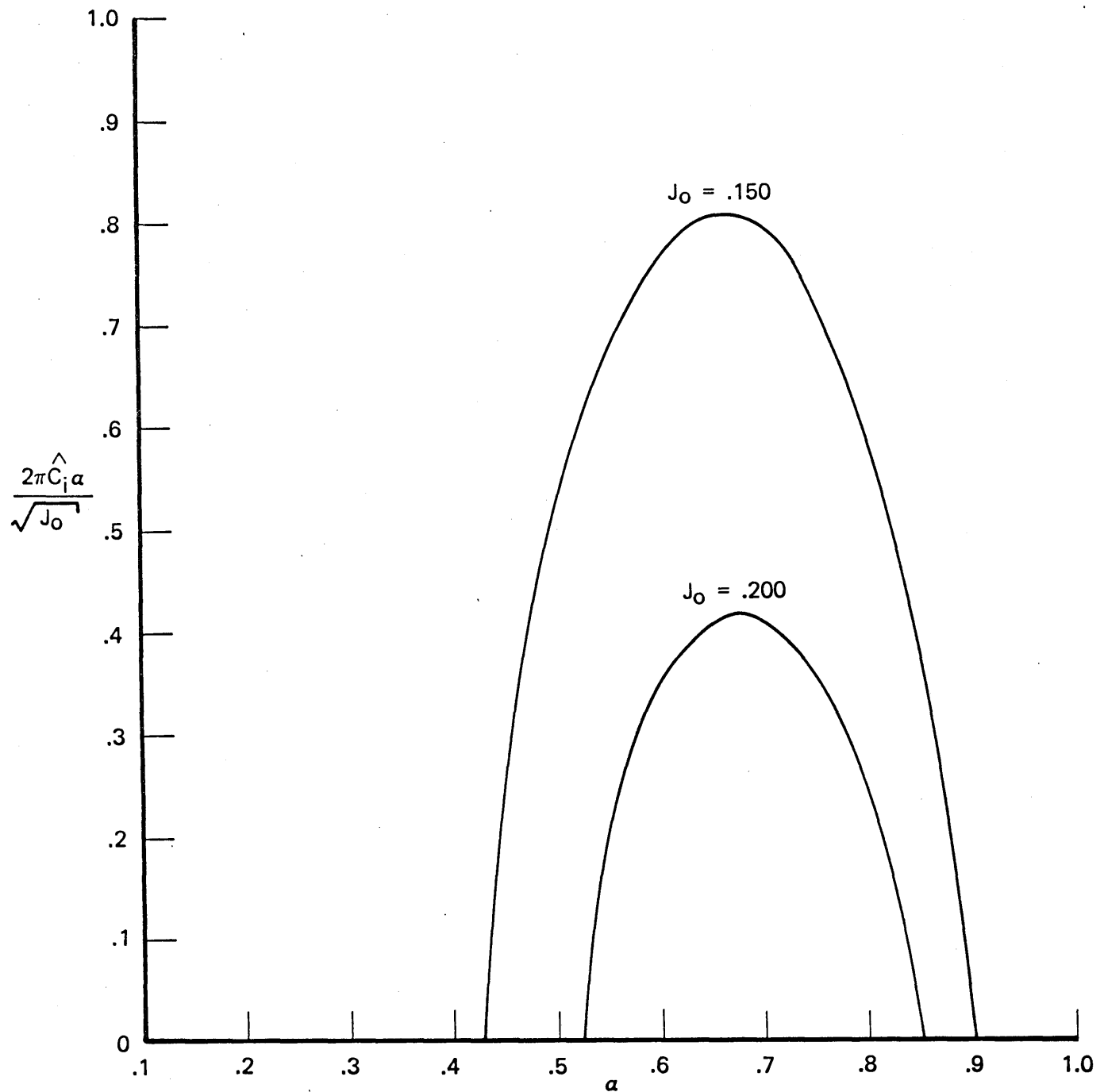
FIGURE 13

NORMALIZED GROWTH RATE VS. WAVE NUMBER
FOR UNSTABLE MODES OF THE HYPERBOLIC TANGENT PROFILE

where $\sigma = \mathrm{Im}(\omega)$ for unstable mode, computed for a hyperbolic tangent shear model with constant Brünt frequency. The nonlinear terms in the horizontal equations of motion are:

$$(4.8) \quad \begin{aligned} Nu_1 &= -2iKu_1^* u_2 + \frac{\partial}{\partial z}\left(w_1^* u_2 + w_2 u_1^*\right) \\ Nu_2 &= -2iKu_1^2 + \frac{\partial}{\partial z}\left(u_1 w_1\right). \end{aligned}$$

Then if we multiply each equation by f_1^* and f_2^* respectively and average over the region $(R,-R)$ corresponding to the Brünt reflection of the unstable mode, we have:

$$(4.9) \quad I_1 \frac{dA}{dt} = c_1 A^* B e^{\sigma t}$$

$$(4.10) \quad I_2 \frac{dB}{dt} = c_2 A^2 e^{-\sigma t}$$

where

$$I_1 = \int_{-R}^{R} dz\, |f_1|^2 \quad , \quad I_2 = \int_{-R}^{R} dz\, |f_2|^2$$

$$c_1 = -iK \int_{-R}^{R} dz\, f_1^* \left[f_1^* f_2 + \frac{df_2}{dz} \int^z d\xi\, f_1^* - 2\frac{df_1^*}{dz}\int^z d\xi\, f_2 \right]$$

$$c_2 = -iK \int_{-R}^{R} dz\, f_2^* \left[f_1^2 + \frac{df_1}{dz}\int^z d\xi\, f_1 \right].$$

The formulation given in equations (4.9) and (4.10) are analogous to those used by Thorpe (1966) and Garret (1968) in discussing resonant interactions in stratified media. For the case of homogeneous media, the vertical distribution functions are simple plane wave solutions and the interaction integrals can be evaluated by inspection. A full discussion of resonant wave-wave interaction for gravity waves in homogeneous media is given by Phillips (1968), with further developments by Craik (1968), Simmons (1969) and Martin, etal (1972). Due to the very restricted phase structure, resonant gravity wave interactions in homogeneous media require a triad resonance such that

$$(4.11) \qquad \underline{K}_1 \pm \underline{K}_2 = \underline{K}_3$$

and

$$(4.12) \qquad \omega_1 \pm \omega_2 = \omega_3 .$$

In stratified shear flow this is not the case, however, due to the possible extensive phase overlap between the unstable mode and its subharmonic.

In order to estimate the integrals, let us assume that the significant contributions to the interaction will occur very near the critical level (which is the same for both modes). The solution of (4.1) for the normalized vertical velocity structure for z/d << 1 can then be approximated for z positive as:

$$(4.13) \qquad W_1 = \eta^{\frac{1}{2}+\mu} \quad , \quad W_2 = (\eta - i\gamma)^{\frac{1}{2}+\mu}$$

$$\eta \equiv z/d \qquad \mu \equiv \sqrt{1/4 - J_0} \qquad \gamma \equiv \frac{Im(c)}{V_0} = \frac{C_i}{V_0} .$$

The corresponding forms for the functions f_1 and f_2 are:

$$(4.14) \quad f_1 = -\frac{i}{\alpha}\frac{dW_1}{d\eta} = -\frac{i}{\alpha}\left(\tfrac{1}{2}+\mu\right)^{\mu-\frac{1}{2}}$$

$$(4.15) \quad f_2 = -\frac{i}{2\alpha}\frac{dW_2}{d\eta} = -\frac{i}{2\alpha}\left(\tfrac{1}{2}+\mu\right)\left(\eta-i\gamma\right)^{\mu-\frac{1}{2}}.$$

Using the fact that near $\eta = 0$,

$$(4.16) \quad \frac{d^2W_1}{d\eta^2} + W_1\frac{J_0}{\eta^2} = 0$$

and

$$(4.17) \quad \frac{d^2W_2}{d\eta^2} + W_2\frac{J_0}{(\eta-i\gamma)^2} = 0$$

we have, defining $h(\eta) \equiv \tan^{-1}\left(\gamma/\eta\right)$:

$$(4.18) \quad \frac{dA}{dt} = \frac{A^*B e^{\sigma t}}{d}\int_0^r d\eta\left[\left(\tfrac{1}{2}+\mu\right)\left(\eta^2+\gamma^2\right)^{-\frac{1}{2}\left(\frac{1}{2}-\mu\right)}e^{i\left(\frac{1}{2}-\mu\right)h(\eta)}\right.$$
$$-\left(\tfrac{1}{2}-\mu\right)\eta\left(\eta^2+\gamma^2\right)^{-\frac{1}{2}\left(\frac{3}{2}-\mu\right)}e^{i\left(\frac{3}{2}-\mu\right)h(\eta}$$
$$\left.+2\left(\tfrac{1}{2}-\mu\right)\eta^{\mu-\frac{3}{2}}\left(\eta^2+\gamma^2\right)^{\frac{1}{2}\left(\frac{1}{2}+\mu\right)}e^{-i\left(\frac{1}{2}+\mu\right)h(\eta}\right.$$

$$(4.19) \quad \frac{dB}{dt} = -\frac{8A^2J_0 e^{-\sigma t}}{d\left(\frac{1}{2}+\mu\right)}\int_0^r d\eta\left[\eta^{2\mu-1}\left(\eta^2+\gamma^2\right)^{\frac{1}{2}\left(\frac{1}{2}-\mu\right)}e^{-i\left(\frac{1}{2}-\mu\right)h(\eta)}\right.$$

Since the solutions to (4.16) and (4.17) apply only near the critical level, the upper limit r is difficult to establish. The criterion for use of (4.16) and (4.17) is that

$$(4.20) \quad \frac{J_0}{\eta^2} \gg \left|z(1-\eta^2) - \alpha^2\right|$$

and since $\alpha^2 < 1$, $\eta^2 << \dfrac{J_0}{2}$.

The integrals cannot be done exactly; however, retaining only the dominant terms ($r << 1$) gives

(4.21) $\quad \dfrac{dA}{dt} \cong \dfrac{A^* B}{d} C_0 e^{\sigma t}$

(4.22) $\quad \dfrac{dB}{dt} \cong -\dfrac{4 A^2 J_0}{d(\frac{1}{2}+\mu)^2} C_0^* e^{-\sigma t}$

where $\quad C_0 = r^{\frac{1}{2}+\mu} e^{i\delta(\frac{1}{2}-\mu)}$

$\delta = \tan^{-1}(\gamma/r)$.

If we further scale the time as

(4.23) $\quad \tau = \Omega_B t$

then (4.21) and (4.22) become

(4.24) $\quad \dfrac{d(A/V_0)}{d\tau} = \dfrac{(A^*/V_0)(B/V_0)}{\sqrt{J_0}} C_0 e^{(\sigma/\Omega_B)\tau}$

(4.25) $\quad \dfrac{d(B/V_0)}{d\tau} = -\dfrac{4(A/V_0)^2 \sqrt{J_0}}{(\frac{1}{2}+\mu)^2} C_0^* e^{-(\sigma/\Omega_B)\tau}$.

There remains the choice for the upper integration limit r. A reasonable choice would be to take z corresponding to r to be one-half of the widths used in the subharmonic transient calculations. If W is the width, then r is given directly as

(4.26) $\quad r = \dfrac{W}{2d} = \dfrac{W \Omega_B}{z\sqrt{J_0} V_0}$.

For values of $T_B = 300$ s., $W = 150$ m and $V_0 = 25$ m/s; $r = .06/J_0$, so that $r^2 << J_0/2$ as required in the approximation. Given an unstable mode corresponding to a (α, Im(c))

pair for a specified Richardson number at $z = 0$ (J_o), we can compute the coupling coefficient C_o. With the initial values of A and B specified, $A(t)$ and $B(t)$ can be found by direct numerical integration of (4.24) and (4.25).

Shown in Figure 14 is the time behavior of the energies for the least stable mode with $R_i(z = 0) = J_o = 0.200$. The eigenvalues of this mode are $\alpha = 0.65$, $Im(C) = 0.044$ and the initial amplitudes were: $|A_o| = |B_o| = .004U_o$ (corresponding to peak horizontal wave velocities of 0.1 m/s for $U_o = 25$ m/s). Also shown is the total energy extracted from the wind to drive the process. In this simple model there is no limit to the energy that can be extracted by the unstable mode. Clearly there will be a point where the energy extracted will have substantially altered the wind, and therefore the interaction. The cutoff line shown in the figure corresponds to an average reduction in the wind of 16%.

The peak amplitude of the subharmonic corresponds to a velocity of about 5 m/s in the source region. Using the parameterized relationship between peak source wave velocity, Richardson number and ground pressure fluctuations, we would expect a peak to peak ground pressure of 0.5 mb, which corresponds very well with observations. In Figure 11 the expected peak to peak ground pressure fluctuations are shown as a function of period as calculated from the peak horizontal subharmonic velocities generated in the simple model considered. Overplotted are the averaged observed values. The simplicity of the model certainly precludes any statement
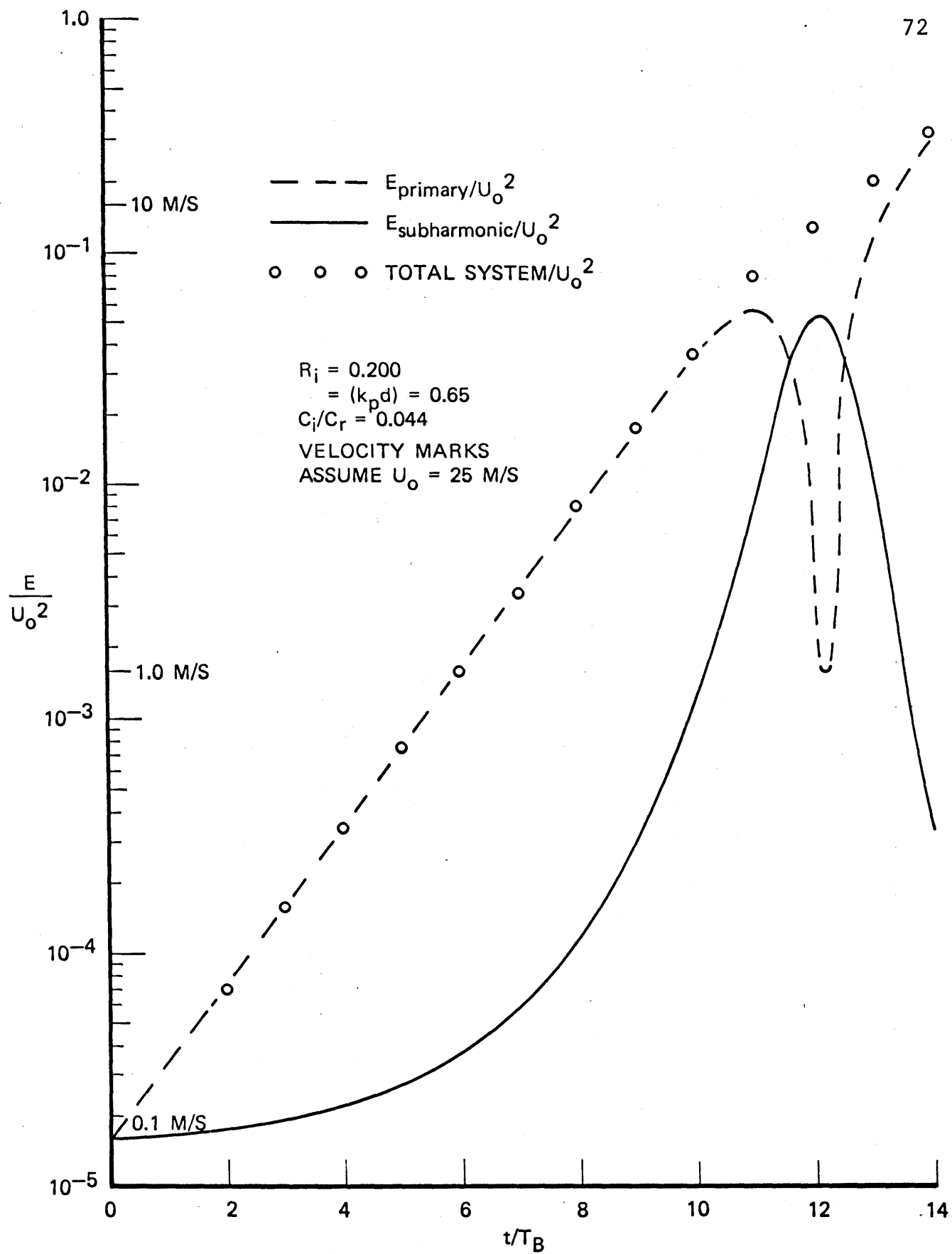
FIGURE 14

TIME BEHAVIOR OF PRIMARY
AND SUBHARMONIC ENERGIES
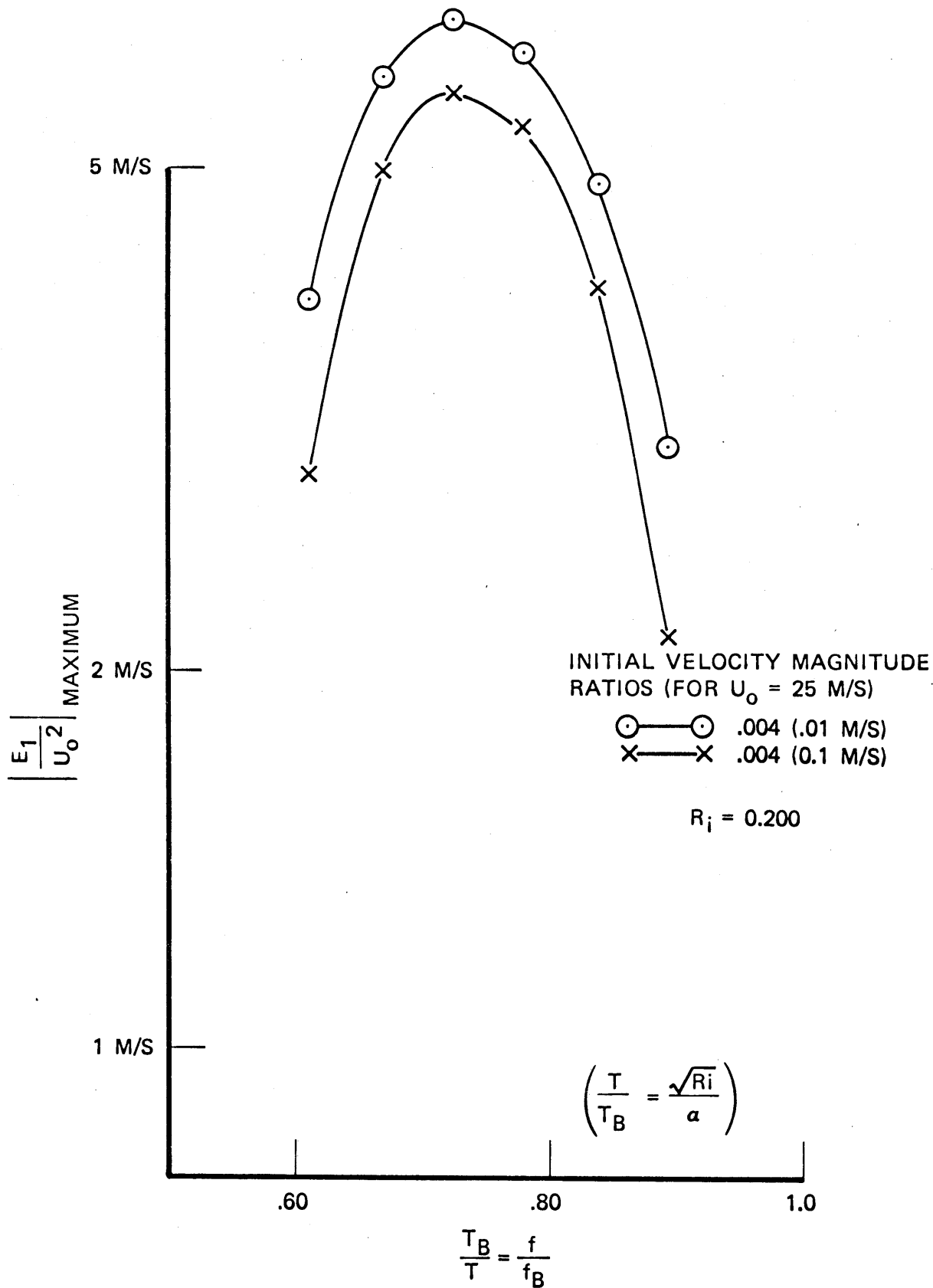
FIGURE 15

SUBHARMONIC ENERGY SPECTRUM
— MAXIMUM OUTPUT VALUES

of the decisiveness of the theory, however, the close similar-
ity of the spectral shape and amplitude do indicate the
plausability of the subharmonic generation mechanism. Figure
14 shows that the subharmonic waves will be present in the
source region with sufficient amplitudes for interaction with
the wind for about two Brünt periods. This is the same time
scale observed for the subharmonic-mean wind interaction
studied in Section III. Additionally, the growth of the
unstable mode is slow relative to the Brünt period and its
amplitude is small enough so that little modification of the
mean wind will occur until substantial subharmonic amplitudes
are reached. The time scales of the subharmonic-unstable mode
interaction are therefore compatible with those of the sub-
harmonic-mean wind interaction found in the transient gravity
wave source calculations.

As a note of numerical interest, accuracy of the
integrations of (4.24) and (4.25) required a time step δt such
that $\delta t \leq .002 T_B$. For a system including the zeroth, first,
and second harmonic, the total computation time would be at
least 20 times as great as that for the zeroth-first harmonic
system for the same vertical grid spacing.

As a final point, although the lowest Richardson
number we have observed on Weather Bureau balloon measurements
is 0.25, the existence of regions for stability with $R_i < 0.25$
seems likely. The absence of observations of Richardson
numbers as low as 0.20 can be explained on the basis of the
vertical sampling of the mean velocity. If the entire lower
jet were modeled by a hyperbolic tangent profile with a source

velocity U_s, Brünt period T_B, and a vertical sampling distance Δz, then the lowest observed Richardson number would be

$$Ri_{OBS} = Ri_{TRUE}\left[\frac{\Delta\xi}{\tanh(\Delta\xi)}\right]^2$$

with the sampling parameter $\Delta\xi$ given as

$$\Delta\xi = \frac{2\pi\,\Delta z}{\sqrt{Ri_{TRUE}}\,T_B\,U_s}\ .$$

Using the balloon measurements for typical values of U_s, T_B, and for minimum Richardson number points and a true value of 0.200, the estimated Richardson number would be 0.243 if the critical level were exactly between the sample points and no noise was present in the observations. An error of half a sample point would give a value of 0.260 for the minimum Richardson number.

V. SUMMARY

The first approach developed to study finite amplitude gravity wave-wind interaction was based on a multiple scale analysis technique. The assumptions are that there exist two time and space scales governing the dynamics of the waves and wind: (1) a "fast" scale corresponding to the relatively rapid temporal-spatial variations of the wave phase, and (2) a "slow" scale corresponding to the variations in wave amplitude and mean flow. The analysis is nonlinear in that wave amplitudes are not considered infinitesimal. The resulting theory is equivalent to a finite amplitude WKB approximation. The limitations of applicability are much like that of linear WKB theory. That is, partial reflections are considered to be second-order effects so that appropriate use of the theory implies that the change in impedance per vertical wavelength be small. For the gravity wave - sheared flow interaction, the change in impedance per wavelength is proportional to $1/R_i^{1/2}$, so the theory is asymptotically correct as $R_i \to \infty$ and will give good results only for $R_i > 1$. If the theory is applied to lower Richardson numbers, the change in the mean wind is overestimated since partial reflections are neglected to first order.

Since observed gravity waves appear to originate from the least stable portions of the jet stream where $R_i < 1$, a theory incorporating partial reflections as well as finite amplitude effects was required. A quasi-linear theory was

76

developed in section II which made no restrictions on the
phase and amplitude structure of the waves and was well suited
to transient source calculations. The equations of motion are
those of linear theory except that time changes in the mean
flow due to wave-wind interaction are incorporated through a
momentum transport equation for the mean flow. The waves then
propagate through a time-varying medium whose time variations
are produced by gradients of the wave Reynold's stress. The
theory has certain appealing features. The nonlinear inter-
action takes place in a small region about the critical level
and these changes are directly incorporated. The induced time
changes in the mean flow near the critical level are included
in equations of motion for the waves, thereby eliminating the
singular nature of the linear theory. Away from critical
levels, linear theory describes the propagation of gravity
waves quite well and the quasi-linear theory becomes essenti-
ally linear there since there is virtually no wave-wind
interaction. The intuitive aspects of linear theory can
therefore be applied except near critical levels. From a
computational point of view, the quasi-linear theory is much
more efficient than a full nonlinear calculation as only one
space and time variable are required since one can consider
waves to be harmonically varying in the direction of the mean
flow. Quite general one-dimensional source and jet models
can be modelled for transient calculations.

Using the quasi-linear theory several numerical
experiments were made using a model jet to examine the trans-
ient behavior of finite amplitude gravity wave sources. The

calculations of the effects of finite sources show that
considerable energy is withdrawn from the wind in the source
region and put into wave energy. The gravity waves very effi-
ciently couple the critical level at the top of the jet with
the critical level at the source region. The steady-state
of all models resulted in a net decrease in the wind energy
at the topside of the jet and a net increase in wind energy
in the source region. The ultimate energy source is then
seen to be this upper critical level. The magnitude of the
gravity waves produced and therefore the amount of wind energy
transported depends strongly on Richardson number, the lower
the Richardson number, the greater the wave amplification
and energy transport. However, the system remains stable
for small sources even at Richardson numbers as low as 0.200.
This would appear to be in keeping with the linear stability
calculations for shears with a ground reflector (Jones, 1968)
which state that for $R_i > .15$ the unstable waves cannot have
frequencies less than the Brünt frequency. The amount of
energy transport by transient gravity wave sources can be an
order of magnitude greater than that of the input source for
$R_i < 0.25$.

Calculations of the ground pressure fluctuations due
to these sources show that observed peak to peak surface
values of from 0.1 to 0.5 millibars can be generated by source
region rms velocities of only 0.5 to 2.0 m/s, which are well
within the limitations of the quasi-linear theory.

The quasi-linear theory has provided a framework for
studying the propagation and energy transport properties of

finite amplitude gravity wave transients, however, the question of spontaneous source generation remains. In section IV a theory of subharmonic wave-wave interaction was discussed. A natural mechanism for spontaneous source generation would seem to be the dynamic instability of highly sheared flows to small perturbations. A considerable volume of literature exists on the determination of unstable regimes in terms of Richardson number and horizontal wavenumber. Since observed gravity waves seemed to originate in localized regions in the jet a small, high shear linear segment or hyperbolic tangent profile is an appropriate model for the wind near a source. Neutral curves, separating stable and unstable regimes, have been found analytically for the hyperbolic tangent shear (Drazin, 1958), and numerically for the linear shear (Jones, 1968). A striking feature of both these curves, however, is that all unstable modes require periods less than a Brünt period and therefore would be severely attenuated before reaching the ground. Observations of surface pressure power spectra confirm this result, showing a sharp cutoff for periods less than the Brünt period. Conversely, the propagating gravity waves observed would be stable in the region of maximum shear for all Richardson numbers greater than zero. Therefore, the source regions responsible for the observed gravity waves do not arise spontaneously as an instability of such waves.

Observed gravity waves with periods greater than the Brünt period can arise from a wave-wave interaction with an

unstable mode through the mechanism of subharmonic genera-
tion. For two waves having the same source region critical
level, a growing disturbance can amplify a wave with twice
its period. The growth rate of the subharmonic is proportion-
al to the amplitude of the unstable mode which is initially
growing exponentially in accordance with linear theory.
Growth of the subharmonic extracts energy directly from the
unstable mode and will eventually stabilize it when both
waves reach approximately the same amplitude. The calculated
growth rate of the subharmonic is shown to be very rapid com-
pared to a wave period and appears to be almost spontaneously
generated, and since it is a propagating mode it will event-
ually be observed at the ground. Calculations have also shown
that through this mechanism a background velocity noise of
1.0 cm/sec can generate surface pressure fluctuations of
approximately 1 millibar.

Lower frequency observed waves could also be generated
through wave-wave interaction as difference waves of two
unstable modes. Although a plausible mechanism, calculations
on the three wave interaction mechanism remain an area for
further work.

A natural extension of the work presented here would
be to include the wave-wave source generation directly into
the quasi-linear theory including unstable modes and wave-wind
interaction. One would also like to use a very realistic wind
and temperature profile and attempt direct comparison with
observed gravity waves. Such a development would require a

far more sophisticated numerical simulator and large amounts of machine time owing to the very short wavelengths and extreme growth rates to be encountered.

APPENDIX A

NUMERICAL DETERMINATION OF THE EIGENVALUES
AND EIGENFUNCTIONS FOR STRATIFIED SHEAR FLOWS.

The linear stability for plane, stratified shear flow is governed by the Taylor-Goldstein equation in the Boussinesq approximation.

For vertical velocity disturbances of the form $w(x, z, t) = \hat{w}(z)e^{i(wt-kx)}$ in a medium with Brünt frequency Ω_B and mean flow structure $\bar{U}(z)$, the governing equation is

$$\frac{d^2\hat{w}}{dz^2} + \hat{w}\left[\frac{\Omega_B^2}{(\bar{U}(z)-\frac{\omega}{K})^2} - \frac{d^2\bar{U}/dz^2}{(\bar{U}(z)-\frac{\omega}{K})} - K^2\right] = 0.$$

Introducing a vertical length scale d and mean velocity scale U_o then define the nondimensional parameters:

$$\alpha \equiv Kd$$

$$c \equiv \frac{\omega/K}{U_o}$$

$$J_o \equiv \Omega_B^2 d^2/U_o^2$$

and scale the flow as $\bar{U}(z) = U_o f(z/d)$ and introduce a new independent variable $\xi = z/d$.

Letting primes denote differentiation with respect to ξ, the nondimensional form of the stability equation is:

$$\hat{w}'' + \hat{w}\left[\frac{J_o}{(f-c)^2} - \frac{f''}{f-c} - \alpha^2\right] = 0.$$

The stability problem is formulated for the complex eigenvalues c, given α, J_o and the flow structure $f(z/d)$, along with the boundary conditions

$$\hat{W}\left(z_a/d\right) = \hat{W}\left(z_b/d\right) = 0$$

where (Z_a, Z_b) are the boundary points of the system and can be infinite.

The Hyperbolic Tangent Flow with Constant Brünt Period.

The functional form of the flow is given as

$$f(z/d) = 1 + \tanh(z/d).$$

Drazin (1958) showed that all the eigenvalues will have the same real part, that is Re(c) = 1, and that the neutral curve for which Im(c) = o is given by

$$J_o = \alpha^2(1-\alpha^2).$$

To specify the boundary value problem we then require:

a) $\lim\limits_{R \to \infty} \hat{W}(R) = \lim\limits_{R \to -\infty} \hat{W}(R) = 0$

b) $Re(c) = 1$ for all J_o, α and $Im(c)$.

The stability problem is then to determine Im(c) given J_o and α. The eigenvalues must be determined numerically away from the neutral curve, but the existence of this curve means the region to be examined is $J_o < \alpha^2(1-\alpha^2)$.

Transformation to Riccati Form for Eigenvalue Determination.

For numerical integration it is useful to map the infinite domain $(\infty, -\infty)$ into the finite domain $(1, -1)$. Clearly, the transformation to use is

$$y = \tanh(z/d)$$

which is monotonic and reduces $f(z/d)-c$ to $y-i\text{Im}(c)$. Then introduce the transformation

$$\hat{W}(z) = \exp\left[\int_0^y \frac{dy}{1-y^2}\,\phi(y)\right]$$

and the stability equation is reduced to a first-order Riccoti equation,

$$\frac{d\phi}{dy} = \frac{1}{1-y^2}\left[\alpha^2 - \phi^2 - \frac{J_0}{(y-ic_i)^2}\right] - \frac{2y}{y-ic_i}$$

where $c_i \equiv \text{Im}(c)$.

The initial values for ϕ at $Y = \pm 1$, can be determined by requiring $d\phi/dy$ to be finite there. Then

a) $\quad y = +1 \qquad \phi^2 = \alpha^2 - \frac{J_0}{(1-ic_i)^2}$

b) $\quad y = -1 \qquad \phi^2 = \alpha^2 - \frac{J_0}{(1+ic_i)^2}$.

The starting values for $d\phi/dy$ can be obtained from L'Hopital's rule:

a) $\quad y = 1 \qquad \frac{d\phi}{dy} = -\frac{1}{(1-ic_i)(1-\phi(1))}\left[2 + \frac{J_0}{(1-ic_i)^2}\right]$

b) $\quad y = -1 \qquad \frac{d\phi}{dy} = \frac{1}{(1+ic_i)(1-\phi(-1))}\left[2 - \frac{J_0}{(1+ic_i)^2}\right]$.

For a given (α, J_0) pair, the solutions for ϕ will only match at $y=0$ if C_i is an eigenvalue. Define

$$\phi = \phi^+ \qquad 0 \le y \le 1$$

$$\phi = \phi^- \qquad -1 \le y \le 0.$$

Now, since $\hat{w}(z/d) \to 0$ as $z \to \pm \infty$, then we require that the initial condition branches at $y = \pm 1$ be chosen such that

$$\text{Re}(\phi^+(1)) < 0 \qquad \text{and} \qquad \text{Re}(\phi^-(-1)) > 0.$$

One can then straight forwardly integrate in from ± 1 and find the zeros of $\Delta = \phi^+(0) - \phi^-(0)$ as a function of c_i for given a(α, Jo) pair. Much work can be saved, however, with some additional analysis. The governing equation is again,

$$\frac{d\phi}{dy} = \frac{\alpha^2 - \phi^2}{1-y^2} - \frac{2y}{y-ic_i} - \frac{Jo}{(1-y^2)(y-ic_i)^2}$$

and at $y = +1$; $\qquad \phi(+1) = \pm \sqrt{\alpha^2 - Jo/(1-ic_i)^2}$

with $\text{Re}(\phi(+1)) < 0$ required. Now let $\theta \equiv -\phi^*(y')$ with $y' = -y$. Then we have

$$\frac{d\theta}{dy'} = \frac{\alpha^2 - \theta^2}{1-y'^2} - \frac{2y'}{y'-ic_i} - \frac{Jo}{(1-y'^2)(y'-ic_i)^2}$$

with

$$\theta(1) = \pm \sqrt{\alpha^2 - Jo/(1-ic_i)^2}$$

and $\text{Re}(\theta(+1)) < 0$. Therefore, since the differential equations and initial values are identical,

$$\phi(y) = -\phi^*(-y) \qquad \qquad \text{by uniqueness.}$$

Therefore,

$$\phi^+(y) = \theta(y) \qquad 0 \le y \le 1$$

$$-\phi^*(-y) = \theta(-y) \qquad 0 \le -y \le 1.$$

For an eigensolution, $\phi^+(0) = \phi^-(0)$, hence

$$\text{Re}(\theta(0)) = 0 \text{ is required.}$$

Further, for an eigensolution, we see that

$$\phi(y) = -\phi^*(-y)$$

$$\text{Re}\left[\phi(y)\right] = -\text{Re}\left[\phi(-y)\right] \quad (\text{odd})$$

$$\text{Im}\left[\phi(y)\right] = \text{Im}\left[\phi(-y)\right] \quad (\text{even}).$$

Therefore, a much easier method for finding C_i is available since

$$\text{Re}\left[\phi(y=0)\right] = 0,$$

so that only one integration from either $y = \pm 1$ to $y = 0$ is required. Initial values of C_i are then iterated until a zero is found in the real part of $\phi(y=0)$ which gives the eigenvalue C_i for a given (J_0, α) pair.

In principle, the nonlinear eigenuvalve problem is now straight forward, however, if care is not taken with the integration technique, substantial errors in the estimate of C_i can result due to the nearly singular term $\dfrac{J_0}{(y-iC_i)^2}$.

Since typically $C_i^2 \ll 1$, then

$$\frac{d\phi}{dy}(y=0) \gg 1$$

and any attempt at direct integration of the equation without regularizing the solution is subject to significant errors in the estimate of C_i.

Regularization of the Solution for Accurate Numerical
    Integration of the Riccati form.

Let us examine the solution as $y = \tanh(z/d) \rightarrow 0$. Let $\widetilde{W} \rightarrow \widehat{W}$ as $y \rightarrow 0$ and define a corresponding Riccati variable $\widehat{\Theta}(y)$ as

$$\widetilde{W}(y) = \exp\left[\int_0^y dy\, \widetilde{\Theta}(y)\right]$$

where $\widetilde{W}$ and $\widetilde{\Theta}$ satisfy

$$\frac{d^2\widetilde{W}}{dy^2} + \widetilde{W}\left[\frac{J_0}{(y-ic_i)^2}\right] = 0$$

and

$$\frac{d\widetilde{\Theta}}{dy} + \widetilde{\Theta}^2 + \frac{J_0}{(y-ic_i)^2} = 0$$

exactly. There is an analytic solution for $\widetilde{\Theta}$ since

$$\widetilde{\Theta} = \frac{1}{\widetilde{W}}\frac{d\widetilde{W}}{dy}$$

; the exact solution for $\widetilde{\Theta}(y)$ is

$$\widetilde{\Theta}(y) = \frac{1}{y-ic_i}\left[\frac{a(\frac{1}{2}-\nu) + b(\frac{1}{2}+\nu)(y-ic_i)^{2\nu}}{a + b(y-ic_i)^{2\nu}}\right]$$

where $\nu \equiv \sqrt{1/4 - J_0}$ (for unstable flows $J_0 < \frac{1}{4}$).

Now, since the previous formulation involved $\phi(y)$, define

$$h(y) \equiv \phi(y) - \widetilde{\Theta}(y)$$

so $\phi(y) \to \widetilde{\Theta}(y)$ as $y \to 0$

so $\frac{dh}{dy}$ will be much reduced from $\frac{d\phi}{dy}$ near y = o,
affording much more accurate estimations of c_i.

There remains to fix the constants a, b for $\widetilde{\Theta}$. Since
$Re(\phi) = 0$ at y = 0, choose $Re(\widetilde{\Theta}) = 0$ at y = o and $\phi = \widetilde{\Theta}$
at y = + 1. The eigenvalue problem is then reformulated as:

$$\frac{dh}{dy} = \frac{1}{1-y^2}\left[\alpha^2 - 2h\widetilde{\Theta} - h^2 + y^2\frac{d\widetilde{\Theta}}{dy}\right] - \frac{2y}{y-ic_i}$$

with initial conditions at y = +1:

   h = 0

$$\frac{dh}{dy} = -\frac{1}{(1-ic_i)(1+\phi(1))}\left[2 + \frac{J_0}{(1-ic_i)^2}\right] + \phi^2(+1) + \frac{J_0}{(1-ic_i)^2}$$

with $\phi(+1) = \pm \sqrt{\alpha^2 - J_0/(1-iC_i)^2}$

such that $\text{Re}(\phi(+1)) < 0$.

The eigenvalues C_i are then found such that $\text{Re}(h) = 0$ at $y = 0$, given values for α and J_0.

Eigenfunction Calculations

Once an accurate determination of C_i for a given (J_0, α) pair has been made, direct calculation of $W(y)$ and $\dfrac{d\hat{W}}{dy}$ can be made by writing

$$F(y) \equiv \hat{W}(y) - \tilde{W}(y)$$

which is governed by

$$(1-y^2)^2 \frac{d^2F}{dy^2} = 2y(1-y^2)\frac{dF}{dy} + F\left[\alpha^2 - \frac{2y(1-y^2)}{y-iC_i}\right]$$
$$+ \tilde{W}\left[\alpha^2 - \frac{2y(1-y^2)}{y-iC_i} - \frac{J_0(y^4-2y^2)}{(y-iC_i)^2}\right]$$
$$+ 2y(1-y^2)\frac{d\tilde{W}}{dy}$$

with the initial conditions

$$F(y=0) = \frac{dF}{dy}(y=0) = 0.$$

APPENDIX B

BRÜNT PERIOD REFLECTION CONDITIONS FOR
UNSTABLE HYPERBOLIC TANGENT FLOWS

Consider the mean flow velocity given as

$$\bar{U}(z) = U_0 \tanh(z/d),$$

then the Richardson number is

$$R_i(z) = \left[\frac{\Omega_B^2 d^2}{U_0^2}\right] \cosh^4(z/d).$$

The condition for waves capable of propagating to infinity is

$$\Omega_B^2 > \Omega^2 \qquad \text{for all } z$$

where $\Omega = \omega - k\bar{U}(z)$ is the doppler-shifted frequency. For the choice of profiles, the source level is z = 0, so w = 0. Therefore the propagation condition is

$$\Omega_B^2 > k^2 U_0^2 \tanh^2(z/d).$$

The minimum Richardson number is

$$J_0 \equiv R_i(z=0) = \frac{\Omega_B^2 d^2}{U_0^2}.$$

Therefore the propagation condition is

$$J_0 > k^2 d^2 \tanh^2(z/d)$$

and since $\tanh^2(z/d) \leq 1$, then the condition is

$$J_0 > k^2 d^2.$$

Further, since a necessary (but not sufficient) condition for unstable modes is

$$J_0 < k^2 d^2 (1 - k^2 d^2)$$

all unstable modes are Brünt reflected for some finite value of z and therefore trapped within the flow.

APPENDIX C

DISTRIBUTION OF VELOCITIES AND ENERGY DENSITIES
IN REGIONS I AND III FOR MODEL A AS A FUNCTION OF
TIME.   CALCULATED GROUND PRESSURE FLUCTUATIONS.

The intermediate computer output for Model A is shown
in the following figures at times corresponding to t = o,
200, 400, 800, 1200, 1600, 2000, 2400, 2800, 3200, 3600 and
4000 sec.   The symbol map is

$$* = 100. DU = 100 \cdot (u_0 - \overline{U})$$
$$1 = 0.5 / R_i$$
$$2 = 10 \cdot u_1 \, (x = 0)$$
$$3 = 10 \cdot W_1 \, (X = 0)$$
$$4 = 10 \cdot \left[u_1 u_1 + w_1 w_1 + \phi_1 \phi_1 / \Omega_B^2 \right]$$
$$5 = 10 \cdot \overline{U} (u_0 - \overline{U}) + 5 \cdot (u_0 - \overline{U})^2 .$$

The final figure shows the calculated ground pressure
fluctuations as a function of time for the model.

91

```
STEP#=  0  TIME=   0.       REGICN I.II:  0KM TO 4KM IN 250M STEPS - 4KM TO 6KM IN 25M STEPS   J=41 CORRESPONDS TO Z=4.0KM
SYMBOL INDEX: *=100.*DU
              1=0.5*INVERSE RIW
              2=10.*U1(X=C)
              3=10.*W1(X=0)
              4=10.*WAVE ENERGY DENSITY
              5=10.*WIND ENERGY DENSITY
              X=COMMON VALUES
              U=MAXIMUM SCALE VALUE EQUALLED OR EXCEEDED
```

J	100.*DU	-5.0	0.0	5.0

```
    J      100.*DU    -5.0                                              0.0                                          5.0
                       +---------+---------+---------+---------+---------+---------+---------+---------+---------+---------
    1      0.0       I                                          X                                                      I
    2      0.0       I                                          X                                                      I
    3      0.0       I                                          X                                                      I
    4      0.0       I                                          X                                                      I
    5      0.0       I                                          X                                                      I
    6      0.0       I                                          X                                                      I
    7      0.0       I                                          X                                                      I
    8      0.0       I                                          X                                                      I
    9      0.0       I                                          X                                                      I
   10      0.0       I                                          X                                                      I
   11      0.0       I                                          X                                                      I
   12      0.0       I                                          X                                                      I
   13      0.0       I                                          X                                                      I
   14      0.0       I                                          X                                                      I
   15      0.0       I                                          X                                                      I
   16      0.0       I                                          X                                                      I
   17      0.0       I                                          X                                                      I
   18      0.0       I                                          X                                                      I
   19      0.0       I                                          X                                                      I
   20      0.0       I                                          X                                                      I
   21      0.0       I                                          X                                                      I
   22      0.0       I                                          X                                                      I
   23      0.0       I                                          X                                                      I
   24      0.0       I                                          X                                                      I
   25      0.0       I                                          X                                                      I
   26      0.0       I                                          X                                                      I
   27      0.0       I                                          X                                                      I
   28      0.0       I                                          X                                                      I
   29      0.0       I                                          X                                                      I
   30      0.0       I                                          X                                                      I
   31      0.0       I                                          X                                                      I
   32      0.0       I                                          X                                                      I
   33      0.0       I                                          X                                                      I
   34      0.0       I                                          X                                                      I
   35      0.0       I                                          X1                                                    I
   36      0.0       I                                          X   1                                                 I
   37      0.0       I                                          X    1                                                I
   38      0.0       I                                          X    1                                                I
   39      0.0       I                                          X    1                                                I
   40      0.0       I                                          X    1                                                I
   41      0.0       I                                          X    1                                                I
   42      0.0       I                                          X    1                                                I
   43      0.0       I                                          X    1                                                I
   44      0.0       I                                          X2   1                                                I
   45      0.0       I                                         X2   1                                                 I
   46      0.0       I                                         X2   1                                                 I
   47      0.0       I                                         X 2 1                                                  I
   48      0.0       I                                         X  21                                                  I
   49      0.0       I                                         X      2       1                                       I
   50      0.0       I                                         X        2               1                             I
   51      0.0       I                                         X         1              1                             I
   52      0.0       I                                         X          2             1                             I
   53      0.0       I                                         X          2             1                             I
   54      0.0       I                                         X         2              1                             I
   55      0.0       I                                         X     2                  1                             I
   56      0.0       I                                         X 2                      1                             I
   57      0.0       I                                         X                        1                             I
   58      0.0       I                                    2    X                        1                             I
   59      0.0       I                                  2      X                        1                             I
   60      0.0       I                                2        X                        1                             I
   61      0.0       I                               2         X                        1                             I
   62      0.0       I                               2         X                        1                             I
   63      0.0       I                                2        X                        1                             I
   64      0.0       I                                 2       X                        1                             I
   65      0.0       I                                  2      X               1                                      I
   66      0.0       I                                    2    X   1                                                  I
   67      0.0       I                                     2  X    1                                                  I
   68      0.0       I                                      2 X    1                                                  I
   69      0.0       I                                      2 X    1                                                  I
   70      0.0       I                                        2X   1                                                  I
   71      0.0       I                                        2X   1                                                  I
   72      0.0       I                                        2X   1                                                  I
   73      0.0       I                                        2X   1                                                  I
   74      0.0       I                                        2X   1                                                  I
   75      0.0       I                                        2X   1                                                  I
   76      0.0       I                                        2X   1                                                  I
   77      0.0       I                                        2X   1                                                  I
   78      0.0       I                                        2X   1                                                  I
   79      0.0       I                                        2X1                                                    I
   80      0.0       I                                        2X                                                     I
   81      0.0       I                                        2X                                                     I
   82      0.0       I                                        2X                                                     I
   83      0.0       I                                        2X                                                     I
   84      0.0       I                                        2X                                                     I
   85      0.0       I                                         X                                                     I
   86      0.0       I                                         X                                                     I
   87      0.0       I                                         X                                                     I
   88      0.0       I                                         X                                                     I
   89      0.0       I                                         X                                                     I
   90      0.0       I                                         X                                                     I
   91      0.0       I                                         X                                                     I
   92      0.0       I                                         X                                                     I
   93      0.0       I                                         X                                                     I
   94      0.0       I                                         X                                                     I
   95      0.0       I                                         X                                                     I
   96      0.0       I                                         X                                                     I
   97      0.0       I                                         X                                                     I
                     +---------+---------+---------+---------+---------+---------+---------+---------+---------+---------
```

```
SYMBOL INDEX: *=100.*DU
              1=0.5*INVERSE RIW
              2=10.*U1(X=0)
              3=10.*W1(X=0)
              4=10.*WAVE ENERGY DENSITY
              5=10.*WIND ENERGY DENSITY
              X=COMMON VALUES
              U=MAXIMUM SCALE VALUE EQUALLED OR EXCEEDED
```

J	100.*DU	-5.0 .... 0.0 .... 5.0
1	0.0	X
2	0.0000	X
3	0.0000	X
4	0.0000	X
5	0.0000	X
6	0.0001	X
7	0.0001	X
8	0.0002	X
9	0.0002	X
10	0.0003	X 3
11	0.0005	X 3
12	0.0007	2X3
13	0.0010	2X3
14	0.0015	2X 3
15	0.0022	2 X 3
16	0.0033	2 X 3
17	0.0049	2 X 3
18	0.0052	2 X 3
19	0.0054	2 X 3
20	0.0056	2 X 3
21	0.0059	2 X 3
22	0.0061	2 X 3
23	0.0064	2 X 3
24	0.0067	2 X 3
25	0.0070	2 X 3
26	0.0073	2 X 3
27	0.0076	2 X 3
28	0.0079	2 X 3
29	0.0083	2 X 3
30	0.0086	2 X 3
31	0.0090	2 X 3
32	0.0094	2 X 3
33	0.0098	2 X 3
34	0.0103	2 X 3
35	0.0108	2 X1 3
36	0.0114	2 X 31
37	0.0121	2 X 31
38	0.0130	2 X 31
39	0.0144	2 X 31
40	0.0168	2 X 31
41	0.0214	X 31
42	0.0298	2 X 31
43	0.0443	2 X 31
44	0.0679	2 X 31
45	0.1026	2 X*3 1
46	0.1485	2 *X3 1
47	0.2016	2 45X 1
48	0.2516	2 4X 1
49	0.2822	2 4X5 1
50	0.2725	2 4X5 1
51	0.2061	2 XX 1
52	0.0882	2 *X4 1
53	-0.0483	2 X 34 1
54	-0.1533	2 5 * 3 4 1
55	-0.1825	2 5 * 3 4 1
56	-0.1224	2 5* 3 4 1
57	-0.0021	X3 4 1
58	0.1188	3 *452 1
59	0.1804	3 *4 5 2 1
60	0.1528	3 *4 5 2 1
61	0.0489	3 *54 2 1
62	-0.0871	53* 4 2 1
63	-0.2050	5 *3 4 2 1
64	-0.2712	5 *3 4 2
65	-0.2807	5 X 4 2 1
66	-0.2499	5 X 4 1 2
67	-0.1998	5 3* 4 1 2
68	-0.1464	5 3* 4 1 2
69	-0.1013	5 3* 4 1 2
70	-0.0670	X *4 1 2
71	-0.0439	35*4 1 2
72	-0.0297	35*4 1 2
73	-0.0215	3 X4 1 2
74	-0.0171	3 X4 1 2
75	-0.0148	3 X4 1 2
76	-0.0135	3 X4 1 2
77	-0.0126	3 X3 1 2
78	-0.0119	3 X4 1 2
79	-0.0113	3 X41 2
80	-0.0107	3 XX 2
81	-0.0103	3 XX 2
82	-0.0098	3 XX 2
83	-0.0094	3 XX 2
84	-0.0090	3 XX 2
85	-0.0086	3 XX 2
86	-0.0082	3 XX 2
87	-0.0078	3 XX 2
88	-0.0075	3 XX 2
89	-0.0072	3 XX 2
90	-0.0069	3 XX 2
91	-0.0066	3 XX 2
92	-0.0063	3 XX 2
93	-0.0060	3 XX 2
94	-0.0057	3 XX 2
95	-0.0055	3 XX 2
96	-0.0053	3 XX 2
97	-0.0050	3 XX 2

```
STEP#= 40  TIME= 400.      REGION I,II:  0KM TC 4KM IN 250M STEPS - 4KM TO 6KM IN 25M STEPS   J=41 CORRESPONDS TO Z=4.0KM
SYMBOL INDEX: *=100.*DU
              1=0.5*INVERSE RIN
              2=10.*U1(X=0)
              3=10.*W1(X=0)
              4=10.*WAVE ENERGY DENSITY
              5=10.*WINC ENERGY DENSITY
              X=COMMON VALUES
              0=MAXIMUM SCALE VALUE EQUALLED OR EXCEEDED
```

```
   J        100.*DU    -5.0                                          0.0                                        5.0
                        +--------+--------+--------+--------+--------+--------+--------+--------+--------+--------+
   1        0.0         I                                       2  X                                            I
   2        0.0001      I                                       2  X                                            I
   3        0.0006      I                                       2  X3                                           I
   4        0.0013      I                                       2  X3                                           I
   5        0.0022      I                                       2  X3                                           I
   6        0.0032      I                                       2  X 3                                          I
   7        0.0044      I                                       2   X 3                                         I
   8        0.0057      I                                       2   X 3                                         I
   9        0.0071      I                                       2   X3                                          I
  10        0.0086      I                                       2  X3                                           I
  11        0.0101      I                                       2   X                                           I
  12        0.0119      I                                       XX                                             I
  13        0.0140      I                                       3X                                             I
  14        0.0165      I                                       3 X 2                                          I
  15        0.0194      I                                      3   X     2                                     I
  16        0.0222      I                                     3    X      2                                    I
  17        0.0244      I                                  3      X        2                                   I
  18        0.0246      I                                  3      X        2                                   I
  19        0.0248      I                                  3      X        2                                   I
  20        0.0249      I                                  3      X         2                                  I
  21        0.0250      I                                  3      X         2                                  I
  22        0.0251      I                                  3      X         2                                  I
  23        0.0252      I                                  3      X         2                                  I
  24        0.0253      I                                  3      X         2                                  I
  25        0.0254      I                                  3      X         2                                  I
  26        0.0255      I                                  3      X         2                                  I
  27        0.0256      I                                  3      X         2                                  I
  28        0.0256      I                                  3      X         2                                  I
  29        0.0257      I                                  3      X         2                                  I
  30        0.0258      I                                  3      X         2                                  I
  31        0.0259      I                                  3      X          2                                 I
  32        0.0260      I                                  3      X          2                                 I
  33        0.0262      I                                  3      X          2                                 I
  34        0.0264      I                                  3      X          2                                 I
  35        0.0288      I                                  3      X1         2                                 I
  36        0.0361      I                                  3      X    1     2                                 I
  37        0.0470      I                                  3      X    1   2                                   I
  38        0.0596      I                                  3      X    1 2                                     I
  39        0.0732      I                                  3      X    1 2                                     I
  40        0.0872      I                                  3      X   1 2                                      I
  41        0.1004      I                                 3      X*  1 2                                       I
  42        0.1119      I                                3      X*   12                                        I
  43        0.1219      I                                3      X*  12                                         I
  44        0.1333      I                                3      5X  X                                          I
  45        0.1527      I                                3       X  X                                          I
  46        0.1898      I                                3       X 21                                          I
  47        0.2536      I                                3      XX 1                                           I
  48        0.3447      I                              3  24 X1                                                I
  49        0.4670      I                            32     4 *5        1                                      I
  50        0.5892      I                        2 3       4  * 5                    1                         I
  51        0.6019      I                        2  3      4  * 5                    1                         I
  52        0.4203      I                        2   3       X 5                     1                         I
  53        0.0810      I                           23 *5     4                      1                         I
  54       -0.2666      I                          5 *32      4                      1                         I
  55       -0.4347      I                    5     *    3 2     4                    1                         I
  56       -0.3234      I                    5     *    3 2        4                 1                         I
  57       -0.0036      I                           XX          4                   1                         I
  58        0.3166      I                           23  *     45                     1                         I
  59        0.4286      I                          X  * 4         5                  1                         I
  60        0.2604      I                            3X    45                        1                         I
  61       -0.0879      I                          5 * 3   X                         1                         I
  62       -0.4268      I                5          *      3 4 2                     1                         I
  63       -0.6054      I          5               *         34   2                  1                         I
  64       -0.5861      I          5               *         X  2                    1                         I
  65       -0.4624      I             5            *         X2           1          I                         I
  66       -0.3396      I               5         *     X 31                         I                         I
  67       -0.2502      I            5         * 2 4 31                              I                         I
  68       -0.1887      I           5       X   4 31                                 I                         I
  69       -0.1537      I           5      2*   4 31                                 I                         I
  70       -0.1356      I               5 2 *   4 31                                 I                         I
  71       -0.1246      I               52  * 4   31                                 I                         I
  72       -0.1141      I               52  * 4     X                                I                         I
  73       -0.1018      I               25  * 4     X                                I                         I
  74       -0.0876      I               25   *4     X                                I                         I
  75       -0.0727      I             2  5   *4     X                                I                         I
  76       -0.0583      I            2      5 *4     X                               I                         I
  77       -0.0453      I            2      5 *4     X                               I                         I
  78       -0.0342      I           2       5*4     X                                I                         I
  79       -0.0270      I          2        5*41   3                                 I                         I
  80       -0.0249      I           2       5*X    3                                 I                         I
  81       -0.0251      I          2        5*X    3                                 I                         I
  82       -0.0253      I          2        5*X    3                                 I                         I
  83       -0.0255      I          2        5*X    3                                 I                         I
  84       -0.0257      I          2        5*X    3                                 I                         I
  85       -0.0259      I          2        5*X    3                                 I                         I
  86       -0.0260      I          2        5*X    3                                 I                         I
  87       -0.0262      I          2        5*X    3                                 I                         I
  88       -0.0263      I          2        5*X    3                                 I                         I
  89       -0.0264      I          2        5*X    3                                 I                         I
  90       -0.0264      I          2        5*X    3                                 I                         I
  91       -0.0264      I          2        5*X    3                                 I                         I
  92       -0.0264      I          2        5*X    3                                 I                         I
  93       -0.0264      I          2        5*X    3                                 I                         I
  94       -0.0263      I          2        5*X    3                                 I                         I
  95       -0.0262      I          2        5*X    3                                 I                         I
  96       -0.0261      I          2        5*X    3                                 I                         I
  97       -0.0259      I          2        5*X    3                                 I                         I
                        +--------+--------+--------+--------+--------+--------+--------+--------+--------+--------+
```

```
STEP#= 80  TIME= 800.     REGION I,II:  0KM TC 4KM IN 250M STEPS - 4KM TO 6KM IN 25M STEPS   J=41 CORRESPONDS TO Z=4.0KM
SYMBOL INDEX:  *=100.*DU
               1=0.5*INVERSE RIW
               2=10.*U1(X=C)
               3=10.*W1(X=C)
               4=10.*WAVE ENERGY DENSITY
               5=10.*WIND ENERGY DENSITY
               X=COMMON VALUES
               U=MAXIMUM SCALE VALUE EQUALLED OR EXCEEDED
```

J	100.*DU	-5.0	0.0	5.0
1	0.0		X 2	
2	0.0038		X32	
3	0.0140		X 23	
4	0.0271		X 23	
5	0.0386		2X 3	
6	0.0447		2 X 3	
7	0.0431		2 X 3	
8	0.0344		2 X 3	
9	0.0217		2X 3	
10	0.0094		X 3	
11	0.0018		X X	
12	0.0014		X 2	
13	0.0076		3X 2	
14	0.0169		3 X 2	
15	0.0243		3 X 2	
16	0.0246		3 X	
17	0.0167		X X	
18	0.0157		X X	
19	0.0146		23 X	
20	0.0136		23 X	
21	0.0126		23 X	
22	0.0117		23 X	
23	0.0108		23 X	
24	0.0100		23 X	
25	0.0094		23 X	
26	0.0088		2 3 X	
27	0.0085		2 3 X	
28	0.0083		2 3 X	
29	0.0083		2 3 X	
30	0.0086		2 3 X	
31	0.0090		2 3 X	
32	0.0098		2 3 X	
33	0.0107		2 3 X	
34	0.0119		2 3 X	
35	0.0142		2 3 X 1	
36	0.0174		2 3 X 1	
37	0.0186		2 3 X 1	
38	0.0156		2 3 X 1	
39	0.0083		2 3 X 1	
40	-0.0021		2 X4 1	
41	-0.0128		2 X4 1	
42	-0.0206		2 X4 1	
43	-0.0224		2 X4 1	
44	-0.0170		2 X4 1	
45	-0.0060		2 X4 1	
46	0.0080		2 3X 1	
47	0.0254		2 3X 1	
48	0.0526		2 3X 1	
49	0.1434		2 34X 1	
50	0.3730		2 34 *5 1	
51	0.6883		2 3 4 * 5 1	
52	0.8814		2 3 4 * * 5 1	
53	0.7524	2	3 4 * * 5 1	
54	0.3246	2	3 * X 1	
55	-0.1050	2	5X 4 1	
56	-0.2261	2	5 * 3 4 1	
57	-0.0380		2 X 4 1	
58	0.1431		3 * 5 2 4 1	
59	0.0268		X 4 2 1	
60	-0.3500	5	* 3 4 2 1	
61	-0.6918	5	* 3 4 2 1	
62	-0.7597	5	* 34 2 1	
63	-0.5676	5	* X2 1	
64	-0.2975	5	X X 1	
65	-0.1117		5 2* X 1	
66	-0.0400		XX4 1	
67	-0.0181		2X4 1	
68	-0.0043		XX 1	
69	0.0058		2X 1	
70	0.0130		X 1	
71	0.0164		X2 1	
72	0.0152		X 2 1	
73	0.0104		X 2 1	
74	0.0042		X 2 1	
75	-0.0014		XX 2 1	
76	-0.0050		XX2 1	
77	-0.0061		XX 1	
78	-0.0050		XX 1	
79	-0.0032		XX1	
80	-0.0021		XX	
81	-0.0017		XX	
82	-0.0014		XX	
83	-0.0011		XX	
84	-0.0010		XX	
85	-0.0009		XX	
86	-0.0009		XX	
87	-0.0010		XX	
88	-0.0011		XX	
89	-0.0013		XX	
90	-0.0015		2XX	
91	-0.0017		2XX	
92	-0.0020		2XX	
93	-0.0022		2XX3	
94	-0.0025		2XX3	
95	-0.0028		2XX3	
96	-0.0030		2XX3	
97	-0.0033		2XX3	

STEP#=120   TIME=1200.   REGICN I,II: 0KM TC 4KM IN 250M STEPS - 4KM TU 6KM IN 25M STEPS   J=41 CORRESPONDS TO Z=4.0KM   96

SYMBOL INDEX: *=100.*DU
              1=0.5*(INVERSE RI#
              2=10.*U1(X=C)
              3=10.*W1(X=0)
              4=10.*WAVE ENERGY DENSITY
              5=10.*WIND ENERGY DENSITY
              X=CUMMON VALUES
              0=MAXIMUM SCALE VALUE EQUALLED CR EXCEEDED

J	100.*DU
1	0.0
2	0.0067
3	0.0228
4	0.0385
5	0.0445
6	0.0374
7	0.0218
8	0.0069
9	-0.0003
10	0.0030
11	0.0095
12	0.0126
13	0.0100
14	0.0059
15	0.0058
16	0.0106
17	0.0169
18	0.0174
19	0.0180
20	0.0185
21	0.0189
22	0.0193
23	0.0155
24	0.0197
25	0.0196
26	0.0194
27	0.0189
28	0.0180
29	0.0168
30	0.0151
31	0.0128
32	0.0097
33	0.0058
34	0.0007
35	-0.0001
36	0.0109
37	0.0314
38	0.0522
39	0.0642
40	0.0605
41	0.0406
42	0.0131
43	-0.0066
44	-0.0036
45	0.0273
46	0.0792
47	0.1438
48	0.2265
49	0.3967
50	0.5851
51	0.4285
52	-0.1988
53	-0.7204
54	-0.5089
55	0.3399
56	1.1783
57	1.4545
58	0.9471
59	-0.1263
60	-1.0481
61	-1.1907
62	-0.7107
63	-0.2370
64	-0.0691
65	-0.0653
66	-0.0644
67	-0.0500
68	-0.0361
69	-0.0194
70	-0.0001
71	0.0159
72	0.0228
73	0.0191
74	0.0085
75	-0.0029
76	-0.0101
77	-0.0109
78	-0.0063
79	-0.0010
80	0.0010
81	0.0011
82	0.0010
83	0.0009
84	0.0007
85	0.0004
86	0.0002
87	-0.0001
88	-0.0004
89	-0.0007
90	-0.0009
91	-0.0011
92	-0.0013
93	-0.0015
94	-0.0016
95	-0.0017
96	-0.0017
97	-0.0017

Scale axis: -5.0 .... 0.0 .... 5.0

SYMBOL INDEX: *=100.*DU
1=0.5*INVERSE RIN
2=10.*U1(X=0)
3=10.*W1(X=0)
4=10.*WAVE ENERGY DENSITY
5=10.*WIND ENERGY DENSITY
X=COMMON VALUES
U=MAXIMUM SCALE VALUE EQUALLED OR EXCEEDED

J	100.*DU	-5.0 .... 0.0 .... 5.0
1	0.0	
2	0.0019	
3	0.0051	
4	0.0054	
5	0.0024	
6	0.0017	
7	0.0091	
8	0.0238	
9	-0.0370	
10	0.0389	
11	0.0277	
12	0.0125	
13	0.0037	
14	0.0045	
15	0.0113	
16	0.0222	
17	0.0317	
18	0.0320	
19	0.0320	
20	0.0317	
21	0.0312	
22	0.0304	
23	0.0293	
24	0.0280	
25	0.0264	
26	0.0247	
27	0.0227	
28	0.0207	
29	0.0187	
30	0.0168	
31	0.0151	
32	0.0139	
33	0.0131	
34	0.0129	
35	0.0207	
36	0.0401	
37	0.0523	
38	0.0405	
39	0.0101	
40	-0.0184	
41	-0.0218	
42	0.0072	
43	0.0510	
44	0.0766	
45	0.0621	
46	0.0152	
47	-0.0339	
48	-0.0570	
49	0.1279	
50	0.7935	
51	1.3971	
52	0.6653	
53	-1.1161	
54	-1.6309	
55	0.0642	
56	1.9024	
57	1.8177	
58	0.2785	
59	-0.8750	
60	-0.8371	
61	-0.3838	
62	-0.2925	
63	-0.3572	
64	-0.2345	
65	-0.0592	
66	0.0060	
67	0.0095	
68	0.0042	
69	-0.0022	
70	-0.0019	
71	0.0061	
72	0.0153	
73	0.0177	
74	0.0114	
75	0.0013	
76	-0.0053	
77	-0.0046	
78	0.0013	
79	0.0060	
80	0.0057	
81	0.0035	
82	0.0018	
83	0.0005	
84	-0.0005	
85	-0.0013	
86	-0.0018	
87	-0.0021	
88	-0.0023	
89	-0.0024	
90	-0.0025	
91	-0.0024	
92	-0.0023	
93	-0.0022	
94	-0.0021	
95	-0.0020	
96	-0.0019	
97	-0.0018	

```
STEP#=200  TIME=2000.      REGION I,II:  0KM TO 4KM IN 250M STEPS - 4KM TO 6KM IN 25M STEPS  J=41 CORRESPONDS TO Z=4.0KM
SYMBOL INDEX:  *=100.*DU
               1=0.5*INVERSE RIN
               2=10.*U1(X=0)
               3=10.*W1(X=C)
               4=10.*WAVE ENERGY DENSITY
               5=10.*WIND ENERGY DENSITY
               X=COMMON VALUES
               U=MAXIMUM SCALE VALUE EQUALLED OR EXCEEDED


   J        100.*DU    -5.0                                                       0.0                                                       5.0
                        +----------+----------+----------+----------+----------+----------+----------+----------+----------+----------+
   1         0.0        I                                                        2    X                                                  I
   2         0.0040     I                                                        2    X                                                  I
   3         0.0117     I                                                        2    X3                                                 I
   4         0.0150     I                                                        2    X3                                                 I
   5         0.0113     I                                                        2    X                                                  I
   6         0.0061     I                                                        2 3X                                                    I
   7         0.0063     I                                                        X X                                                     I
   8         0.0127     I                                                        3  X                                                    I
   9         0.0198     I                                                        3   X2                                                  I
  10         0.0217     I                                                        3   X 2                                                 I
  11         0.0171     I                                                        3   X    2                                              I
  12         0.0091     I                                                        3   X      2                                            I
  13         0.0031     I                                                        3   X        2                                          I
  14         0.0021     I                                                        3  X          2                                         I
  15         0.0039     I                                                        3  X         2                                          I
  16         0.0062     I                                                        3 X       2                                             I
  17         0.0138     I                                                        3 X 2                                                   I
  18         0.0147     I                                                        3 X 2                                                   I
  19         0.0155     I                                                        3 X2                                                    I
  20         0.0161     I                                                        3 X2                                                    I
  21         0.0165     I                                                        3 X2                                                    I
  22         0.0167     I                                                        3 X                                                     I
  23         0.0165     I                                                        3 X                                                     I
  24         0.0161     I                                                        3 X                                                     I
  25         0.0154     I                                                        3 X                                                     I
  26         0.0143     I                                                        32X                                                     I
  27         0.0129     I                                                        32X                                                     I
  28         0.0114     I                                                        32X                                                     I
  29         0.0097     I                                                        32X                                                     I
  30         0.0081     I                                                        32X                                                     I
  31         0.0070     I                                                        32X                                                     I
  32         0.0064     I                                                        32X                                                     I
  33         0.0069     I                                                        X X                                                     I
  34         0.0085     I                                                        X X                                                     I
  35         0.0193     I                                                        X X1                                                    I
  36         0.0384     I                                                      23 X      1                                               I
  37         0.0395     I                                                      2 3 X     1                                               I
  38         0.0111     I                                                      2 3 X     1                                               I
  39        -0.0194     I                                                      2 3X4     1                                               I
  40        -0.0162     I                                                      23X4      1                                               I
  41         0.0270     I                                                      23 X      1                                               I
  42         0.0725     I                                                      2  3 X    1                                               I
  43         0.0723     I                                                    2   3 X     1                                               I
  44         0.0231     I                                                    2   3 X     1                                               I
  45        -0.0183     I                                                    2   3X4     1                                               I
  46         0.0163     I                                                    2   3 X     1                                               I
  47         0.1104     I                                                    2   3 4X    1                                               I
  48         0.2268     I                                                  2     3 4 X 1                                                 I
  49         0.1254     I                                                2       3 4X        1                                           I
  50        -0.0749     I                                                2     3X4            1                                          I
  51         0.8698     I                                              2   3 4        *   5      1                                       I
  52         2.2524     I                             2              3       4    * 4 5      *  1              5                         I
  53         0.6233     I                    2                       3       4 5                                                        I
  54        -2.0357     I        5                   *            2         3         4            1                                     I
  55        -0.0500     I                                         2         5X4                    1                                    I
  56         3.1056     I                              2                     3              4              1         *                   O
  57         1.0463     I                           *                        3          2  *      4       1 5                           I
  58        -1.9423     O                        *                           3             4             2 1                            I
  59        -0.6554     I                      5                   *   2     34                  1                                      I
  60         0.8354     I                              2           3     4        *           X                                         I
  61        -0.2864     I                         5        *   3    4   2             1                                                 I
  62        -0.8755     I                   5          *      X     2                1                                                  I
  63        -0.2252     I                            5   * 2X                 1                                                         I
  64        -0.0513     I                                5*43 2                     1                                                   I
  65        -0.1859     I                           5      * 43  2          1                                                          I
  66        -0.1216     I                           5  * 4X  1                                                                         I
  67        -0.0250     I                                5X43  1                                                                       I
  68         0.0070     I                                2X3  1                                                                        I
  69        -0.0156     I                                XX3  1                                                                        I
  70        -0.0434     I                                5X43  1                                                                       I
  71        -0.0355     I                                X*43  1                                                                       I
  72        -0.0008     I                               2 X43  1                                                                       I
  73         0.0216     I                               2  X3  1                                                                       I
  74         0.0118     I                               2  X3  1                                                                       I
  75        -0.0126     I                               2X43  1                                                                        I
  76        -0.0229     I                               X*43  1                                                                        I
  77        -0.0114     I                               2 X43  1                                                                       I
  78         0.0055     I                               2  X3  1                                                                       I
  79         0.0103     I                               2  XX                                                                          I
  80         0.0046     I                               2  X3                                                                          I
  81        -0.0019     I                               2 XX3                                                                          I
  82        -0.0057     I                               2 XX 3                                                                         I
  83        -0.0077     I                               2 XX 3                                                                         I
  84        -0.0084     I                               2 XX  3                                                                        I
  85        -0.0083     I                               2 XX  3                                                                        I
  86        -0.0078     I                               2 XX 3                                                                         I
  87        -0.0069     I                               2 XX 3                                                                         I
  88        -0.0070     I                               2 XX 3                                                                         I
  89        -0.0051     I                               2 XX 3                                                                         I
  90        -0.0044     I                               2  XX 3                                                                        I
  91        -0.0038     I                               2  XX 3                                                                        I
  92        -0.0034     I                               2  XX 3                                                                        I
  93        -0.0031     I                               2  XX 3                                                                        I
  94        -0.0031     I                               2  XX 3                                                                        I
  95        -0.0031     I                               2  XX 3                                                                        I
  96        -0.0033     I                               2  XX 3                                                                        I
  97        -0.0035     I                               2  XX 3                                                                        I
                        +----------+----------+----------+----------+----------+----------+----------+----------+----------+----------+
```
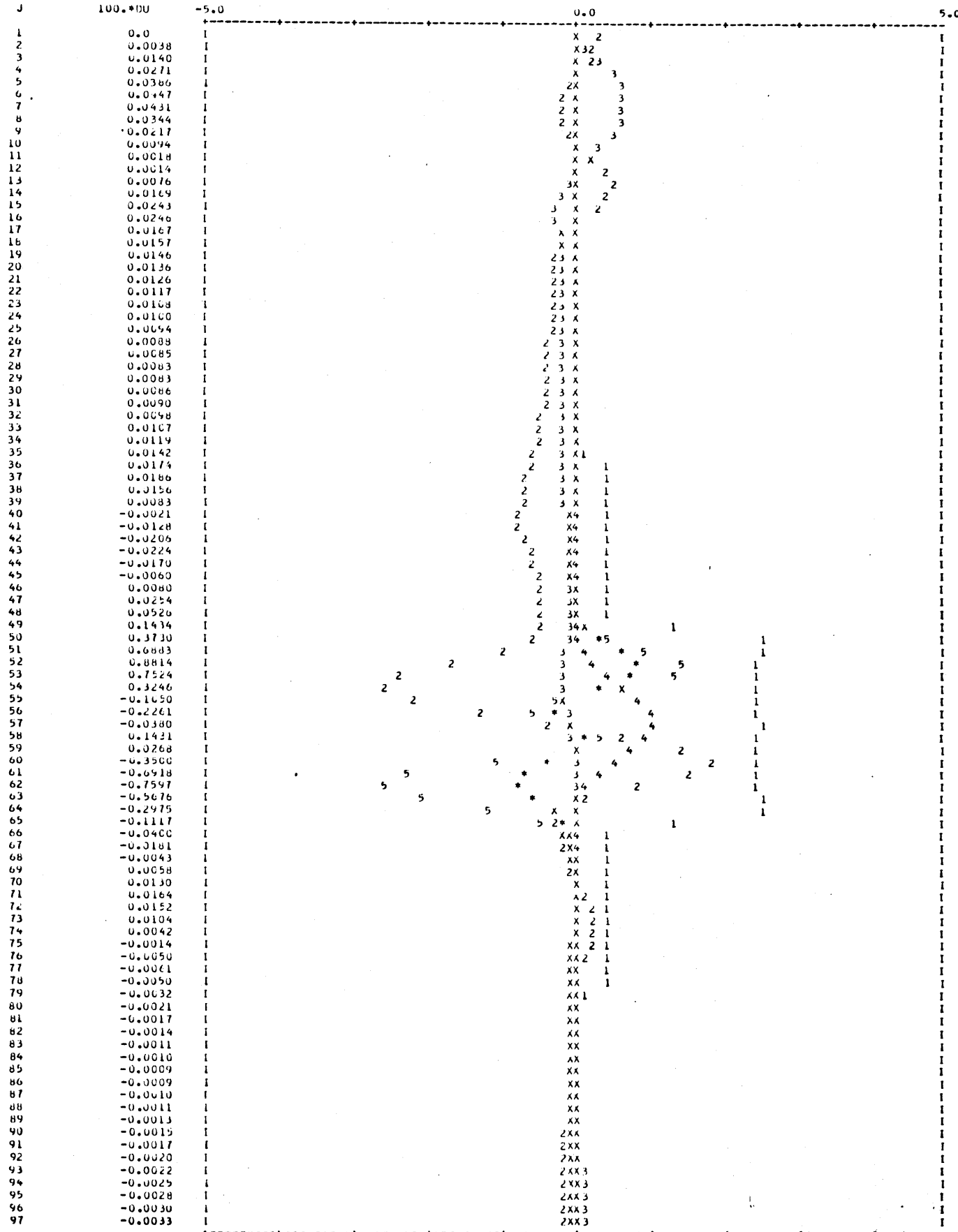
SYMBUL INDEX: *=100.*DU
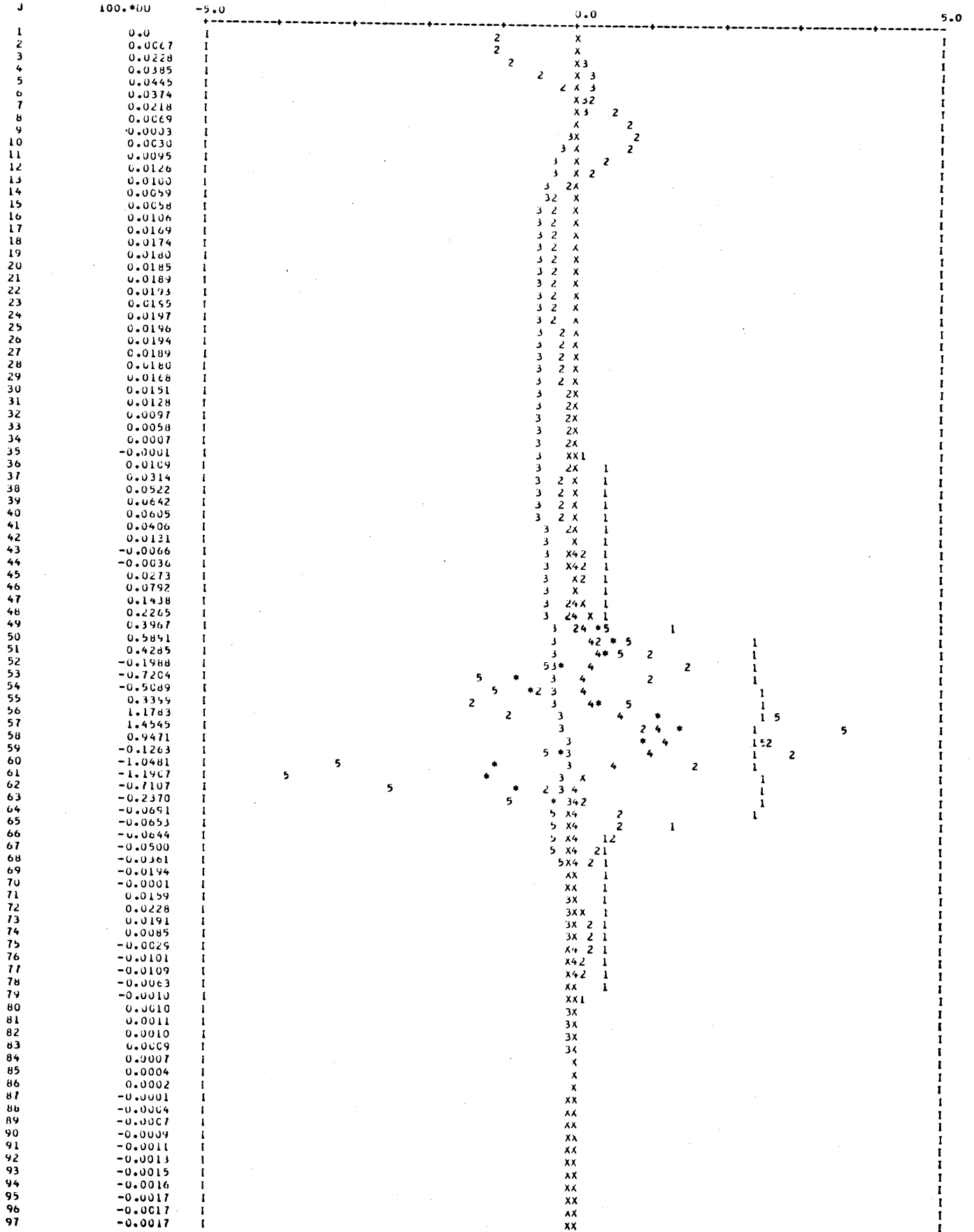   1=0.5*INVERSE RI#
              2=10.*U1(X=0)
              3=10.*W1(X=0)
              4=10.*WAVE ENERGY DENSITY
              5=10.*WIND ENERGY DENSITY
              X=COMMON VALUES
              U=MAXIMUM SCALE VALUE EQUALLED OR EXCEEDED

J	100.*DU
1	0.0
2	0.0048
3	0.0151
4	0.0228
5	0.0246
6	0.0222
7	0.0182
8	0.0137
9	0.0096
10	0.0076
11	0.0070
12	0.0059
13	0.0047
14	0.0044
15	0.0032
16	0.0002
17	0.0020
18	0.0024
19	0.0029
20	0.0033
21	0.0036
22	0.0037
23	0.0037
24	0.0034
25	0.0028
26	0.0020
27	0.0011
28	-0.0000
29	-0.0010
30	-0.0016
31	-0.0014
32	0.0003
33	0.0042
34	0.0111
35	0.0175
36	0.0102
37	-0.0114
38	-0.0193
39	0.0042
40	0.0313
41	0.0226
42	-0.0111
43	-0.0122
44	0.0385
45	0.0794
46	0.0544
47	0.0158
48	0.0803
49	0.3279
50	0.1453
51	0.1610
52	1.9133
53	1.6100
54	-1.4165
55	-0.1255
56	2.3061
57	-0.0438
58	-1.2897
59	0.2336
60	0.2812
61	-0.3992
62	-0.4519
63	-0.2677
64	-0.0813
65	-0.0596
66	-0.0649
67	-0.0144
68	0.0127
69	0.0083
70	-0.0043
71	-0.0030
72	0.0088
73	0.0145
74	0.0087
75	0.0006
76	-0.0005
77	0.0041
78	0.0069
79	0.0050
80	0.0020
81	0.0003
82	-0.0004
83	-0.0006
84	-0.0006
85	-0.0004
86	-0.0001
87	0.0001
88	0.0003
89	0.0004
90	0.0005
91	0.0006
92	0.0005
93	0.0005
94	0.0004
95	0.0003
96	0.0002
97	0.0001

SYMBUL INDEX: *=100.*DU
1=0.5*INVERSF RIW
2=10.*U1(X=0)
3=10.*w1(X=C)
4=10.*WAVE ENEKGY DENSITY
5=10.*WIND ENEPGY DENSITY
X=CUMMON VALUES
L=MAXIMUM SCALE VALUE EQUALLED OR EXCEEDED

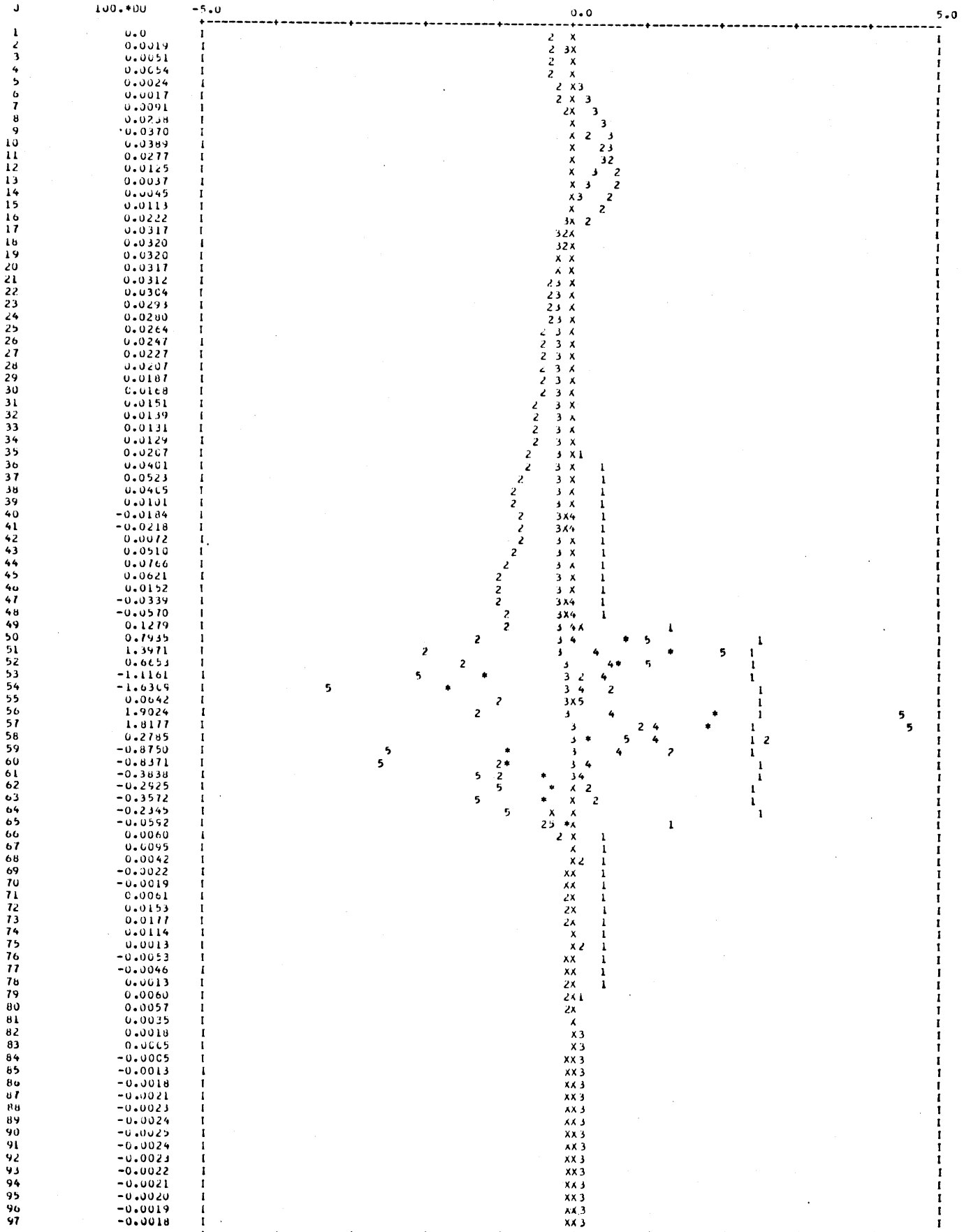| J	100.*DU	-5.0	0.0	5.0
1	0.0		2 X	
2	-0.0002		2 XX	
3	-0.0003		23*X	
4	0.0005		23 X	
5	0.0036		X X	
6	0.0088		32 X	
7	0.0143		32 X	
8	0.0178		3 2X	
9	0.0171		3 X	
10	0.0115		3 X 2	
11	0.0045		3 X 2	
12	0.0013		3 X 2	
13	0.0024		3 X 2	
14	0.0058		3X 2	
15	0.0110		3 X 2	
16	0.0124		3 X2	
17	0.0115		3 X	
18	0.0120		3 2X	
19	0.0128		3 2X	
20	0.0137		3 2X	
21	0.0147		3 2X	
22	0.0158		3 2X	
23	0.0170		32 X	
24	0.0181		32 X	
25	0.0191		32 X	
26	0.0198		X X	
27	0.0202		X X	
28	0.0201		X X	
29	0.0193		X X	
30	0.0176		X X	
31	0.0147		23 X	
32	0.0105		23 X	
33	0.0043		23 X	
34	-0.0047		X *X	
35	0.0021		X X1	
36	0.0341		23 X 1	
37	0.0425		2 3 X 1	
38	0.0C54		2 3 X 1	
39	-0.0128		23 X4 1	
40	0.0304		23 X 1	
41	0.0712		2 3 X 1	
42	0.0402		2 3 X 1	
43	-0.0015		2 3 X4 1	
44	0.0471		2 3 X 1	
45	0.1306		2 3 4X 1	
46	0.1160		2 3 X* 1	
47	0.0550		2 3 X 1	
48	0.1495		2 3 4X 1	
49	0.2523		2 3 4 X 1	
50	-0.0156		3X24	
51	0.2994		X 4 * 5 1	
52	1.0557		3 24 * 5 1	
53	0.5681		3 4 * 2 5 1	
54	-0.8957	5 X 3 4	1	
55	0.7601	2	3 4 * 5 1	
56	3.2416	2	3 4 *	0
57	-0.0530		5X 2 4 1	
58	-1.6540	5 *	3 4 2 1	
59	0.5385		23 4* 5 1	
60	-0.0115		X 4 2 1	
61	-0.3438	5	* X4 1	
62	-0.1655	5	*3 4 2 1	
63	-0.3009	5	* 34 2 1	
64	-0.0691		5 *34 2	
65	-0.1728	5	* X 2 1	
66	-0.1305	5	2 * X	
67	-0.0412		5*X 21	
68	-0.0650		5 *X 2 1	
69	-0.0540		5 *x 1	
70	0.0021		2X 1	
71	0.0096		X 1	
72	-0.0201		5*X 1	
73	-0.0250		5XX 1	
74	0.0088		2 X 1	
75	0.0125		2 X 1	
76	-0.0126		XX 1	
77	-0.0162		2XX 1	
78	0.0033		2 X 1	
79	0.0108		2 X1	
80	0.0024		2 X	
81	-0.0052		2XX	
82	-0.0080		2XX	
83	-0.0082		2XX	
84	-0.0070		2XX	
85	-0.0053		2 XX	
86	-0.0036		2 XX	
87	-0.0023		2 XX	
88	-0.0014		2 XX	
89	-0.0009		2 XX	
90	-0.0007		2 XX	
91	-0.0009		2 XX	
92	-0.0012		2 XX	
93	-0.0017		2 XX	
94	-0.0021		2 XX	
95	-0.0025		2 XX3	
96	-0.0029		2 XX3	
97	-0.0031		2 XX3	

SYMBOL INDEX: *=100.*DU
              1=0.5*INVERSE RIW
              2=10.*UI(X=C)
              3=10.*WI(X=C)
              4=10.*WAVE ENERGY DENSITY
              5=10.*WIND ENERGY DENSITY
              X=COMMON VALUES
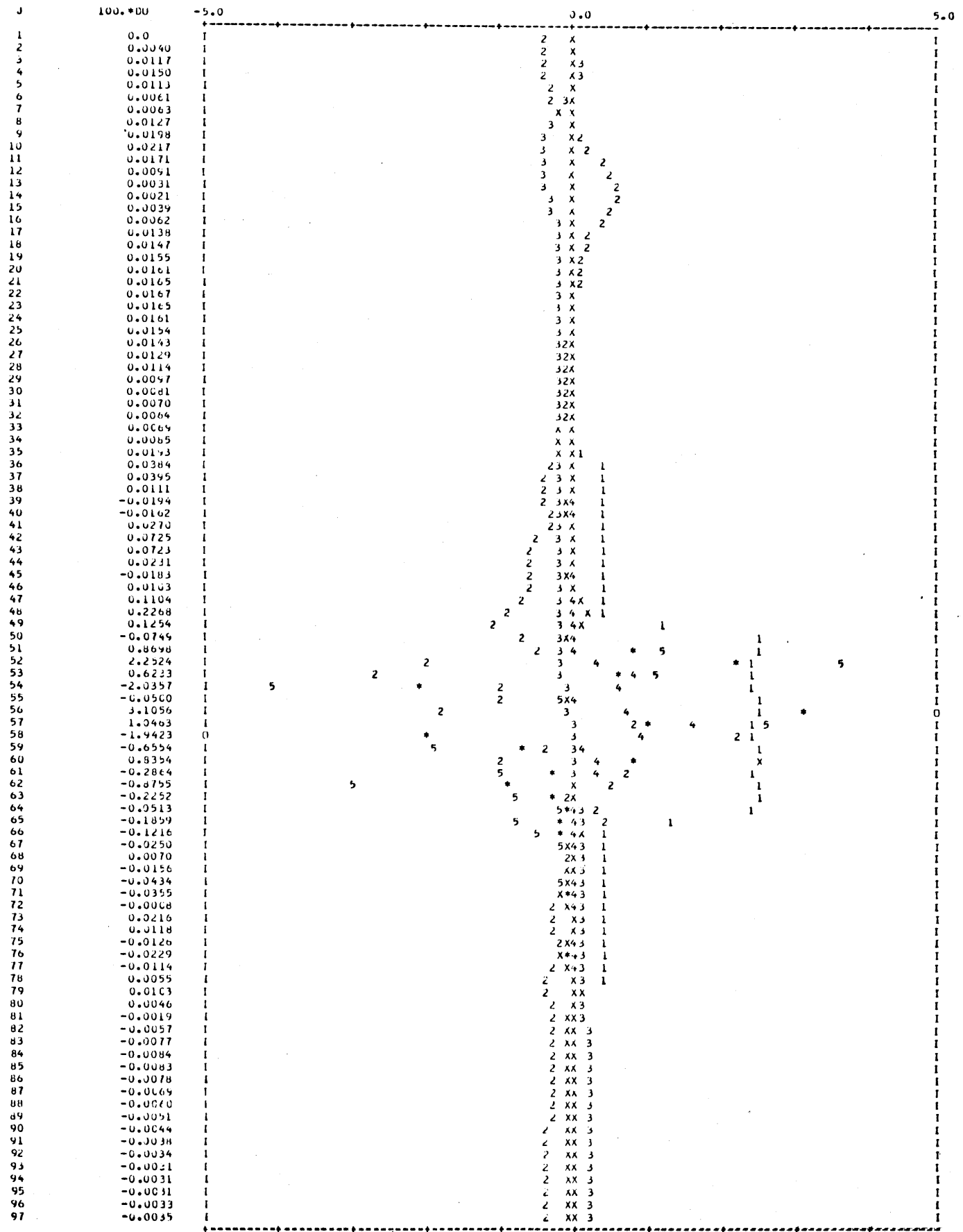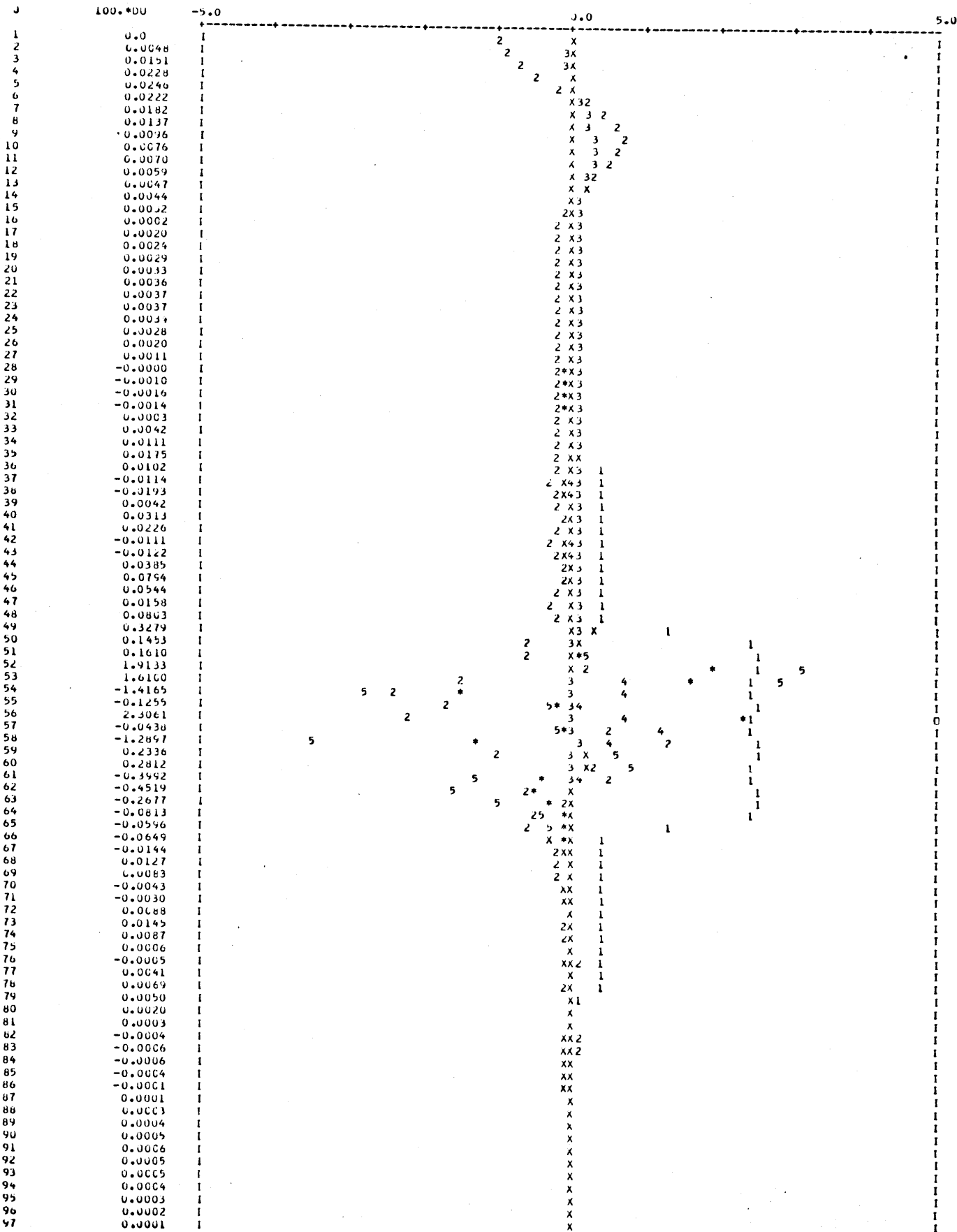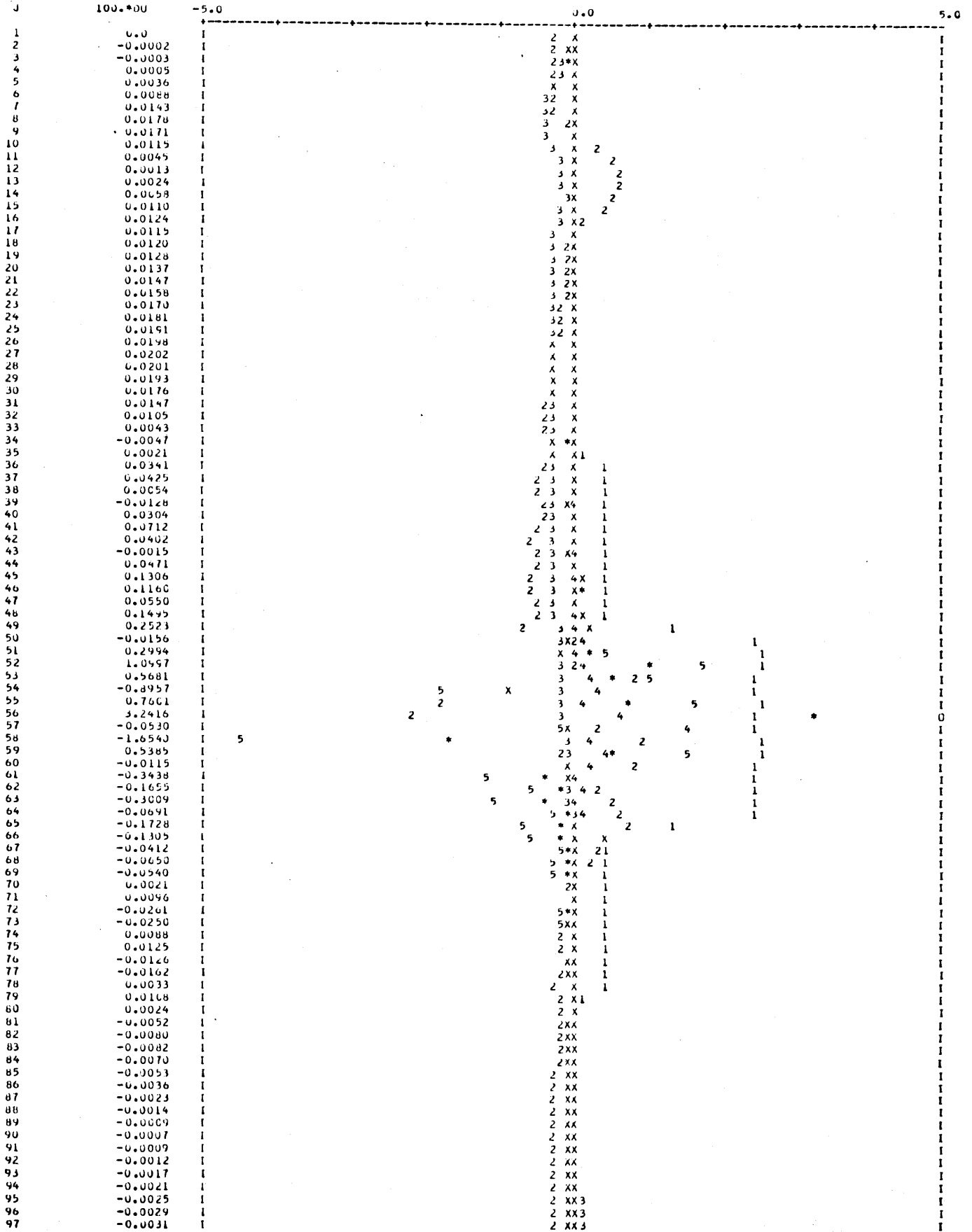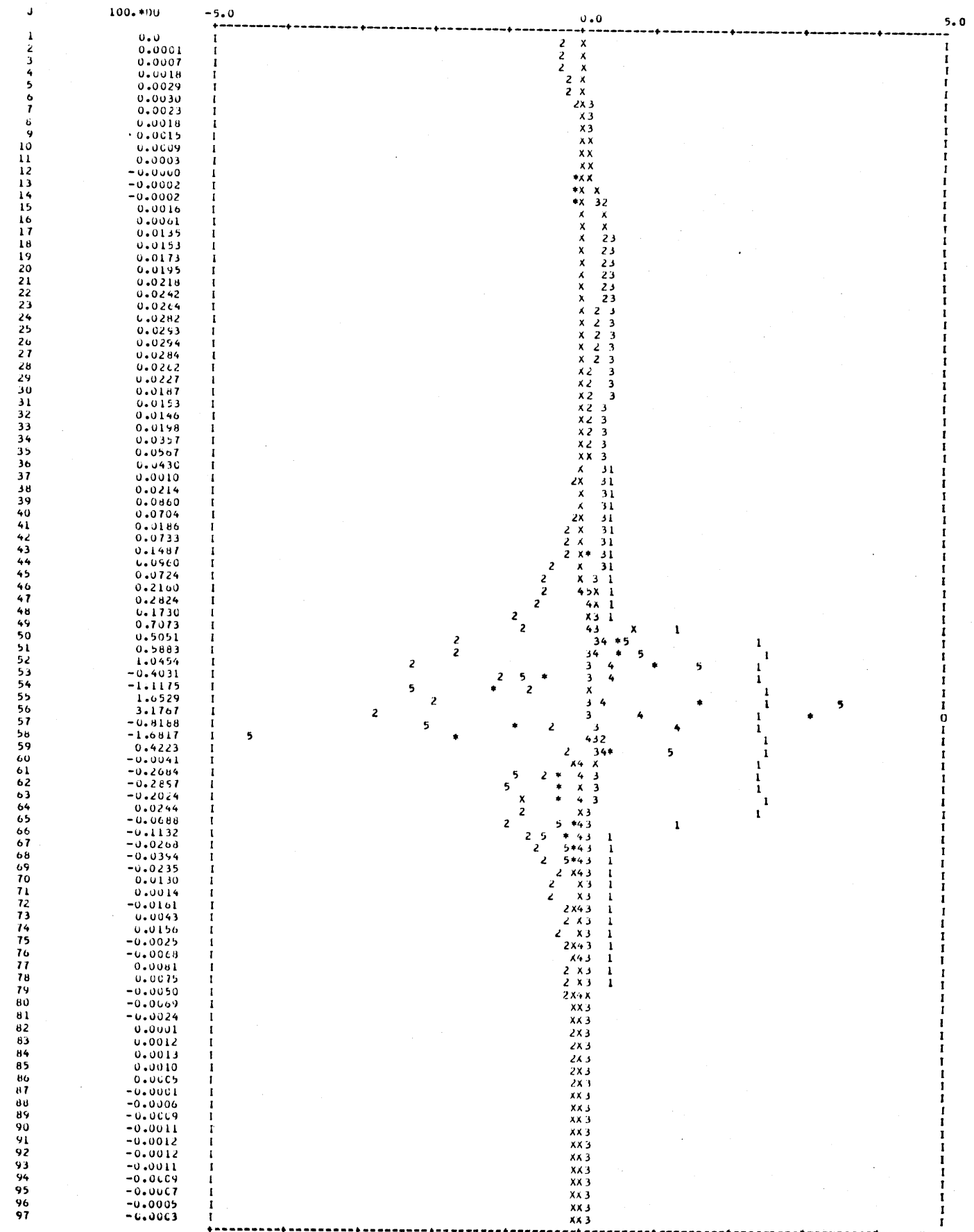   G=MAXIMUM SCALE VALUE EQUALLED OR EXCEEDED

J	100.*DU
1	0.0
2	0.0001
3	0.0007
4	0.0018
5	0.0029
6	0.0030
7	0.0023
8	0.0018
9	0.0015
10	0.0009
11	0.0003
12	-0.0000
13	-0.0002
14	-0.0002
15	0.0016
16	0.0001
17	0.0135
18	0.0153
19	0.0173
20	0.0195
21	0.0218
22	0.0242
23	0.0264
24	0.0282
25	0.0293
26	0.0294
27	0.0284
28	0.0262
29	0.0227
30	0.0187
31	0.0153
32	0.0146
33	0.0198
34	0.0357
35	0.0567
36	0.0430
37	0.0010
38	0.0214
39	0.0860
40	0.0704
41	0.0186
42	0.0733
43	0.1487
44	0.0960
45	0.0724
46	0.2160
47	0.2824
48	0.1730
49	0.7073
50	0.5051
51	0.5883
52	1.0454
53	-0.4031
54	-1.1175
55	1.6529
56	3.1767
57	-0.8168
58	-1.6817
59	0.4223
60	-0.0041
61	-0.2604
62	-0.2857
63	-0.2024
64	0.0244
65	-0.0688
66	-0.1132
67	-0.0268
68	-0.0394
69	-0.0235
70	0.0130
71	0.0014
72	-0.0161
73	0.0043
74	0.0156
75	-0.0025
76	-0.0068
77	0.0081
78	0.0075
79	-0.0050
80	-0.0069
81	-0.0024
82	0.0001
83	0.0012
84	0.0013
85	0.0010
86	0.0005
87	-0.0001
88	-0.0006
89	-0.0009
90	-0.0011
91	-0.0012
92	-0.0012
93	-0.0011
94	-0.0009
95	-0.0007
96	-0.0005
97	-0.0003

Plot scale: -5.0 ... 0.0 ... 5.0

STEP#=360 TIME=3600.   REGION 1,11: 0KM TC 4KM IN 250M STEPS - 4KM TO 6KM IN 25M STEPS   J=41 CORRESPCNDS TO Z=4.0KM
SYMBOL INDEX: *=100.*DU
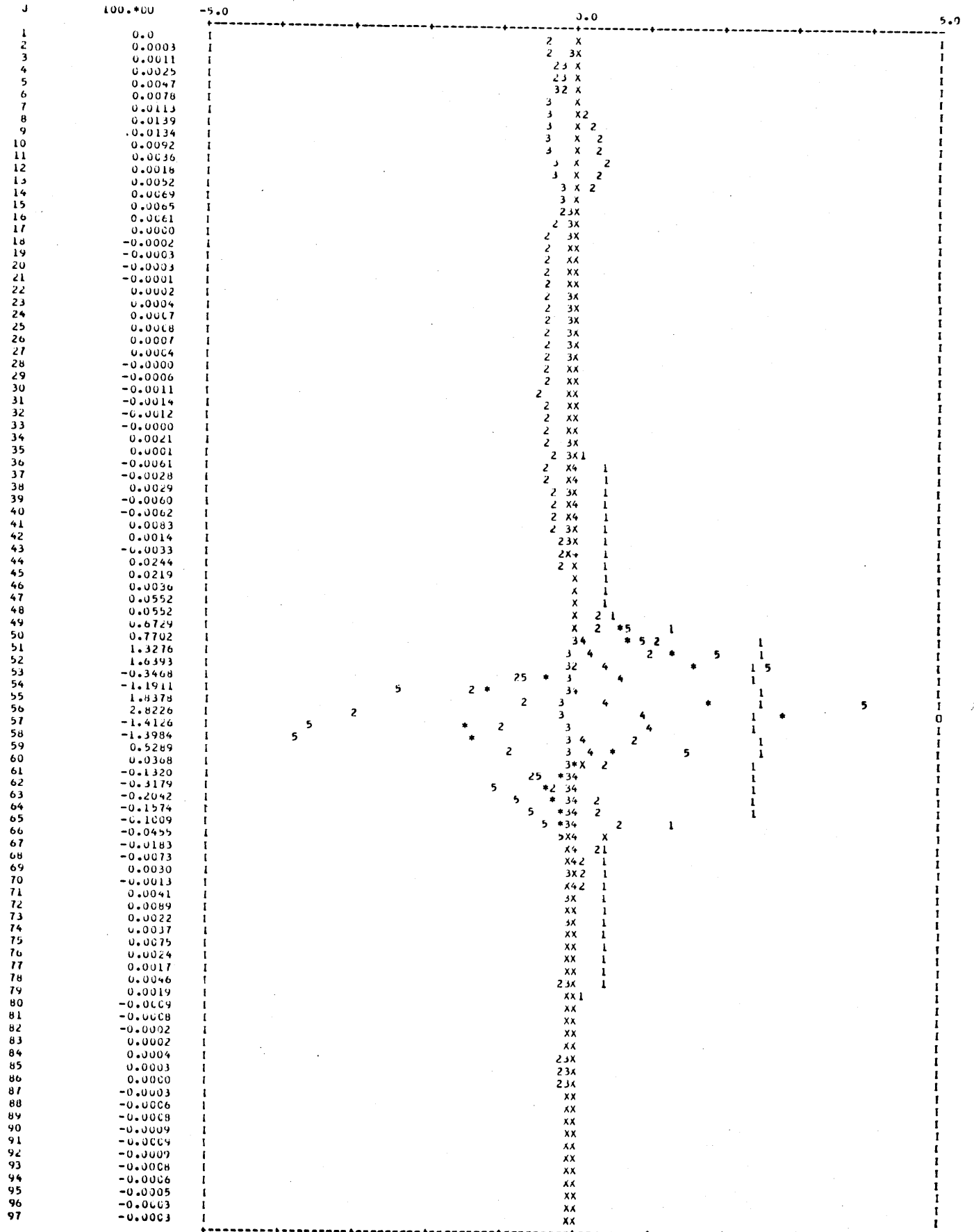   1=0.5*INVERSE RI#
             2=10.*UI(X=0)
             3=10.*WI(X=C)
             4=10.*WAVE ENERGY DENSITY
             5=10.*WIND ENERGY DENSITY
             X=COMMON VALUES
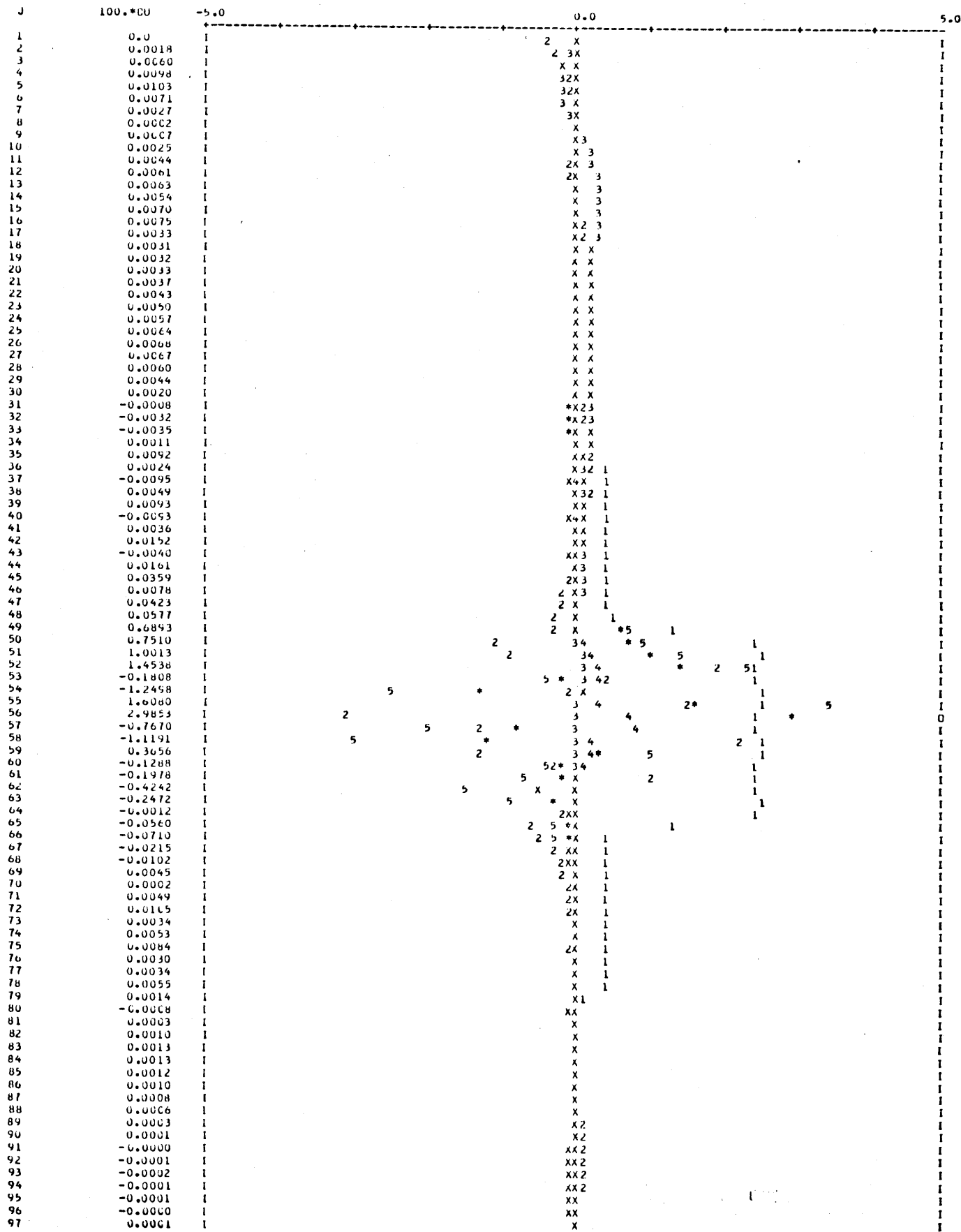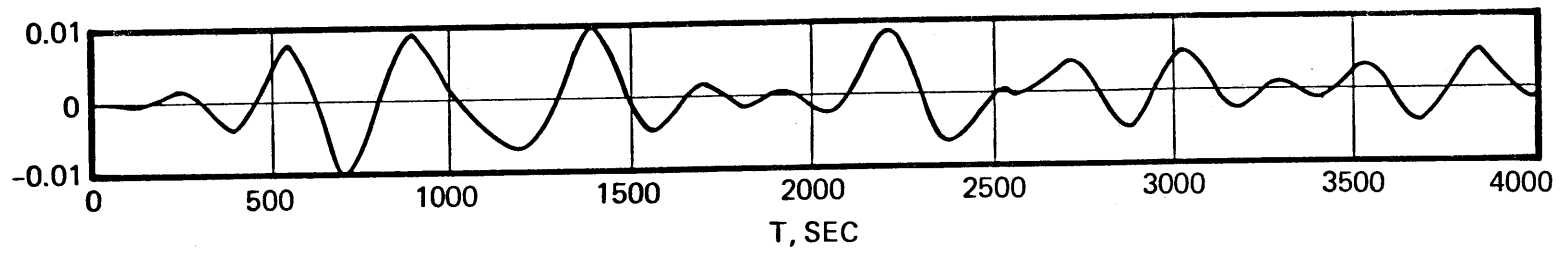   0=MAXIMUM SCALE VALUE EQUALLED OR EXCEEDED

J	100.*DU
1	0.0
2	0.0003
3	0.0011
4	0.0025
5	0.0047
6	0.0078
7	0.0113
8	0.0139
9	.0.0134
10	0.0092
11	0.0036
12	0.0018
13	0.0052
14	0.0069
15	0.0065
16	0.0061
17	0.0000
18	-0.0002
19	-0.0003
20	-0.0003
21	-0.0001
22	0.0002
23	0.0004
24	0.0007
25	0.0008
26	0.0007
27	0.0004
28	-0.0000
29	-0.0006
30	-0.0011
31	-0.0014
32	-0.0012
33	-0.0000
34	0.0021
35	0.0001
36	-0.0061
37	-0.0028
38	0.0029
39	-0.0060
40	-0.0062
41	0.0083
42	0.0014
43	-0.0033
44	0.0244
45	0.0219
46	0.0036
47	0.0552
48	0.0552
49	0.6729
50	0.7702
51	1.3276
52	1.6393
53	-0.3468
54	-1.1911
55	1.8378
56	2.8226
57	-1.4126
58	-1.3984
59	0.5289
60	0.0368
61	-0.1320
62	-0.3179
63	-0.2042
64	-0.1574
65	-0.1009
66	-0.0455
67	-0.0183
68	-0.0073
69	0.0030
70	-0.0013
71	0.0041
72	0.0089
73	0.0022
74	0.0037
75	0.0075
76	0.0024
77	0.0017
78	0.0046
79	0.0019
80	-0.0009
81	-0.0008
82	-0.0002
83	0.0002
84	0.0004
85	0.0003
86	0.0000
87	-0.0003
88	-0.0006
89	-0.0008
90	-0.0009
91	-0.0009
92	-0.0009
93	-0.0008
94	-0.0006
95	-0.0005
96	-0.0003
97	-0.0003

Scale: -5.0 .... 0.0 .... 5.0

STEP#=400   TIME=4000.   REGION I,II: 0KM TO 4KM IN 250M STEPS - 4KM TO 6KM IN 25M STEPS   J=41 CORRESPONDS TO Z=4.0KM
SYMBOL INDEX: *=100.*DU
              1=0.5*INVERSE RI#
              2=10.*U1(X=0)
              3=10.*W1(X=0)
              4=10.*WAVE ENERGY DENSITY
              5=10.*WIND ENERGY DENSITY
              X=COMMON VALUES
              U=MAXIMUM SCALE VALUE EQUALLED OR EXCEEDED

J	100.*CU	-5.0	0.0	5.0
1	0.0		2 X	
2	0.0018		2 3X	
3	0.0060		X X	
4	0.0098		32X	
5	0.0103		32X	
6	0.0071		3 X	
7	0.0027		3X	
8	0.0002		X	
9	0.0007		X3	
10	0.0025		X 3	
11	0.0044		2X 3	
12	0.0061		2X 3	
13	0.0063		X 3	
14	0.0054		X 3	
15	0.0070		X 3	
16	0.0075		X2 3	
17	0.0033		X2 3	
18	0.0031		X X	
19	0.0032		X X	
20	0.0033		X X	
21	0.0037		X X	
22	0.0043		X X	
23	0.0050		X X	
24	0.0057		X X	
25	0.0064		X X	
26	0.0068		X X	
27	0.0067		X X	
28	0.0060		X X	
29	0.0044		X X	
30	0.0020		X X	
31	-0.0008		*X23	
32	-0.0032		*X23	
33	-0.0035		*X X	
34	0.0011		X X	
35	0.0092		XX2	
36	0.0024		X32 1	
37	-0.0095		X4X 1	
38	0.0049		X32 1	
39	0.0093		XX 1	
40	-0.0093		X4X 1	
41	0.0036		XX 1	
42	0.0152		XX 1	
43	-0.0040		XX3 1	
44	0.0161		X3 1	
45	0.0359		2X3 1	
46	0.0078		2 X3 1	
47	0.0423		2 X 1	
48	0.0577		2 X 1	
49	0.6893		2 X *5 1	
50	0.7510		2 34 * 5 1	
51	1.0013		2 34 * 5 1	
52	1.4538		3 4 * 2 51	
53	-0.1808		5 * 3 42 1	
54	-1.2498	5 *	2 X 1	
55	1.6060		3 4 2* 1 5	
56	2.9853	2	3 4 1 *	0
57	-0.7670	5 2 *	3 1	
58	-1.1191	5	* 3 4 2 1	
59	0.3056		2 3 4* 5 1	
60	-0.1288		52* 34 1	
61	-0.1978		5 * X 2 1	
62	-0.4242	5	X X 1	
63	-0.2472	5	* X 1	
64	-0.0012		2XX 1	
65	-0.0560		2 5 *X 1	
66	-0.0710		2 5 *X 1	
67	-0.0215		2 XX 1	
68	-0.0102		2XX 1	
69	0.0045		2 X 1	
70	0.0002		2X 1	
71	0.0049		2X 1	
72	0.0105		2X 1	
73	0.0034		X 1	
74	0.0053		X 1	
75	0.0084		2X 1	
76	0.0030		X 1	
77	0.0034		X 1	
78	0.0055		X 1	
79	0.0014		X1	
80	-0.0008		XX	
81	0.0003		X	
82	0.0010		X	
83	0.0013		X	
84	0.0013		X	
85	0.0012		X	
86	0.0010		X	
87	0.0008		X	
88	0.0006		X	
89	0.0003		X2	
90	0.0001		X2	
91	-0.0000		XX2	
92	-0.0001		XX2	
93	-0.0002		XX2	
94	-0.0001		XX2	
95	-0.0001		XX 1	
96	-0.0000		XX	
97	0.0001		X	

CALCULATED PRESSURE AT Z = 0 IN MB FOR MODEL A

REFERENCES

Boer, G. "Atmospheric Gravity Waves, an Observational and Numerical Study," MIT, Dept. of Meteorology, Ph.D Thesis, (1970).

Booker, J. R. & F. P. Bretherton, "The critical layer for internal gravity waves in a shear flow." 1967, JFM, 17, p. 513.

Breeding, R. J., "A non-linear investigation of critical levels for internal atmospheric gravity waves." 1971, JFM, 50, p. 545.

Bretherton, F. P., "Momentum transport by gravity waves." 1969, Quart. J. Roy. Met. Soc., 95, p. 213.

Bretherton, F. P., "On the mean motion induced by internal gravity waves." 1969, JFM, 36, p. 735.

Browland, F. K. (1965), MIT Aeroelastic & Structures, Res. Lab. Report. TR-92-4.

Claerbout, J., "Electromagnetic Effects of Atmospheric Gravity Waves," MIT, Dept. of Earth and Planetary Science, Ph.D Thesis (1967).

Collyer, M. R., "The stability of stratified shear flows." 1970, JFM, 42, p. 367.

Craik, A.D.D., "Resonant gravity wave interactions in a shear flow." 1968, JFM, 34, p. 531.

Drazin, P. G. & L. N. Howard, "Hydrodynamic stability of parallel flow of inviscid fluid." 1966, Adv. Appl. Mech., 9, p. 1.

Drazin, P. G., "The stability of a shear layer in air unbounded inviscid fluid." 1958, JFM, 4, p. 214.

Garrett, C.J.R., "On the interaction between internal gravity waves and a shear flow." 1968, JFM, 34, p. 711.

Grimshaw, R., "Nonlinear internal gravity waves in a slowly varying medium." 1972, JFM, 54, p. 193.

Hazel, P., "Numerical studies of the stability of inviscid stratified shear flows." 1972, JFM, 51, p. 39.

Houghton, D. D. & W. L. Jones, "Gravity wave propagation with a time-dependent critical level." 1968, Proceedings from symposium on acoustic=gravity waves in the atmosphere, p. 249.

105

Howard, L. N., "Neutral curves and stability boundaries in stratified flows." 1963, JFM, 16, p. 333.

Jones, W. L., "Reflexion and stability of waves in stably stratified fluids with shear flow: a numerical study." 1968, JFM, 34, p. 609.

Kelley, R. D., Nat. Phys. Lab. Aero Report #1161 (1965).

Louquet-Higgin, M. S., "Resonant interactions between two trains of gravity waves." 1962, JFM, 12, p. 321.

Madden, R. T. & J. F. Claerbout, "Jet stream associated gravity waves and implications concerning jet stream stability." 1968, Proceedings from symposium on acoustic-gravity waves in the atmosphere, p. 121.

Martin, S., W. Simmons, & C. Wunch, "The excitation of resonant triads by single internal waves." 1972, JFM, 53, p. 17.

Maslowe, S. A. & R. E. Kelly, "Inviscid instability of an unbounded heterogeneous shear layer." 1971, JFM, 48, p. 405.

Midsad, R. W., "Experiments on Free Shear Layer Transition," Sc.D. Thesis, Dept. of Meteorology, M.I.T. (1970).

Miles, J. W., "On the stability of heterogeneous shear flows, Part I." 1963, JFM, 16, p. 209 "Part II."

Miles, J. W. & L. N. Howard, "Note on a heterogeneous shear flow." 1964, JFM, 20, p. 331.

Nayfeh, A. H. & S. D. Hassan, "The method of multiple scales and nonlinear dispersive waves." 1971, JFM, 48, p. 463.

Scotti, R. S. & G. M. Corcos, "An experiment on the stability of small disturbances in a stratified free shear layer." 1972, JFM, 52, p. 499.

Simmons, W. F., "A variational method for weak resonant wave interactions." 1969, Proc. Roy. Soc., 309, p. 551.

Spiegel, E. A. & G. Veronis, "On the Boussinesq approximation for a compressible fluid." 1960, Astrophys, J., 131, p. 442.

Thorpe, S. A., "On wave interactions in a stratified fluid." 1966, JFM, 24, p. 737

Thorpe, S. A., "Neutral eigensolutions of the stability equation for stratified shear flow." 1969, JFM, 36, p. 673.

Whitham, G. B., "A general approach to linear and non-linear dispersive waves using a Lagrangian." 1965, JFM, 22, p. 273.

Whitham, G. B., "Two-timing, variational principles and waves." 1970, JFM, 44, p. 373.

Yanowitch, M., "Effect of viscosity on gravity waves and the upper boundary condition." 1967, JFM, 29, p. 209.

BIBLIOGRAPHY

Benjamin, T. Brooke, "Internal Waves of Finite Amplitude and Permanent Form." 1966, JFM, 25, p. 241.

Benjamin, T. Brooke, "Internal Waves of Permanent Form in Fluids of Great Depth." 1967, JFM, 29, 0. 559.

Benney, D. J., "A nonlinear theory for oscillations in a parallel flow." 1961, JFM, 10, p. 209.

Benney, D. J., "A nonlinear theory for oscillations in a parallel flow." 1961, JFM, 14, p. 209.

Benney, D. J., "Nonlinear gravity wave interactions." 1962, JFM, 14, p. 577.

Benney, D. J., & R. F. Bergeron, "A new class of nonlinear waves in parallel flows." 1969, Studies in Applied Mathematics, 48, p. 181.

Bretherton, F. P., "Resonant interactions between saves: the case of discrete oscillations." 1964, JFM, 20, p. 457.

Bretherton, F. P., "The propagation of groups of internal gravity waves in a shear flow." 1966, Quart. J. Roy. Met. Soc., 92, p. 466.

Case, K. M., "Hydrodynamic stability and the inviscid limit." 1961, JFM, 10, p. 420.

Crapper, G. D., "Nonlinear gravity waves on steady non-uniform currents." 1972, JFM, 52, p. 713.

Davey, R. F. & A. Roshko, "The effect of density difference on shear-layer instability." 1972, JFM, 53, p. 523.

Davis, R. E., "On high Reynolds number flow over a wavy boundary." 1969, JFM, 36, p. 337.

Davis, S. H., "Finite amplitude instability of time-dependent flows." 1971, JFM, 45, p. 33.

Drazin, P. G., "Nonlinear internal gravity waves in a slightly stratified atmosphere." 1969, JFM, 36, p. 433.

Eckart, C., "Variational principles of hydrodynamics." 1960, Physics of Fluids, 3, p. 421.

Freeman, N. C., "Simple waves on shear flows: similarity solutions." 1972, JFM, 56, p. 257.

Gossard, E. E. & W. B. Sweeney, "Dispersion and spectra of gravity waves in the atmosphere." 1974, J. Atm. Sci., 31, p. 1540.

Greenspan, H. P. & D. J. Benney, "On shear-layer instability, breakdown and transition." 1963, JFM, 15, p. 133.

Haberman, R., "Critical layers in parallel flows." 1972, Studies in App. Math., 51, p. 139.

Hasselman, K., "On the non-linear energy transfer in a gravity wave spectrum. Part I. General Theory." 1962, JFM, 12, p. 481.

Hasselman, K., "Part II. Conservation therems; wave-particle analogy; irreversibility." 1963, JFM, 15, p. 273.

Hasselman, K., "Feynman diagrams and interaction rules of wave-wave scattering proce-ses." 1966, Rev. Geophys., 4, p.1.

Hasselman, K., "Part III. Evaluation of the energy flux and swell-sea interaction for a Neumann spectrum." 1963, JFM, 15, p. 385.

Hasselman, K., "A criterion for nonlinear wave stability." 1967, JFM, 30, p. 737.

Hines, C. O., "Generalizations of the Richardson criterion for the onset of atmospheric turbulence." 1971, Quart. J. Roy. Met. Soc., 97, p. 429.

Howard, L. N., "Note on a paper by John W. Miles." 1961, JFM, 10, p. 509.

Kelly, R. E. & S. A. Maslowe, "The nonlinear critical layer in a slightly stratified shear flow." 1970, Studies in App. Math., 49, p. 301.

Lin, C. C., "Some mathematical problems in the theory of the stability of parallel flows." 1961, JFM, 10, p. 430.

Lindzen, R. S., "Some speculations on the roles of critical level interactions between internal gravity waves and mean flows." 1968, Proceedings from symposium on acoustic-gravity waves in the atmosphere, p. 231.

McEwan, A. D., etal., "Forced resonant second-order interaction between damped internal waves." 1972, JFM, 55, p. 589.

Phillips, O. M., "The interaction trapping of internal gravity waves." 1968, JFM, 34, p. 407.

Richardson, L. F., "The supply of energy from and to atmospheric eddies." 1920, <u>Proc. Roy. Soc.</u>, <u>97</u>, p. 354.

Townsend, A. A., "Excitation of internal waves in a stably-stratified atmosphere with considerable shear." 1968, <u>JFM</u>, <u>32</u>, p. 145.

Whitham, G. B., <u>Linear and Nonlinear R Waves</u>, 1974, John Wiley & Sons.

Woods, J. D., "On Richardson's number as a criterion for laminar-turbulent-laminar transition in the atmosphere and ocean." 1969, <u>Radio Science</u>, <u>4</u>, p. 1289.

ACKNOWLEDGMENT

BIOGRAPHICAL NOTE

The author was born on 15 April 1946 in Los Angeles, California, and attended Covina High School. He received his Bachelor's Degree in Mathematics from M.I.T. in 1967 and his Master's Degree from M.I.T. in Geophysics in 1969. He has been employed as a Research Geophysicist at Chevron Oil Field Research Company since September 1975.